

**NASA CONTRACTOR
REPORT**



NASA CR

C.1



0060323

NASA CR-1204

LOAN COPY: RETURN TO
AFWL (WLIL-2)
KIRTLAND AFB, N MEX

**A STUDY OF JIMSPHERE WIND
PROFILES AS RELATED TO SPACE
VEHICLE DESIGN AND OPERATIONS**

by S. I. Adelfang, E. V. Ashburn, and A. Court

Prepared by
LOCKHEED CALIFORNIA COMPANY
Burbank, Calif.
for George C. Marshall Space Flight Center



0060323

NASA CR-1204

**A STUDY OF JIMSPHERE WIND PROFILES AS RELATED TO
SPACE VEHICLE DESIGN AND OPERATIONS**

By S. I. Adelfang, E. V. Ashburn, and A. Court

Distribution of this report is provided in the interest of information exchange. Responsibility for the contents resides in the author or organization that prepared it.

Issued by Originator as Report No. LR 21588

Prepared under Contract No. NAS 8-20747 by
LOCKHEED CALIFORNIA COMPANY
Burbank, Calif.

for George C. Marshall Space Flight Center

NATIONAL AERONAUTICS AND SPACE ADMINISTRATION

For sale by the Clearinghouse for Federal Scientific and Technical Information
Springfield, Virginia 22151 - CFSTI price \$3.00



FOREWORD

This report was prepared by the Lockheed-California Company, Burbank, California for the National Aeronautics and Space Administration, George C. Marshall Space Flight Center, Huntsville, Alabama under Contract NAS 8-20747. The contract title is "Jimsphere Wind Profiles Related to Space Vehicle Design and Operations".

Dr. J. R. Scoggins and Mr. W. W. Vaughan of the George C. Marshall Space Flight Center, Aero-Astroynamics Laboratory, were the technical monitors on behalf of the Contracting Officer Mr. L. Garrison, during the administration of the contract, and Mr. G. H. Fichtl assisted in review of the draft copy of the final report. Mr. E. V. Ashburn was the Principal Investigator for the Lockheed-California Company.

ABSTRACT

During the period December 1964 through April 1967, Jimsphere wind sensors were used to obtain 1194 profiles in the altitude range 1 km to 20 km over Cape Kennedy. This report consists of an analysis of the winds and wind shears derived from the Jimsphere data. The zonal and meridional components of the wind were found to have a distribution that is significantly closer to a normal distribution than the distribution of the components determined for the winds measured by conventional radiosonde methods. Extreme ($\geq 95\%$) Jimsphere wind speeds at 7 km through 15 km are not independent of the extreme wind speeds at 12 km altitude. Mean shears at 8, 12, and 16 km are a function of a power of the shear layer thickness, Δz for $\Delta z \leq 1$ km. The power is 1 for mean zonal and scalar shears, not clearly defined for mean meridional shears, and $2/3$ for mean vector shears. The standard deviation and the 95% scalar, vector, zonal, and meridional shears are also a function of the altitude interval Δz to the $2/3$ power. Given that the shear is extreme at 12 km altitude the simultaneous occurrence of non-overlapping extreme vector and zonal shears measured over altitude layers of 50 to 1000 meters, is a low probability event. Definitions of steady state wind and gusts are discussed in terms of filtering the wind data for the relevant frequency ranges and in terms of space vehicle characteristics.

TABLE OF CONTENTS

Section	Page
FOREWORD	iii
ABSTRACT	v
LIST OF FIGURES	ix
LIST OF TABLES	xii
SYMBOLS	xiii
1 INTRODUCTION	1
2 CHARACTERISTICS OF THE ZONAL, MERIDIONAL, AND SCALAR WIND SPEEDS IN THE FIRST 18 km OF THE ATMOSPHERE OVER CAPE KENNEDY	3
3 THEORY OF WIND SHEAR EXTREMES	18
3.1 Introduction	18
3.2 Statistical Properties	20
3.3 The Chi Distribution	21
3.4 Characteristic Extremes	24
3.5 Interval Effect	26
3.6 Variances of Averages	27
3.7 Correlations	29
3.8 Linear Decrease	31
3.9 Wind Differences	33
3.10 Conclusions	36
4 OBSERVED RELATIONS BETWEEN WIND SHEAR OVER VARIOUS ALTITUDE INTERVALS	38
4.1 Introduction	38
4.2 Means and Variances of Shears	38
4.3 Observed Distribution of Zonal, Meridional, and Vector Shears	43
4.4 Mean, Standard Deviation, and Extreme Shear as a Function of Shear Layer Thickness	55
4.5 Correlation of Shears	61
4.6 Empirical Conditional Probabilities of 95% Zonal and Vector Shears	68
5 SHEAR ENVELOPES FOR 95 AND 99 PERCENT ZONAL AND VECTOR SHEARS	71

TABLE OF CONTENTS (Cont.)

Section		Page
6	THE DEFINITION OF THE STEADY STATE WIND AND GUSTS	79
7	RELATION BETWEEN WIND SPEEDS, SHEARS, AND GUSTS	92
8	RECOMMENDATIONS FOR FUTURE ANALYSIS OF DETAILED WIND PROFILES	97
9	REFERENCES	100

LIST OF FIGURES

Figures	Page
1.1 Jimsphere	2
2.1 Monthly Distribution of Jimsphere Balloon Releases, Cape Kennedy, Florida, 1964 - 1967	4
2.2 Means, Variances, and Number of Observations as a Function of Altitude for Jimsphere Winds	5
2.3 50%, 95%, and 99% Scalar Winds	6
2.4 50%, 95%, and 99% Zonal Winds	7
2.5 50%, 95%, and 99% Meridional Winds	8
2.6 Conditional Probability of Exceedance of 95% Scalar Wind at 12 km in Combination with Exceedance of 95% Scalar Wind, at Altitudes from 7 to 14 km	10
2.7 Observed and Normal Distribution of Zonal Winds at 1, 4, and 7 km	11
2.8 Observed and Normal Distribution of Zonal Winds at 10, 13, and 16 km	12
2.9 Observed and Normal Distribution of Meridional Winds at 1, 4, and 7 km	13
2.10 Observed and Normal Distribution of Meridional Winds at 10, 13 and 16 km	14
2.11 Correlation Coefficient Between Zonal Component at Altitude Z and $Z - \Delta z$	16
2.12 Correlation Coefficient Between Meridional Component at Altitude Z and Component at Altitude $Z - \Delta z$	17
4.1 Mean Scalar Shear as a Function of Altitude for Various Shear Layer Thicknesses, Δz (m)	39
4.2 Mean Vector Shear as a Function of Altitude for Various Shear Layer Thicknesses, Δz (m)	40
4.3 Mean Zonal Shear as a Function of Altitude for Various Shear Layer Thicknesses, Δz (m)	41
4.4 Mean Meridional Shear as a Function of Altitude for Various Shear Layer Thicknesses, Δz (m)	42
4.5 Variance of Scalar Shear as a Function of Altitude for Various Shear Layer Thicknesses, Δz (m)	44
4.6 Variance of Vector Shear as a Function of Altitude for Various Shear Layer Thicknesses, Δz (m)	45

LIST OF FIGURES (Cont.)

Figures		Page
4.7	Variance of Zonal Shear as a Function of Altitude for Various Shear Layer Thicknesses, Δz (m)	46
4.8	Variance of Meridional Shear as a Function of Altitude for Various Shear Layer Thicknesses, Δz (m)	47
4.9	Observed and Normal Distribution of 50 m Zonal and Meridional Shears	48
4.10	Observed and Normal Distribution of 100 m Zonal and Meridional Shears	49
4.11	Observed and Normal Distribution of 400 m Zonal and Meridional Shears	50
4.12	Observed and Normal Distribution of 1000 m Zonal and Meridional Shears	51
4.13	Observed and Normal Distribution of 3000 m Zonal and Meridional Shears	52
4.14	Observed and Normal Distribution of 5000 m Zonal and Meridional Shears	53
4.15	The Cumulative Distribution of Vector Shears at 12 km for Shear Layer Thicknesses of 50, 100, 400, 1000, 3000, and 5000 Meters	54
4.16	The Mean Zonal, Meridional, Scalar and Vector Shear at 8, 12, and 16 km, as a Function of Shear Layer Thickness	56
4.17	Standard Deviation of Zonal, Meridional, Scalar, and Vector Shears as a Function of Shear Layer Thickness at 8, 12, and 16 km	58
4.18	95% and 99% Zonal, Meridional, and Vector Shears at 12 km as a Function of Shear Layer Thickness	60
4.19	Comparison of Observed and Predicted 95% Zonal Shear at 12 km as a Function of Shear Layer Thickness	62
4.20	Correlation of Adjacent Pairs of Scalar, Vector, Zonal, and Meridional Shears Over Non-Overlapping Intervals (Δz) of 50, 100, 400, and 1000 Meters at and Immediately Below 10, 12, and 14 km	63
4.21	The Correlation of 50 m Vector Shears with Vector Shears of Various Thicknesses at 12 km	65
4.22	The Correlation Between Zonal and Meridional Shears, as a Function of Altitude, for Shear Layer Thicknesses, Δz , of 50, 400, 1000, 3000, and 5000 m	66
4.23	Conditional Probability of Exceedance in Combination of 95% Zonal Shear at Indicated Altitude, Given the 95% Zonal Shear at 12 km, for Shear Layer Thicknesses (Δz) of 50, 100, 800, and 1000 Meters	69

LIST OF FIGURES (Cont.)

Figures		Page
4.24	Conditional Probability of Exceedance in Combination of 95% Vector Shear at the Indicated Altitude Given the 95% Vector Shear at 12 km for Shear Layer Thicknesses (Δz) of 50, 100, 800, and 1000 Meters	70
5.1	95% Zonal Shear as a Function of Altitude for Various Shear Layer Thicknesses	72
5.2	99% Zonal Shear as a Function of Altitude for Various Shear Layer Thicknesses, Δz (m)	73
5.3	95% Vector Shear as a Function of Altitude for Various Shear Layer Thicknesses, Δz (m)	74
5.4	99% Vector Shear as a Function of Altitude for Various Shear Layer Thicknesses, Δz (m)	75
5.5	Conditional Probability of Exceedance in Combination of Non-Overlapping 95% Zonal (Vector) Shears at Altitudes Between 12 km and the Indicated Altitude Given the 95% Zonal (Vector) Shear at 12 km, for Shear Layer Layer Thicknesses (Δz) of 50, 100, 800, and 1000 Meters	77
5.6	Conditional Probability of Exceedance in Combination of 95% 50, 100, and 400 Meter Zonal (Vector) at the Indicated Altitude Given the 95%, 1000 Meter Shear at 12 km	78
6.1	Spectral Window for Jimsphere Profiles	81
6.2	Vertical Velocity of Various Vehicles as a Function of Flight Time	86
6.3	Altitude of Various Vehicles as a Function of Flight Time	87
6.4	Maximum Observable Frequency of Wind Fluctuations from Wind Profiles with an Altitude Resolution of 50 Meters as a Function of Flight Time for Various Vehicles	88
6.5	Maximum Observable Frequency from Wind Profiles with an Altitude Resolution of 50 Meters as a Function of Altitude for Various Vehicles	90
7.1	Conditional Probability for Exceedance of the Indicated Vector Shear Percentiles at 12 km, for Shear Layer Thicknesses of 100, 400, 1000, 3000 and 5000 m, Given that the Scalar Wind Speed at 12 km Exceeds the 95 Percent Value	93
7.2	Conditional Probability for Exceedance of the Indicated Zonal Shear Percentiles at 12 km, for Shear Layer Thicknesses of 100, 400, 1000, 3000, and 5000 m, Given that the Zonal Wind Speed at 12 km Exceeds the 95 Percent Value	94

LIST OF TABLES

Tables		Page
3.1	Independent Bivariate Normal and Related χ_2 Distributions	23
4.1	The Value of the Constant D of Equation 4.5	59
4.2	$R_{x/yz}$ The Coefficient of Multiple Correlation for Vector Shears at 12 km	67
6.1	Frequency Range of Jimsphere Data in the Time Domain for the Saturn AS-504 Vehicle	82
6.2	Cut-Off Frequency of the Alfriend Filter as a Function of Flight Time of the Saturn AS-504 Vehicle	83
7.1	Comparison of Conditional Probabilities of Dependent and Independent Scalar Wind Speed and Vector Shear with Conditional Probabilities Estimated from Jimsphere Observations for Various Shear Layer Thicknesses, Δz	95
7.2	Comparison of Conditional Probabilities of Dependent and Independent Zonal Wind Speed and Zonal Shear with Conditional Probabilities Estimated from Jimsphere Observations for Various Shear Layer Thicknesses, Δz	96

LIST OF SYMBOLS

a	Sample size factor (Eqs. 3.13, 3.14)
b	Ratio of the thicknesses of elemental layers
C	Constant of proportionality (Eq. 4.1)
C_L	Weighted sum of correlations in Eq. 7.2
c_{ij}	Generalized covariance matrix
$c_{i, i+1}$	Covariance matrix (Eq. 3.18)
D	Constant of proportionality (Eq. 4.5)
E	Expectation
F	Cumulative probability
f_c^*	Cut-off frequency of the Alfriend filter in the time domain
f_m	Maximum frequency of Jimsphere wind profile perturbations seen by a space vehicle
G	Constant of proportionality (Eq. 4.7)
H(n)	Transfer function (Eq. 6.1)
I_0	Zero order Bessel function of the first kind
k	Number of degrees of freedom of a chi distribution
L	Correlation distance
l	Number of independent variables
m	Average random sample size between occurrences of the characteristic extreme V_m^*
m_j	Mean of the jth component (Eq. 3.5)
$N(m_j, \sigma_j^2)$	Normal distribution with mean m_j and variance σ_j^2
N	Number of Jimsphere wind observations per unit time seen by a space vehicle
N_0	Number of soundings which have shears which exceed the 95% value at level z
N_1	Subset of N_0
N_2	Subset of N_1
n	Number of standard deviations from the mean of the P th percentile of a normal variable (Eq. 4.9)
n	Frequency (Eq. 6.1)

n	Any linear coordinate axis in the horizontal plane
P	Percentile
p	Probability
R	Resolution of the Jimsphere data
$R_{x/yz}$	Coefficient of multiple correlation where x is the dependent variable and y and z are the independent variables
S	Averaging interval for Jimsphere winds (Eq. 6.1)
T	Length of the data record
V	Two-dimensional horizontal wind vector
v	Magnitude of V
v_x	Magnitude of the component of V in the x direction
v_y	Magnitude of the component of V in the y direction
v_m^*	Characteristic extreme (Eq. 3.11)
$v(t)$	Magnitude of the vertical velocity of the booster
\bar{v}_ℓ	Mean of the resultant ℓ -layer winds
W	Vector wind shear
w	Magnitude of the vector wind shear
w_x	Zonal wind shear or magnitude of the component of W in the x direction
w_y	Meridional wind shear or magnitude of the component of W in the y direction
w_s	Scalar wind shear
w/95	95 percent vector shear
w/99	99 percent vector shear
$w_{x/95}$	95 percent zonal shear
$w_{y/95}$	95 percent meridional shear
x	Dependent variable (Eqs. 4.12 and 4.13)
x	Designated eastward for a Euclidean x-y-z space
y	Independent variable (Eqs. 4.12 and 4.13)
y	Designated northward for a Euclidean x-y-z space
z	Independent variable (Eqs. 4.12 and 4.13)
z	Designated upward for a Euclidean x-y-z space
z	Altitude
Δz	Vertical shear layer thickness

η	Coefficient in correlation models (Eqs. 7.3, 7.4, 7.5)
λ	Wavelength for the damped wave correlation model (Eq. 7.5)
ρ_{ik}	Linear correlation coefficient between components with subscripts j and k
σ_j^2	Variance of the jth component
σ	Standard deviation of shear (Eq. 4.5)
$\frac{\sigma^2}{\bar{x}}/l$	Variance of the mean over l elemental layers
$\frac{\sigma^2}{\bar{x}/bl}$	Variance of the mean over bl elemental layers
χ_K	Chi distribution with K degrees of freedom

Section 1

INTRODUCTION

This report consists of an analysis of the characteristics of the winds and wind shears in the 1 to 18 km altitude range over Cape Kennedy that are important for the design and operation of space vehicles. This analysis is based upon 1194 wind profiles that cover the period December 1964 through April 1967. These wind profiles were derived by the Aerospace Environment Division, Aero-Astro dynamics Laboratory of the George C. Marshall Space Flight Center from AN/FPS-16 radar observations of Jimspheres. Jimsphere wind sensors are 2 meter diameter spherical superpressure balloons with large roughness elements irregularly spaced on the surface. The purpose of the rough surface is to control the random vortex shedding or aerodynamic noise associated with smooth balloons operating in the supercritical Reynolds number region. The result is the Jimsphere balloon which will follow the small scale wind motions very accurately (Figure 1.1). Details of the properties of Jimspheres and the method of computing the scalar, zonal, and meridional magnitudes and the wind directions are given by Scoggins (Ref. 14). The combination of the Jimsphere higher precision radar and the computing techniques yields details of the variation of wind with altitude far beyond the capabilities of the conventional RAWIN system. Thus, for the first time, a detailed analysis of the wind shears for an altitude increment as small as 50 m has been feasible.

The following sections present an analysis of the characteristics of the zonal, meridional, and scalar wind speeds, theory of wind shear extremes, relations between wind shears over various altitude increments, determination of shear envelopes, definitions of steady wind and gusts, and a discussion of the use of detailed wind profiles in the design and operation of space vehicles.

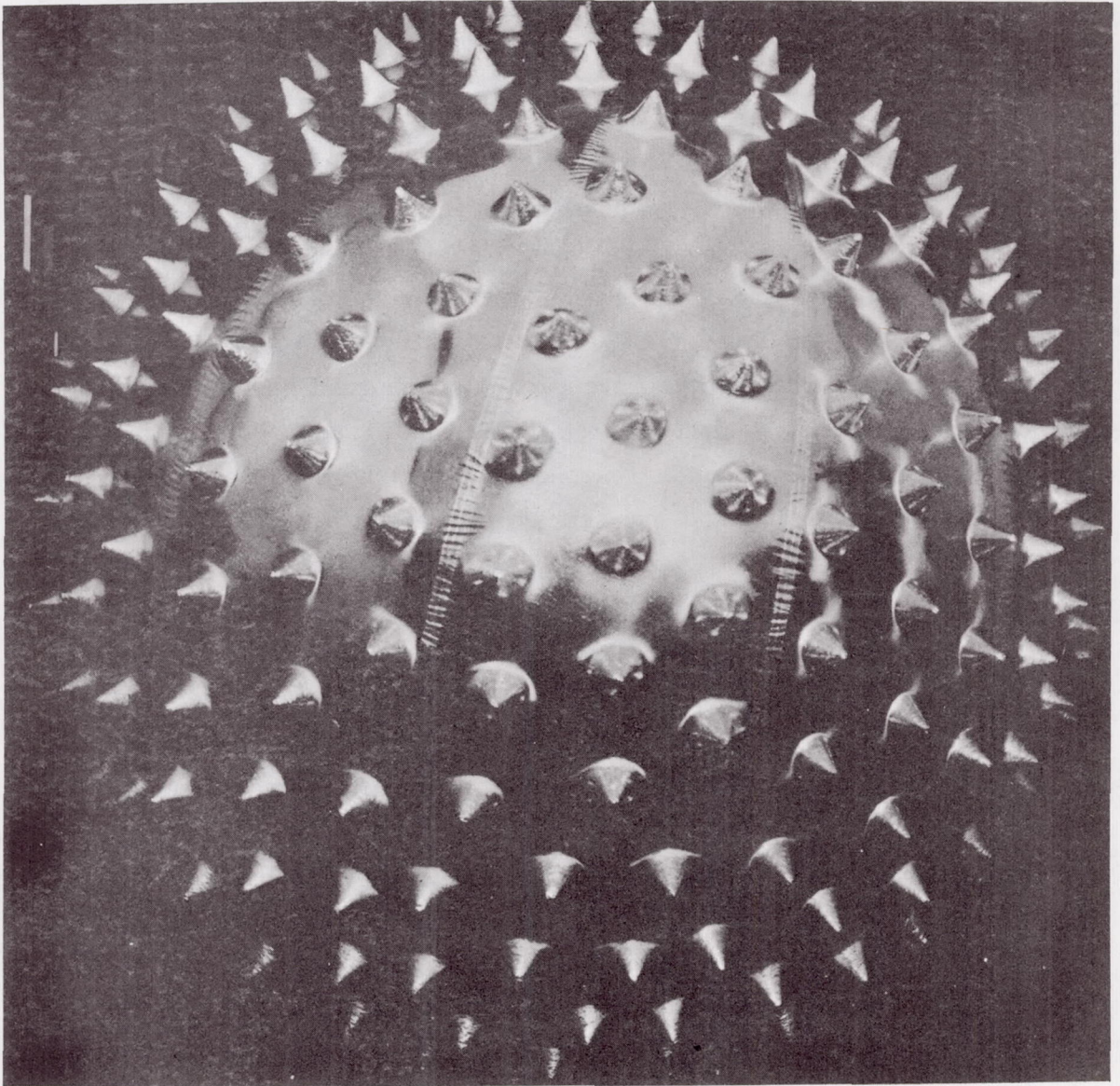


Figure 1.1 Jimsphere

Section 2

CHARACTERISTICS OF THE ZONAL, MERIDIONAL, AND SCALAR WIND SPEEDS IN THE FIRST 18 km OF THE ATMOSPHERE OVER CAPE KENNEDY

In this study the data provided are used as one sample without stratification. This sample contains wind information obtained from 1194 distinct soundings made at Cape Kennedy during the period 28 November 1964 through 11 May 1967. The distribution of the soundings by months is indicated in Figure 2.1. The histogram indicates that the Jimsphere wind observations were not uniformly distributed throughout all months of the observation period. A relatively high percentage of the observations were made during February, March, and April.

The number of observations as a function of altitude is shown in Figure 2.2. There were 1000 or more observations for all altitudes 625 m to 14075 m, 800 or more observations for altitudes 250 m to 16275 m and 500 or more observations for altitudes 175 m to 17125 m. Figure 2.2 also illustrates the means and variances of the scalar, zonal and meridional winds as a function of altitude. The points represent 50 m intervals.

Published Tables of the monthly and annual wind distributions derived from rawinsonde observations as a function of altitude for Cape Canaveral and Patrick Air Force Base (Ref. 16). This summary included data obtained during the period January 1956 to December 1961. Figures 2.3, 2.4, and 2.5 illustrate a comparison of the results obtained from the Jimsphere soundings from Cape Kennedy. The comparison indicated that the 50% Jimsphere scalar winds are significantly higher at all altitudes, the 95% Jimsphere scalar winds are nearly the same at all altitudes up to approximately 9 km; above 9 km the 50% Jimsphere winds are significantly smaller. In contrast, the 99% scalar winds for the 1956 - 61 period show significantly higher wind speeds at all altitudes. The difference between the 99% Jimsphere scalar winds and the 99% rawinsonde scalar winds is largest for rawinsonde scalar winds near 80 m/sec. Perhaps the statement in "Synoptic Meteorology as Practiced by the National Meteorological Center" (NAWAC Manual 1963, page 17) "This error

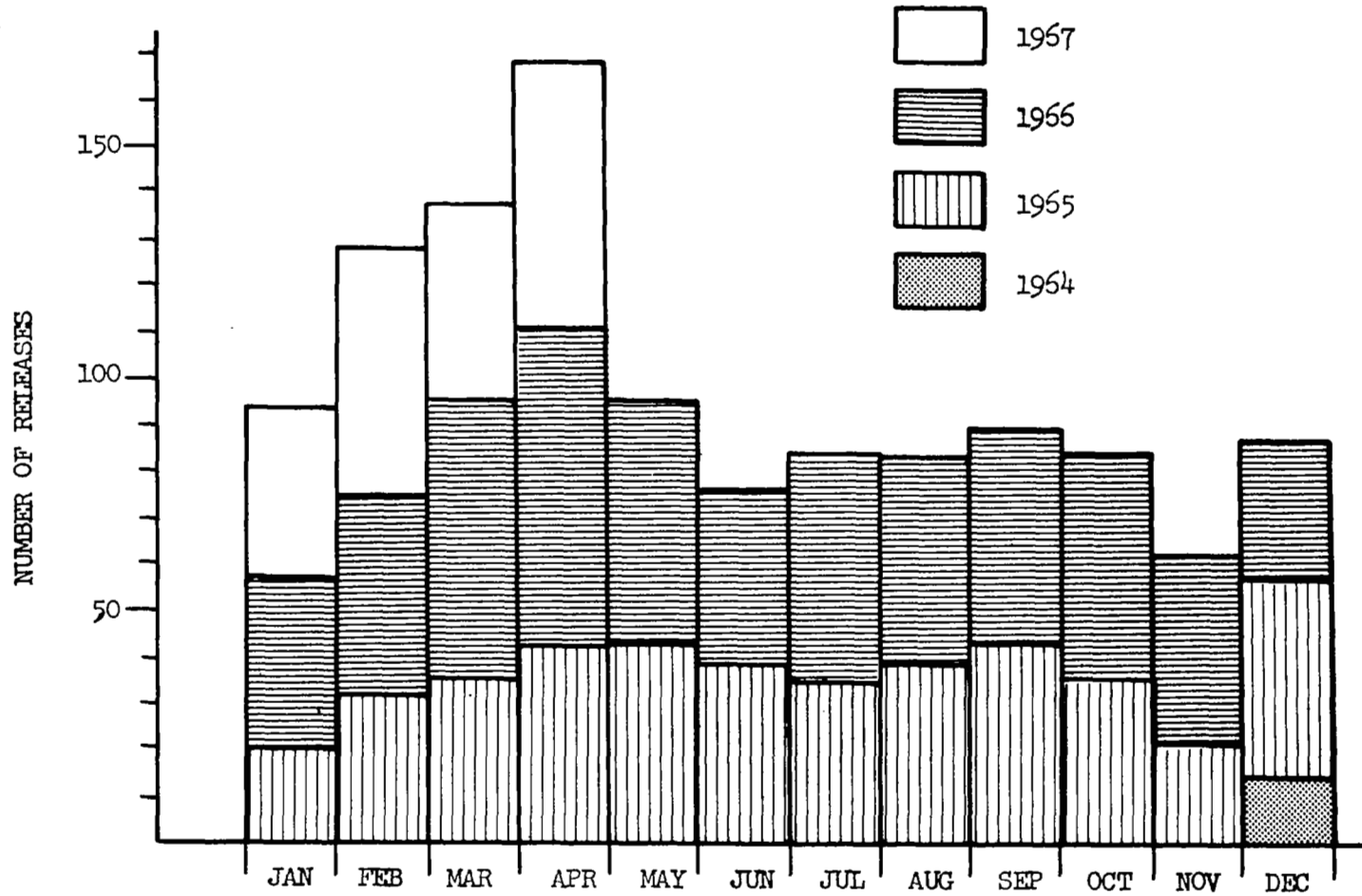


Figure 2.1 Monthly Distribution of Jimsphere Balloon Releases, Cape Kennedy, Florida, 1964 - 1967

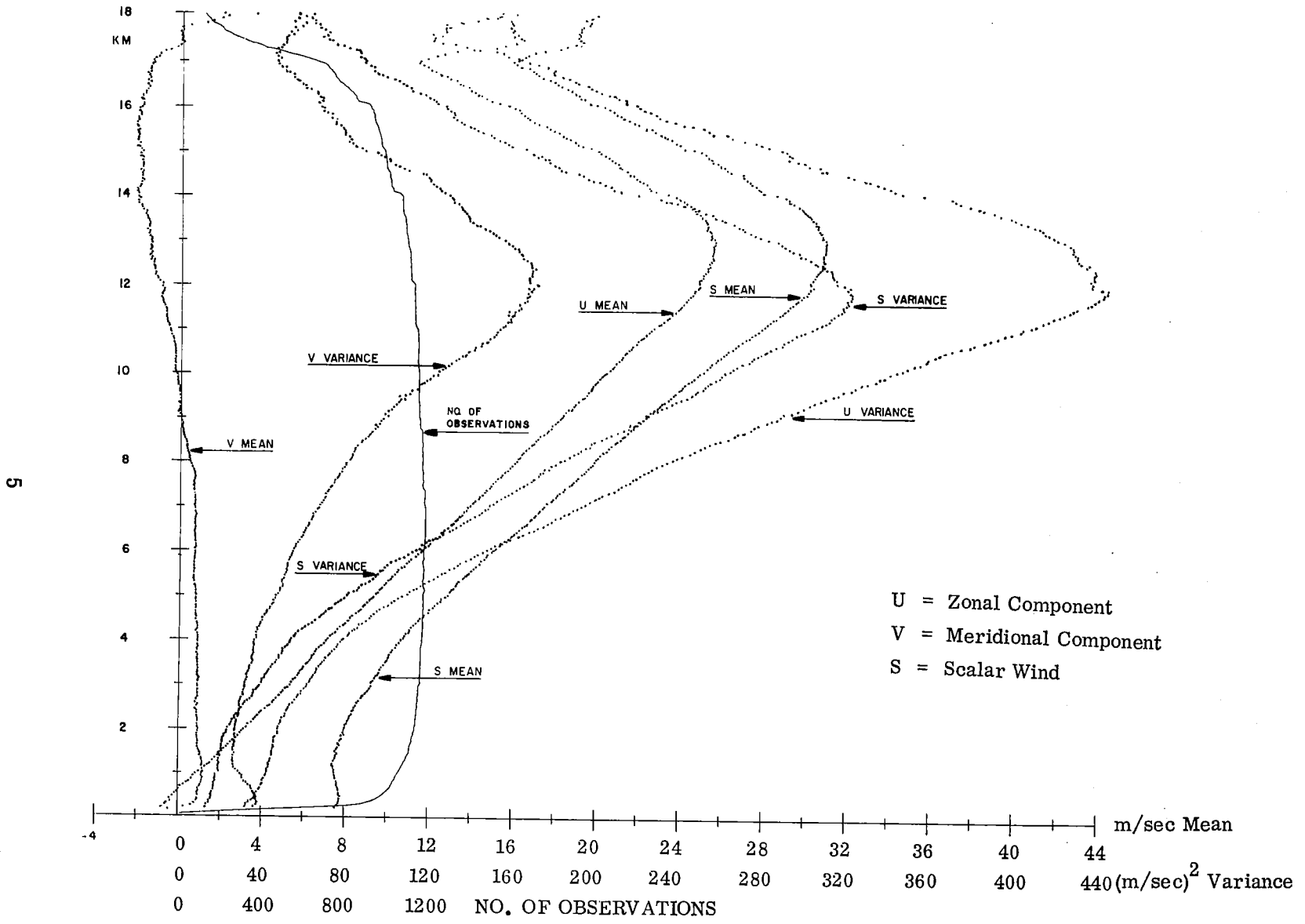


Figure 2.2 Means, Variances, and Number of Observations as a Function of Altitude for Jimsphere Winds

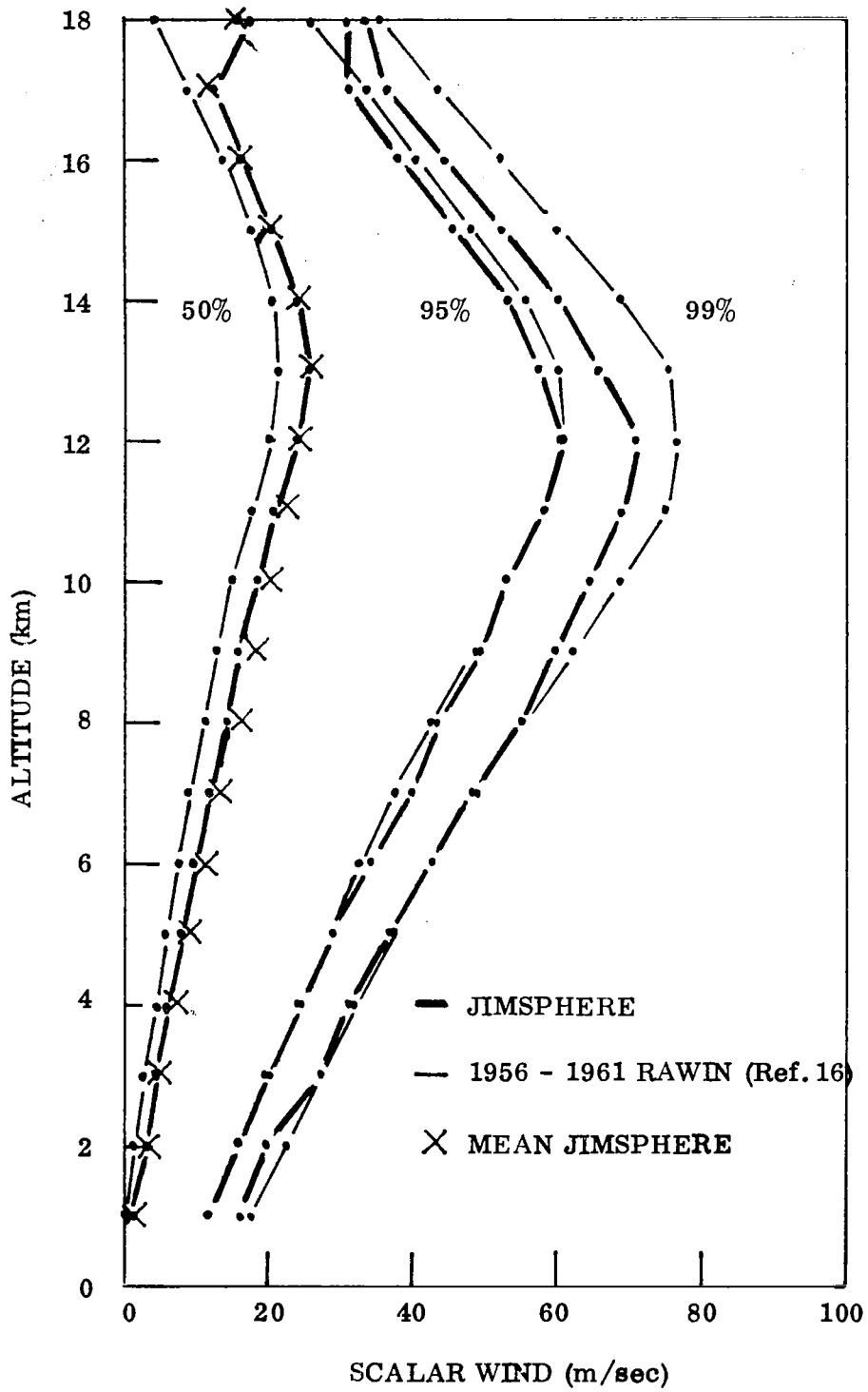


Figure 2.3 50%, 95%, and 99% Scalar Winds

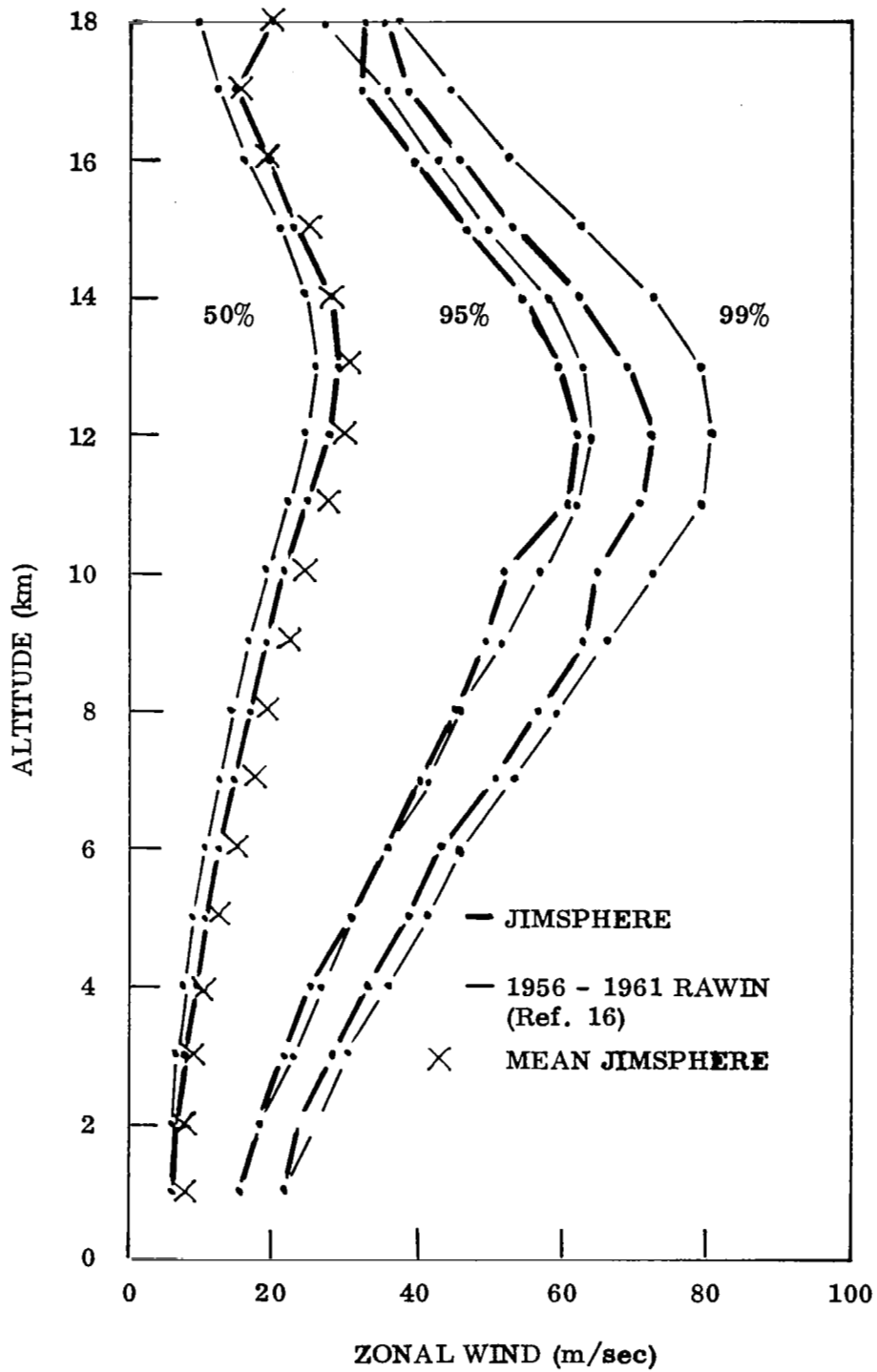


Figure 2.4 50%, 95%, and 99% Zonal Winds

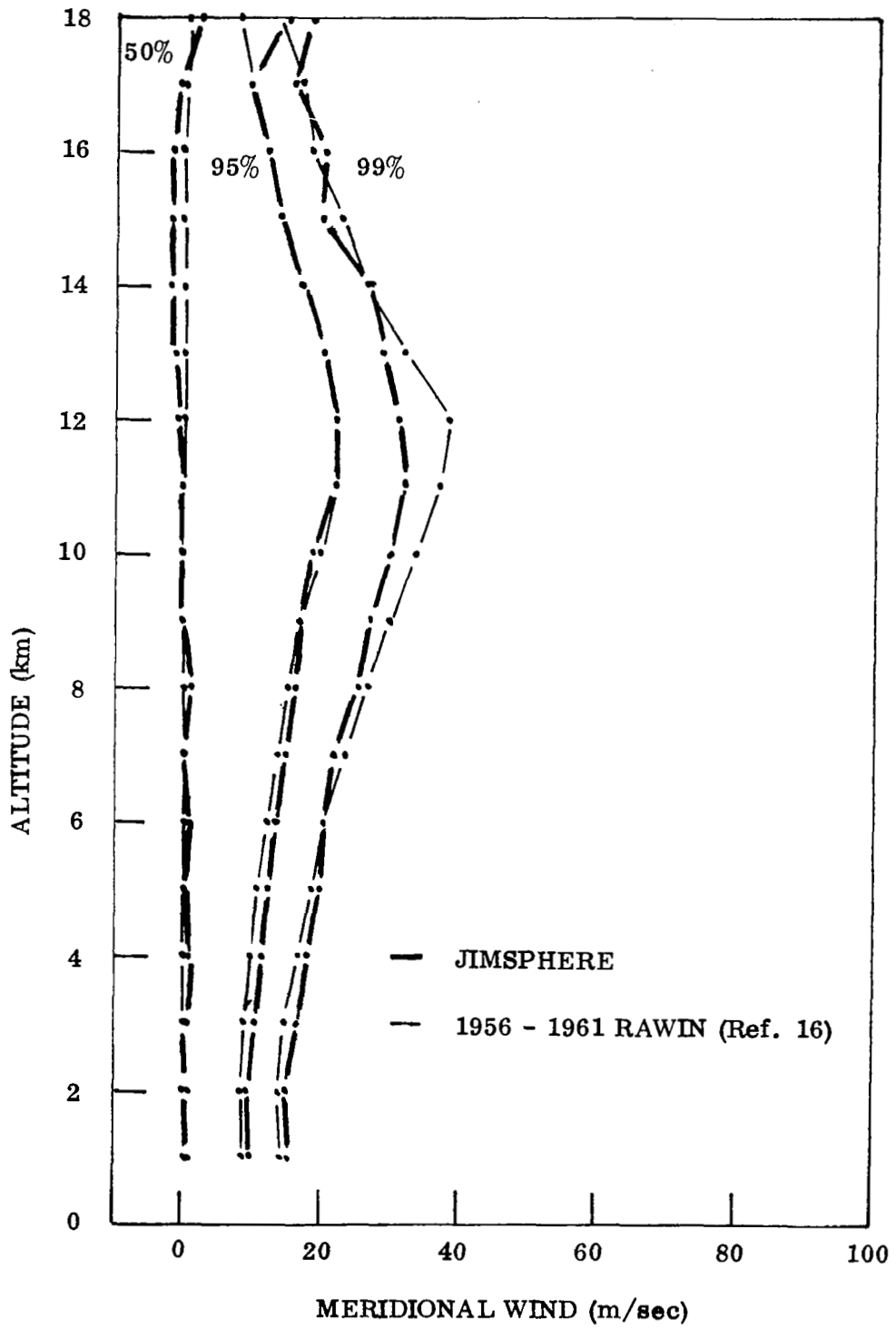


Figure 2.5 50%, 95%, and 99% Meridional Winds

(in wind speeds) increases rapidly, especially for winds over 100 kt., . . ." is pertinent to the explanation of the relatively large differences in the 99% winds for the Jimsphere and the rawinsonde. Are these differences due to the short record for the Jimsphere or are the rawinsondes in error? In any case it appears that investigation of the reality of the extreme wind speeds is in order.

Figure 2.4 illustrates that the comments made above relative to the scalar winds apply to the zonal component except that the 95% zonal winds are nearly the same for both sets of data up to an altitude of 12 km.

The comparison between the Jimsphere and rawinsonde meridional components (Figure 2.5) illustrates essentially small differences for the 50% and 95% winds; the 99% Jimsphere meridional winds are significantly smaller than the rawinsonde winds at altitudes between 8 and 13 km.

An interesting statistic relating to the extreme profiles of wind speed is an estimate of the probability that extreme wind speeds occur simultaneously over large altitude intervals. Conditional probabilities were computed of the simultaneous occurrence of extreme wind speed ($\geq 95\%$ value), as observed at 1 km intervals, from 7 to 14 km, given that the wind speed is extreme at 12 km. The results support the conclusion that these extreme wind speeds are not independent. For example, if the extreme wind speeds were independent, the conditional probability that the extreme winds at 10 and 11 km occur simultaneously, given that the extreme wind occurred at 12 km, is $(.05)^2$. The results shown in Figure 2.6 for the Jimsphere data indicate that the observed conditional probability is 0.55.

Figure 2.7 through 2.10 were prepared to illustrate the extent to which the distribution of zonal and meridional winds depart from a normal distribution. The results shown in these Figures when combined with those illustrated in Figure 2.4 and 2.5 indicated that the zonal and meridional winds from the Jimsphere records are more nearly normally distributed than the rawinsonde observations. The distributions

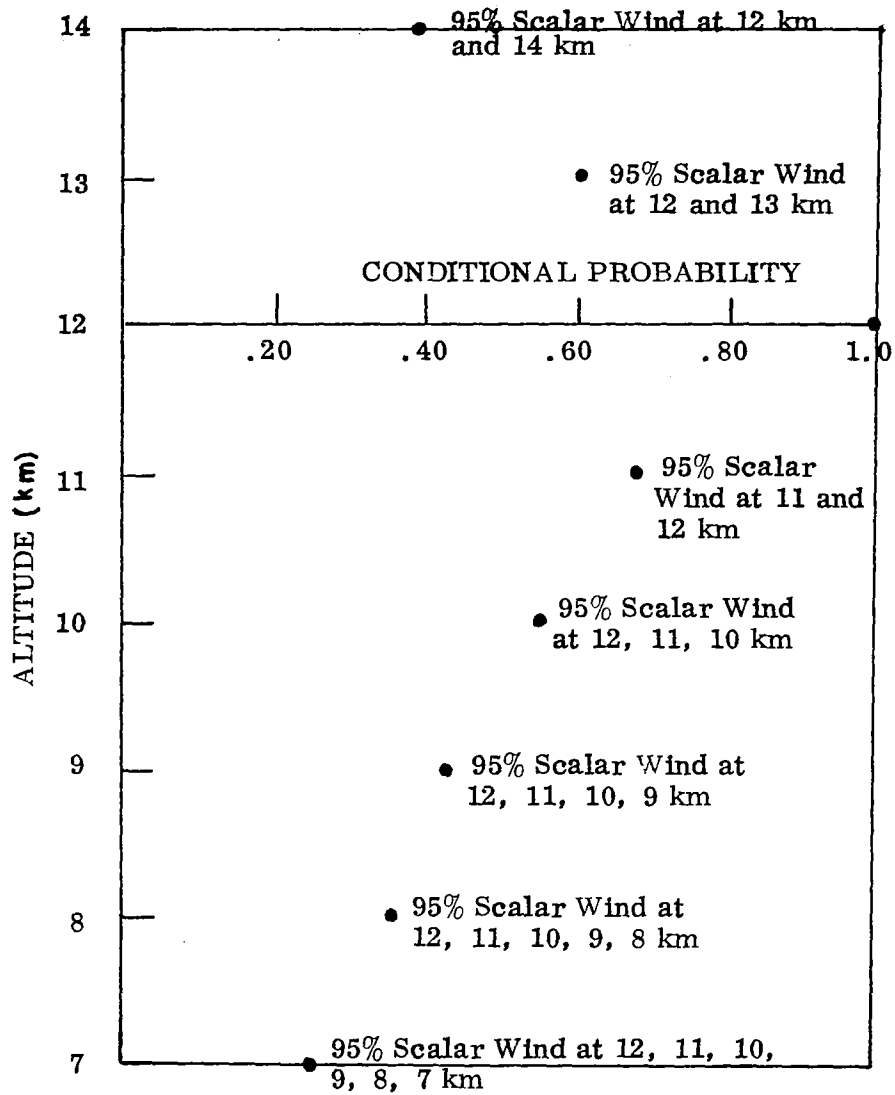


Figure 2.6 Conditional Probability of Exceedance of 95% Scalar Wind at 12 km in Combination with Exceedance of 95% Scalar Wind, at Altitudes from 7 to 14 km

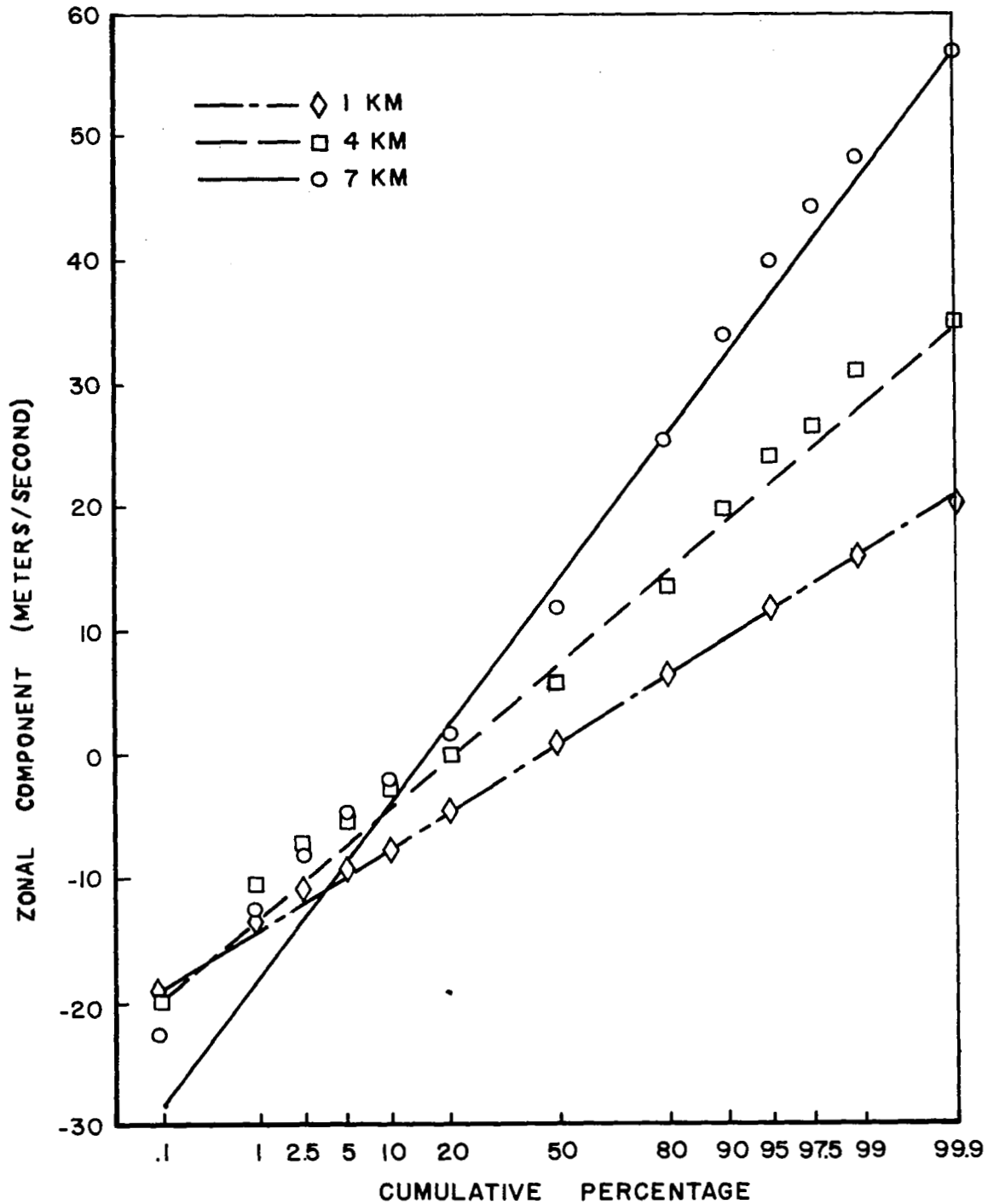


Figure 2.7 Observed and Normal Distribution of Zonal Winds at 1, 4, and 7 km

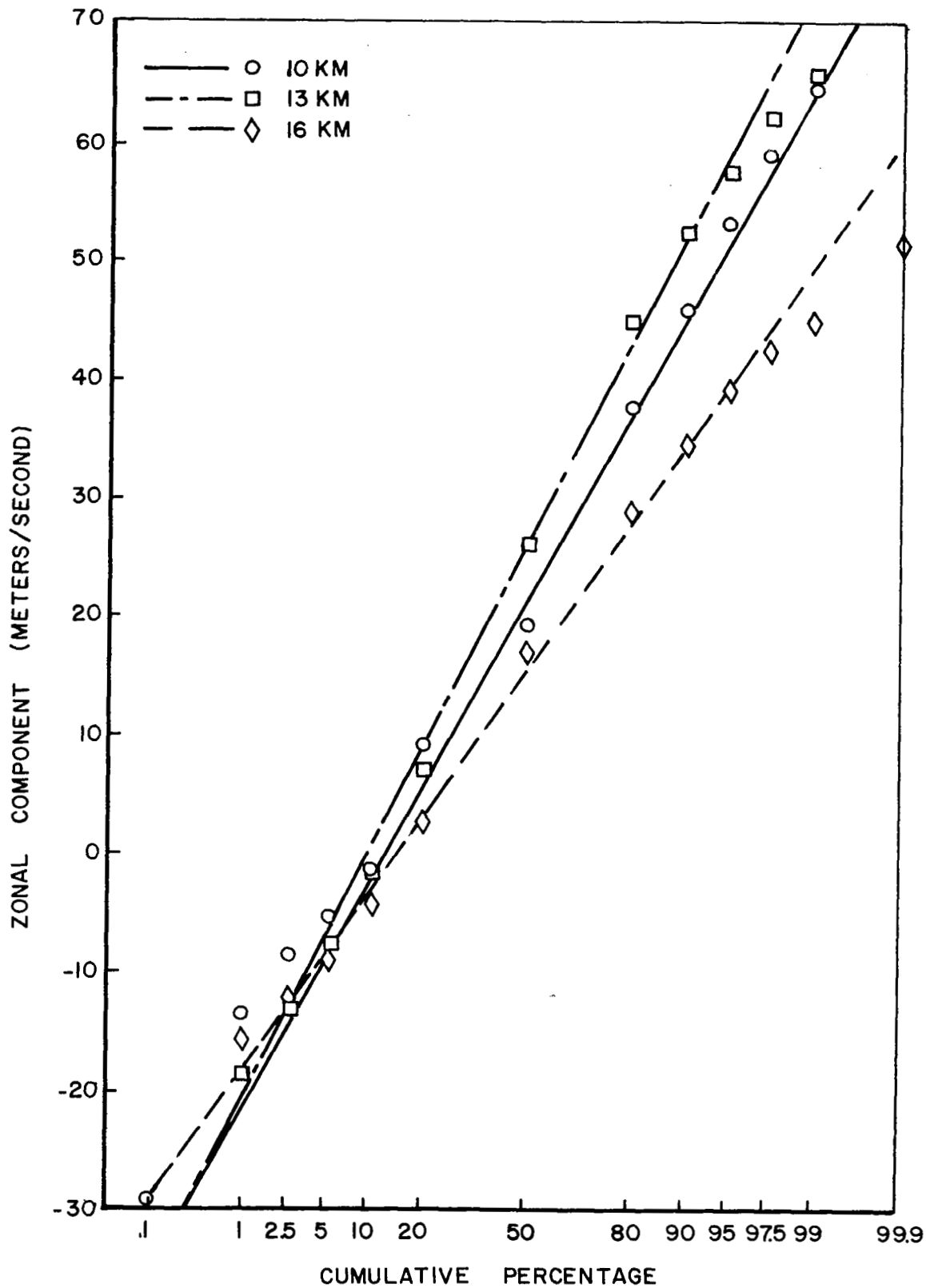


Figure 2.8 Observed and Normal Distribution of Zonal Winds at 10, 13, and 16 km

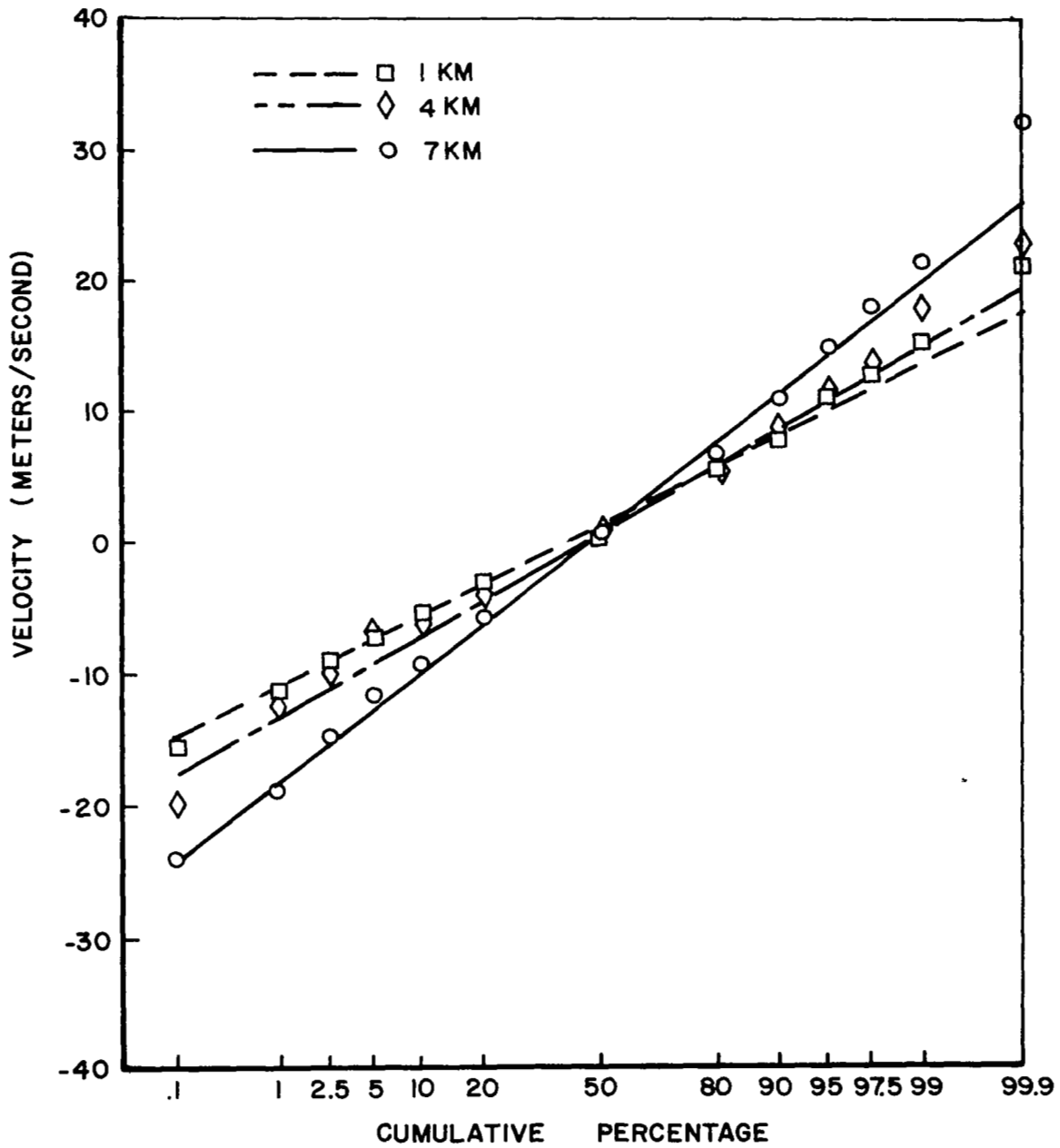


Figure 2.9 Observed and Normal Distribution of Meridional Winds at 1, 4, and 7 km

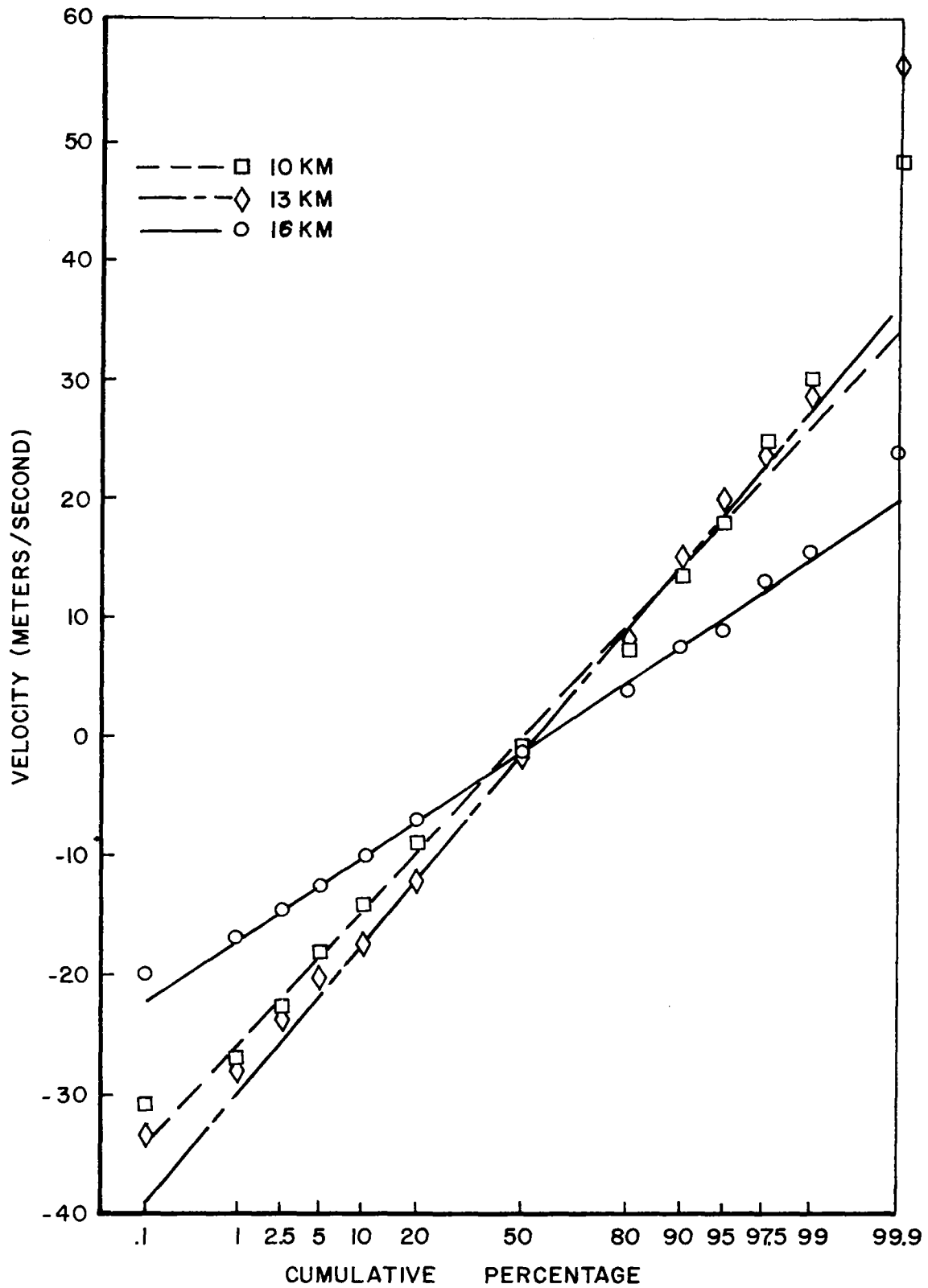


Figure 2.10 Observed and Normal Distribution of Meridional Winds at 10, 13, and 16 km

for the Jimsphere meridional winds for altitudes 10 km and 13 km are the only ones that depart greatly from a normal distribution.

A further comparison between the Jimsphere winds and the rawinsonde winds is illustrated in Figures 2.11 and 2.12. In these Figures the interlevel correlations of the wind components are shown for the Jimsphere observations and the rawinsonde observations as given by Vaughan (Ref. 17). The correlation coefficients for the Jimsphere observations are slightly higher at nearly all altitudes for both the zonal and the meridional components.

In summary,

1. More Jimsphere observations were made during the months of February, March, and April than for the rest of the year. These months are those when the maximum winds were observed using rawinsondes.
2. The winds as measured by the Jimsphere show significantly lower values for the 99% and 95% winds and higher for the 50% level. Possible explanation lie in one or more of the following:
 - a. Errors in the rawinsonde values
 - b. Too small a sample for the Jimsphere values
 - c. Difference in sample period between rawinsonde and Jimsphere data.
3. The distribution of the zonal and meridional components of the Jimsphere winds are more nearly normally distributed than the rawinsonde winds.
4. The extreme ($\geq 95\%$) wind speeds at 7 through 11 and 13 and 14 km are not independent of the extreme wind speeds at 12 km.

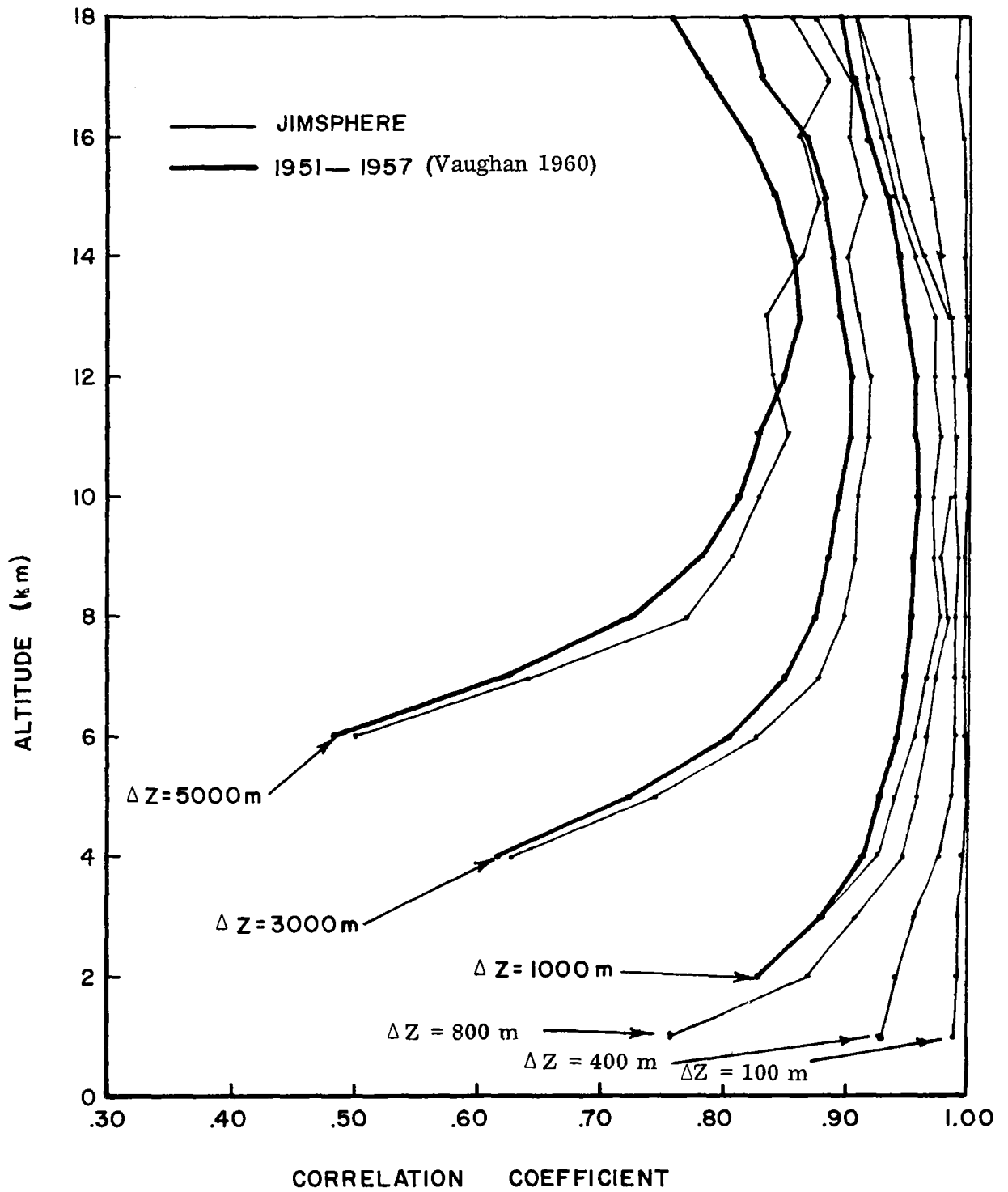


Figure 2.11 Correlation Coefficient Between Zonal Component at Altitude Z and $Z - \Delta z$

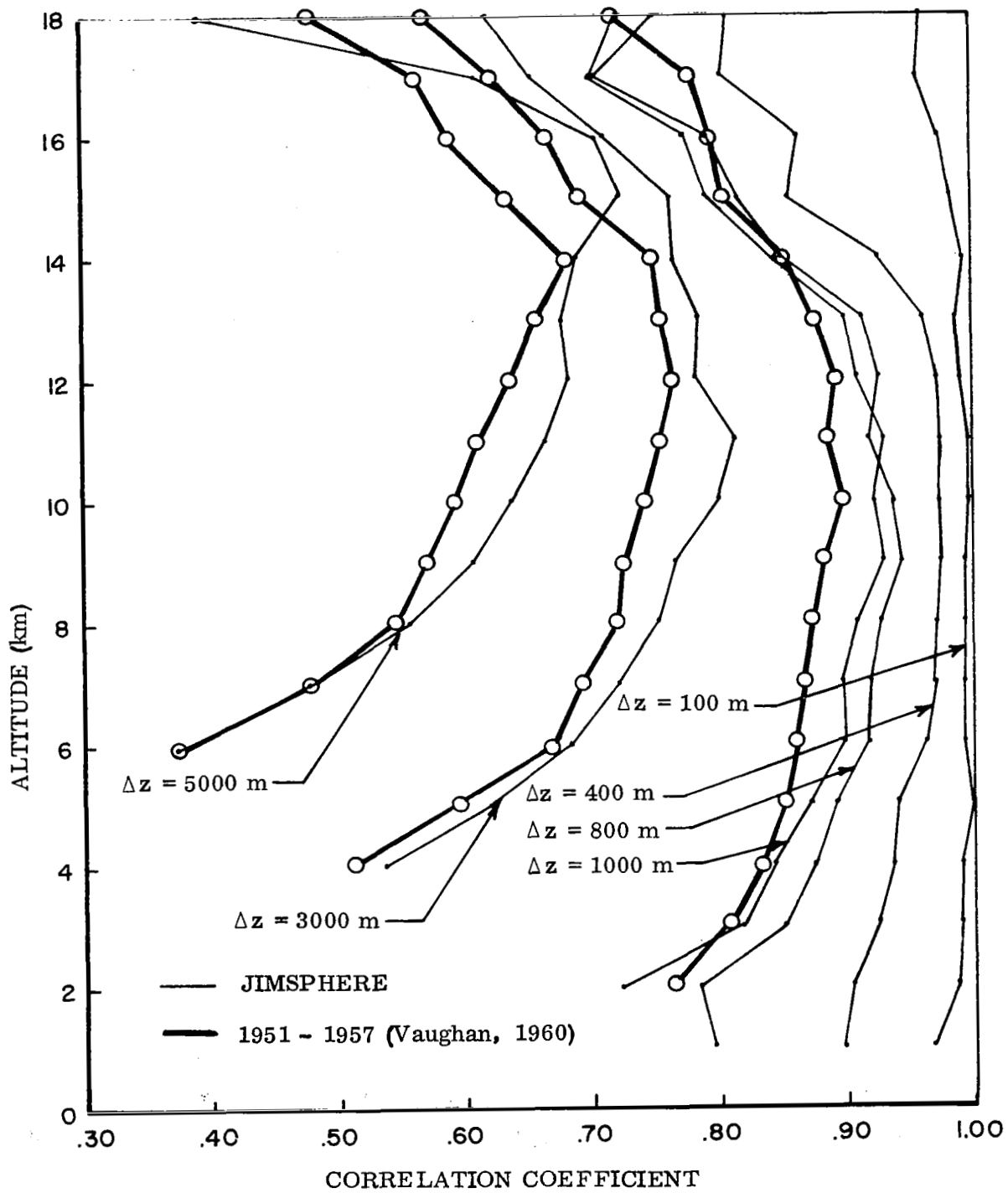


Figure 2.12 Correlation Coefficient Between Meridional Component at Altitude Z and Component at Altitude $Z - \Delta z$

Section 3

THEORY OF WIND SHEAR EXTREMES

3.1 INTRODUCTION

Wind shear is very easy to define but hard to measure, and still harder to describe and predict, either operationally or climatically. Yet it is a very important atmospheric property which must be considered in the design and operation of vehicles, from small aircraft to massive space boosters. The statistical properties of wind shear are the topics of this section. Major emphasis is placed on the description, analysis, and behavior of wind shear extremes.

Wind is air movement, and hence is represented mathematically as a vector, having both orientation (direction) and length (speed). Vectors will be denoted by capital letters, their lengths (which are ordinary scalar quantities) by the corresponding lower case letters.

Wind shear is the rate of change of wind along a direction perpendicular to that of the movement. This definition (Gordon, Ref. 7, p. 113) is preferable to the less specific "directional derivation" in a given direction (Huschke, Ref. 9).

In Euclidean x-y-z space, with x eastward, y northward, z upward, wind is a 3-dimensional vector. But the vertical component usually is about two orders of magnitude smaller than the resultant of the two horizontal components. For most purposes, including the present discussion, wind may be considered as a two-dimensional horizontal vector V with components of magnitudes v_x and v_y in the x and y directions, respectively. The length (or "modulus") of this vector is

$$v = (v_x^2 + v_y^2)^{1/2}. \quad 3.1$$

The entire atmosphere at any given instant forms a continuous field of vectors V . At any point and any time, the horizontal wind vector has three derivatives, or rates of change, that are of interest. The derivative with respect to time, t , at a given point represents the wind gustiness, while the two space derivatives, vertically and horizontally, perpendicular to the wind vector, represent the shears:

$$\text{gustiness:} \quad \frac{d}{dt} V = \frac{d}{dt} V_x + \frac{d}{dt} V_y ;$$

$$\text{horizontal:} \quad \frac{d}{dn} V = \frac{d}{dx} V_x + \frac{d}{dy} V_y ; \quad 3.2$$

$$\text{vertical:} \quad \frac{d}{dz} V = \frac{d}{dz} V_x + \frac{d}{dz} V_y ;$$

The horizontal (or lateral) wind shear, derivative is taken in the horizontal direction, n , normal to the wind vector. The vertical wind shear vector, representing the vertical shear of the horizontal wind vector, or vector wind shear, is denoted by W , in the horizontal plane, with magnitude w and components of magnitudes w_x and w_y :

$$w = (w_x^2 + w_y^2)^{1/2} . \quad 3.3$$

Scalar shears also are of interest, primarily because they are much easier to compute than vector shears. The horizontal and vertical scalar shears represent simply the changes in the wind speed (length of the wind vector) without regard to directional changes:

$$\text{horizontal:} \quad \frac{d}{dn} v = \frac{d}{dn} (v_x^2 + v_y^2)^{1/2} ;$$

$$\text{vertical:} \quad \frac{d}{dz} v = \frac{d}{dz} (v_x^2 + v_y^2)^{1/2} . \quad 3.4$$

Only when the direction of the wind vector is constant, horizontally or vertically, are the corresponding scalar and vector shears numerically equal. In general, the scalar shear is smaller than the magnitude of the vector shear.

3.2 STATISTICAL PROPERTIES

Vector shear is a point function, a space derivative of a vector at a point in space. But no such point function is actually computed or measured. The manner in which the wind vector V varies continuously with height is not known, so that derivatives cannot be obtained. Instead, wind shear at a point customarily is approximated by finite differences, giving the wind shear through a layer. However, in this Section, and the three following, wind derivatives will be assumed to apply to points, or at most to tiny volumes of space; the extent to which actual observations are incompatible with such an assumption will be examined later.

Wind components (zonal and meridional, or west-to-east and south-to-north) at some given atmospheric level usually are assumed to have a joint bivariate normal distribution. At the next higher level, a similar bivariate normal distribution would exist. Each of these four components may be correlated, linearly or otherwise, with each of the others. A complete description of the statistical properties of the wind at two adjacent levels involves the means and variances of four normal variables, and their six correlations (presumably linear), or 14 different quantities in all.

The vector (layer) wind shear, W , between two levels is the resultant of two orthogonal difference vectors, one for each wind component. No matter what the correlation of the corresponding components is at the two levels, their difference has a normal distribution. Thus the components of the difference vector, the layer wind shear, have a bivariate normal distribution. The two means depend on the difference between the respective component means, the two variances on the variances and covariances for each component separately, and the correlation between the two wind shear components depends on all four variances and six correlations.

For convenience in notation, in this paragraph only, the zonal and meridional components of wind at the first level may be denoted as v_1, v_2 , those at the second level as v_3, v_4 , with m_j and σ_j^2 denoting the mean and variance of the j th component ($j = 1, 2, 3, 4$) and ρ_{jk} the linear correlation between v_j and v_k , $k \neq j$. Then the magnitudes of the two components of the layer wind shear vector W are

$$\begin{aligned} w_x &= v_3 - v_1 : N(m_3 - m_1, \sigma_1^2 - 2\sigma_1\rho_{13}\sigma_3 + \sigma_3^2), \\ w_y &= v_4 - v_2 : N(m_4 - m_2, \sigma_2^2 - 2\sigma_2\rho_{24}\sigma_4 + \sigma_4^2). \end{aligned} \tag{3.5}$$

The linear correlation between the magnitudes of these two difference vectors is

$$\rho_{w_x w_y} = \frac{(\sigma_1\rho_{12}\sigma_2 + \sigma_3\rho_{34}\sigma_4) - (\sigma_1\rho_{14}\sigma_4 + \sigma_2\rho_{23}\sigma_3)}{\left[(\sigma_1^2 - 2\sigma_1\rho_{13}\sigma_3 + \sigma_3^2)(\sigma_2^2 - 2\sigma_2\rho_{24}\sigma_4 + \sigma_4^2) \right]^{1/2}} \tag{3.6}$$

3.3 THE CHI DISTRIBUTION

The chi distribution with k degrees of freedom, denoted as χ_k , applies to the square root of the sum of the squares of k independent normal variables, each with mean zero and the same variance. For $k = 2$ the chi distribution is sometimes called the Rayleigh distribution, for $k = 3$ the Maxwell distribution, although neither of these 19th century British physicists was the first to discover or use it. The χ_2 distribution applies to the length of the radius vector, in polar coordinates, of a bivariate normal variate of which the cartesian components have the same variance and no correlation. In particular, therefore, it applies to the scalar wind speed, and to the magnitude of the vector wind shear, if all components have the same variance and no correlation.

In this circular bivariate case, when the two cartesian components, v_x and v_y , are each normally distributed with mean zero and the same variance, σ^2 , the

strength of the resultant wind, v , should follow the χ_2 distribution:

$$p(v) = (v/\sigma^2) \exp(-v^2/2\sigma^2), \quad 3.7$$

where $v^2 = v_x^2 + v_y^2$. The mode of the distribution is at $v = \sigma$, and the mean and variance are:

$$m_v = E(v) = \sigma\sqrt{\pi/2}; \quad \sigma_v^2 = (2 - \pi/2)\sigma^2 = (4/\pi - 1) [E(v)]^2 \quad 3.8$$

The cumulative probability,

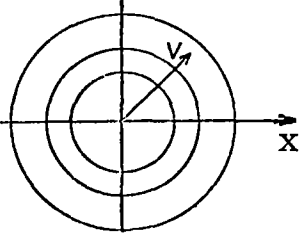
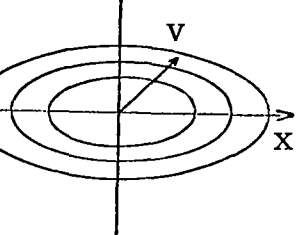
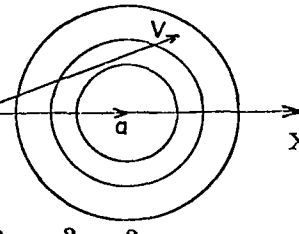
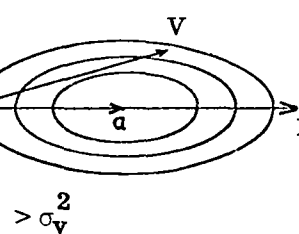
$$F(v) = \int_0^v x \sigma^{-2} \exp(-x^2/2\sigma^2) dx = 1 - \exp(-v^2/2\sigma^2) \quad 3.9$$

is 0.30347σ at the mode and 0.54407σ at the mean; the median is at $v = 1.1774 \sigma$.

When the variances are unequal, and when correlations are not zero, a bivariate normal distribution can be converted into a circular normal distribution by suitable rotation of axes and by scaling the variables to have the same variance, i. e., by expressing them in units of standard deviation. Without such transformation, in terms of the original unequal variances of possibly correlated variables, the chi distribution is quite cumbersome. Such elliptical and non-central chi distributions, with 2 degrees of freedom, corresponding to elliptical and non-central bivariate normal distributions, are given in Table 3.1. All except the simplest, already discussed, contain Bessel functions, but the general form, and particularly the extreme behavior, of such chi distributions appear to be essentially the same as for the simplest case.

While some form of chi distribution describes scalar wind speeds, as well as the magnitude of vector resultant winds and of vector wind shears, a more complicated function applies to scalar wind shears. Since scalar winds have chi distributions, the differences of two such winds, the scalar wind shear, has the distribution of

TABLE 3.1 INDEPENDENT BIVARIATE NORMAL AND RELATED χ_2 DISTRIBUTIONS

<p>central circular</p>  <p>$\sigma_x^2 = \sigma_y^2 = \sigma^2$</p>	$p(x, y) = \frac{1}{2\pi\sigma^2} \exp\left(-\frac{x^2 + y^2}{2\sigma^2}\right)$ $p(v) = \frac{v}{\sigma^2} \exp(-v^2/2\sigma^2)$
<p>central elliptical</p>  <p>$\sigma_x^2 > \sigma_y^2$</p>	$p(x, y) = \frac{1}{2\pi\sigma_x\sigma_y} \exp\left(-\frac{x^2}{2\sigma_x^2} - \frac{y^2}{2\sigma_y^2}\right)$ $p(v) = \frac{v}{\sigma_x\sigma_y} \exp\left[-v^2 \frac{\sigma_x^{-2} + \sigma_y^{-2}}{4}\right] I_0\left[v^2 \frac{\sigma_x^{-2} - \sigma_y^{-2}}{4}\right]$
<p>Y non-central circular</p>  <p>$\sigma_x^2 = \sigma_y^2 = \sigma^2$</p>	$p(x, y) = \frac{1}{2\pi\sigma^2} \exp\left[-\frac{(x-a)^2 + y^2}{2\sigma^2}\right]$ $p(v) = \frac{v}{\sigma^2} \exp\left[-\frac{(v-a)^2}{2\sigma^2}\right] \exp\left[-\frac{av}{\sigma^2}\right] I_0\left[\frac{av}{\sigma^2}\right]$
<p>Y non-central elliptical</p>  <p>$\sigma_x^2 > \sigma_y^2$</p>	$p(x, y) = \frac{1}{2\pi\sigma_x\sigma_y} \exp\left[-\frac{(x-a)^2}{2\sigma_x^2} - \frac{y^2}{2\sigma_y^2}\right]$ $p(v) = \frac{\sigma_y}{\sigma_x} \exp\left(\frac{-a^2}{2\sigma_x^2}\right) \frac{v}{\sigma_y} \exp\left(\frac{-v^2}{2\sigma_y^2}\right) \cdot \sum_{j=1}^{\infty} \left(v^2 \frac{\sigma_y^{-2} - \sigma_x^{-2}}{2}\right)^j \frac{1}{j!} I_0^{(2j)}\left(\frac{av}{\sigma_x^2}\right)$

Bessel function of first kind and of zero order, for pure imaginary argument

$$I_0(v) = \frac{1}{\pi} \int_0^\pi \exp(v \cos \theta) d\theta$$

the difference of two chi variates. This "chi-dif" distribution, not generally known (Court, Ref. 5), closely resembles a normal distribution over most of its domain but a chi distribution in the "tails".

Thus, when the individual zonal and meridional components of wind speed have normal distributions, the distributions of their resultants (vector sums) and shears (differences) are:

	<u>Components</u>	<u>Resultants</u>	<u>Scalar</u>
Speeds	Normal	Chi	Chi
Shears	Normal	Chi	Chi-dif

3.4 CHARACTERISTIC EXTREMES

The chi distribution, introduced in the preceding sub-section as applying to wind speeds and the magnitudes of the vector (layer) wind shear, provides a basis for discussing the behavior of extremes of these quantities. For this, elements of the statistical theory of extreme values are needed (Gumbel, Ref. 8). Extreme value theory is concerned not with the entire sample of observations from some population, but with the behavior of only the extreme values in each of many samples.

The extremes are not necessarily the largest or smallest elements in each sample, but may be the next-to-largest, third-from-smallest, etc. In the simplest case, the theory applies to a set of n values, each of which is the largest (or other defined "extreme") of a sample of m values from some population.

One fundamental concept of the theory is that of the characteristic extreme. (Formerly it was called, somewhat ambiguously, the "expected extreme", although it is not an expected value in the usual statistical sense.) The characteristic extreme, v_m^* , is the value that has a probability of $1/m$ of being exceeded by the largest value in a random sample of size m :

$$P (v \geq v_m^*) = 1/m . \quad 3.10$$

The quantity m is the return period or return interval of the extreme v_m^* ; it is the average interval between occurrences, or recurrences, of a value of v at least as large as v_m^* . For a χ_2 distribution, the cumulative distribution (3.9) gives

$$P(v \geq v_m^*) = 1 - 1/m = 1 - \exp(-v_m^{*2}/2\sigma^2). \quad 3.11$$

Hence $m = \exp(v_m^{*2}/2\sigma^2)$ and

$$v_m^* = \sigma \sqrt{2 \ln m}. \quad 3.12$$

This same relation also applies asymptotically (for large samples) to the normal distribution and to many others. The characteristic extreme of a random sample of χ_2 variables increases quite slowly as the sample size is enlarged. To double the magnitude of the characteristic extreme, the size of a sample from a chi distribution must be increased $e^4 = 53.6$ times.

If the sample size is changed by a factor of a , the characteristic extreme of the resulting sample of am elements will be

$$\begin{aligned} v_{am}^* &= \sigma \sqrt{2 \ln(am)} \\ &= v_m^* \sqrt{2 \ln(am)} / \sqrt{2 \ln m} \end{aligned} \quad 3.13$$

Thus the characteristic extremes of two independent samples from a chi distribution are in the ratio of the square roots of the logarithms of the sample sizes:

$$v_{am}^*/v_m^* = \sqrt{\ln(am)/\ln(m)} = \sqrt{1 + \ln a/\ln m} \quad 3.14$$

When m is large relative to a , this makes little difference: the characteristic extreme of 1,000 observations is only $\sqrt{1.5} = 1.225$ that for 100 observations. But in smaller samples the effect is important.

The monthly average of wind speeds and shears measured 2 or 4 times daily would not be significantly different, but the maximum winds, or maximum interval shears, of the twice per day soundings would be, on the average, only about

$$\sqrt{\ln 60 / \ln 120} = \sqrt{0.855} = 0.9248$$

those of the corresponding maxima of soundings made four times daily.

3.5 INTERVAL EFFECT

Even more important in applying extreme value analysis to winds and wind shears is another sampling effect, termed the "interval length effect" by Dr. Julius Lieblein in an unpublished talk before the Institute of Mathematical Statistics in 1955. This effect arises when the items of a sample are themselves sums of averages of other variables.

Summing or averaging over either time or space intervals can introduce this effect. The total number of plants tallied on a 1-km botanical transect is the sum of the plants in each of 1,000 intervals of 1 meter each. The total number of lightning flashes counted in an hour is the sum of the flashes in 3,600 consecutive 1-second intervals. The speed of a moving object, or of the wind, over 1 km or during 1 minute is the average of its speeds over 1,000 successive meters, or during 60 consecutive seconds.

Thus, the distribution of 1-minute wind speeds is the distribution of the mean of 1-second winds -- and the distribution of 1-second wind speeds is the distribution of the mean of 1-millisecond winds. Exactly the same arguments apply to the motions of adjacent layers of the atmosphere. The resultant motion, or wind, averaged over a 1-km layer is the mean of the motions of all the thousand 1-meter

layers in that kilometer, or of all the million 1-millimeter layers in the kilometer, or of all elemental layers, however thin they are.

The smallest individual air parcel for which a velocity can be assumed must be at least an order of magnitude greater than the mean free path of the individual air molecules. The mean free path is about 0.05μ at sea level, 0.1μ at 5 km, 1μ at 21 km, 1 mm at 70 km and 1 m at 115 km. Hence the concept of wind cannot apply, in the troposphere, to parcels smaller than about 10μ in diameter.

A body of air may be considered as composed of many elemental cubes, each 10μ on a side. Viewed in the vertical, moving air is a collection of layers, each 10μ or 0.001 cm thick. The actual thickness of such elemental layers is unimportant; the concept of such layers serves only as the basis for showing that the characteristics of winds measured over layers of differing thickness vary according to the layer thicknesses.

In each elemental layer, the two components of motion have a bivariate normal distribution, so that their resultant, the wind speed, has a χ_2 distribution (Eq. 3.7). In this distribution, the parameter is the standard deviation of each of the wind components if they are equal, or some function of their standard deviations if they differ (Table 3.1).

The wind speed through a layer composed of many elemental layers is the resultant of the two components, each averaged through the layer. It also will have a χ_2 distribution with parameter depending on the variances of each of the two component averages. Hence the characteristic extreme of wind speeds averaged through a layer, and of vector shear through a layer, depend on the variances of the wind components within the layer.

3.6 VARIANCES OF AVERAGES

The variance of the sum of ℓ variables, with $c_{i,j}$ denoting the covariance between the i th and j th variables, so that $c_{i,i} = \sigma_i^2$, the variance of the i th variable is

$$\begin{aligned}
\text{Var} \left(\sum_1^{\ell} x_i \right) &= \sum_{i=1}^{\ell} \sum_{j=1}^{\ell} c_{i,j} \\
&= \sum_1^{\ell} \sigma_i^2 + 2 \sum_{i=1}^{\ell-1} \sum_{t=1}^{\ell-i} c_{i,i+t} \\
&= \sum_1^{\ell} \sigma_i^2 + 2 \sum_{i=1}^{\ell-1} \sum_{t=1}^{\ell-i} \sigma_i \rho_{i,i+t} \sigma_{i+t} ,
\end{aligned} \tag{3.15}$$

because $c_{i,j} / \sigma_i \sigma_j = \rho_{i,j}$, the linear correlation coefficient between the i th and j th variables. The variance of the mean of the ℓ variables is ℓ^{-2} that of their sum.

Two special cases are of interest: (1) when the ℓ variables are all mutually independent, so that $\rho_{ij} = c_{ij} = 0$ for $i \neq j$; and (2) when the correlation depends only on the difference $|i - j| = |t|$, so that $\rho_{i,i+1} = \rho_t$ for any i and t .

When the variables are independent ($\rho_{ij} = 0$), the variance of their sum is the sum of the variances, and the variance of the mean of the ℓ independent variables is $1/\ell$ times the mean of their variances. If zonal winds in adjacent elemental layers were independent, and each had the same variance σ^2 , the mean zonal wind over ℓ layers would have a variance of σ^2/ℓ . If, in addition, the components were independent of each other, the resultant of these average winds would have a χ_2^2 distribution with parameter σ^2/ℓ .

Hence the mean of these resultant ℓ -layer winds, \bar{v}_ℓ , would be, from Eq. 3.8

$$E(\bar{v}_\ell) = \sigma_\ell \sqrt{\pi/2} = \sigma \sqrt{\pi/2 \ell} \tag{3.16}$$

Similarly, the characteristic extreme of m such mean l -layer winds would be, from Eq. 3.12

$$v_m^* = (\sigma / \sqrt{l}) \sqrt{2 \ln m} \quad 3.17$$

For m winds averaged over bl independent elemental layers, the mean and characteristic extreme would each be $(bl)^{-1/2}$, where b is the ratio of the thicknesses. In this highly simplified and unrealistic case of inter-component and inter-layer independence, with all variances equal, the means and characteristic extremes of winds and wind shears should vary inversely according to the square root of the thickness of the averaging layer. For example, winds averaged over 1 km would have means and characteristic extremes only $10^{-1/2} = 0.316$ those of winds averaged through 100-meter layers, if winds in all layers are mutually independent.

3.7 CORRELATIONS

Independence of wind components in adjacent elemental layers, however, is hardly plausible. Instead, some sort of correlation, decreasing with separation (at least initially), is more tenable. If this decrease depends only on the separation $|i - j| = t$, and not on the particular i or j , the sum of all covariances in Eq. 3.15 becomes

$$\begin{aligned} 2 \sum_{i=1}^{l-1} \sum_{t=1}^{l-i} c_{i,i+t} &= 2 \left[(l-1) c_1 + (l-2) c_2 + \dots + 2c_{l-2} + c_{l-1} \right] \\ &= 2 \sum_{t=1}^{l-1} (l-t) c_t \end{aligned} \quad 3.18$$

If all variances σ_i^2 are equal, $c_t = \sigma^2 \rho_t$ and (3.15) reduces to

$$\begin{aligned} \frac{\sigma_x^2}{x} | \ell &= \ell^{-2} \left[\ell s^2 + 2\sigma^2 \sum_{t=1}^{\ell-1} (\ell-t) \rho_t \right] \\ &= \left(\frac{\sigma}{\ell} \right)^2 \left[\ell + 2 \sum_{t=1}^{\ell-1} (\ell-t) \rho_t \right] \end{aligned} \quad 3.19$$

Further application of this result requires some assumptions about the behavior of ρ_ℓ , which presumably decreases with ℓ , at least initially. Three models, of increasing complexity and validity, are available to describe the manner of decrease, or "decay", of correlation with increasing separation. One is a highly artificial but usefully simple model of linear decrease. A second is the exponential decay model, widely used although not applicable to most meteorological phenomena, including winds layer-by-layer, on either theoretical or observational grounds. The third is the damped wave model, little used largely because its complexity has thus far defied efforts at fitting it objectively to data, and partly because no physical basis for it has yet appeared, although many sets of observations appear to follow it. The three models are:

$$\text{Linear decrease:} \quad \rho_\ell = \begin{cases} (1 - \eta)(L - \ell)/L, & \ell < L \\ 0 & \ell > L \end{cases} \quad 3.20$$

$$\text{Exponential decay:} \quad \rho_\ell = (1 - \eta) e^{-b\ell} \quad 3.21$$

$$\text{Damped wave:} \quad \rho_\ell = (1 - \eta) \cos(2\pi\ell/\lambda) e^{-b\ell} \quad 3.22$$

The coefficient $(1 - \eta)$ permits each model to be fitted to actual observations of correlations at different lags (separations in time or space). Two observations on the same variable at different lags will differ because of instrumental and observational errors as well as because the variable actually changes with lag. Even if the true value of the variable did not change, the correlation between observations at a given lag would be $1 - \eta$ rather than unity. Hence, observed lag correlations generally underestimate the true lag correlation, for which $\eta = 0$.

In the linear decrease model, the constant L is the "correlation distance", at which the correlation becomes zero, and is zero for all greater lags. In the other two models, the correlation never remains at zero, but a corresponding "effective correlation distance" can be found such that correlation at greater lags is less than some value, such as 0.01 or 0.001.

In the damped wave model, the constant λ is not the correlation distance; instead it is the wavelength of the correlation, which, in this model, decreases to zero at $\ell = \lambda/4$, becomes negative until $\ell = 3\lambda/4$ and attains a second maximum at $\ell = \lambda$. Hence the linear model can be considered a crude approximation of the first quarter, with L approximately $\lambda/4$.

3.8 LINEAR DECREASE

In the linear decrease model, when $\ell < L$, the number of layers forming the correlation distance, the correlation sum in Eq. (3.18) is

$$\begin{aligned} 2 \sum_{t=1}^{\ell-1} (\ell - t) \rho_t &= 2 \sum_{t=1}^{\ell-1} (\ell - t) \frac{L - t}{t} \\ &= \ell \frac{\ell - 1}{3L} (3L - \ell - 1) \end{aligned} \quad 3.23$$

Thus the variance of a wind component averaged over ℓ layers, throughout which the correlation remains appreciable, is

$$\begin{aligned} \sigma_{\bar{X}}^2 |_{\ell < L} &= \left(\frac{\sigma}{\ell}\right)^2 \left[\ell + \ell \frac{\ell - 1}{3L} (3L - \ell - 1) \right] \\ &= \sigma^2 \left(1 - \frac{\ell^2 - 1}{3\ell L} \right) \end{aligned} \quad 3.24$$

or approximately $\sigma^2 (1 - \ell/3L)$. As wind is averaged over an increasing number of layers, the variance of the average decreases until, when $\ell = L$, it is slightly more than 2/3 the variance of the wind in an elemental layer.

The actual variance of winds averaged over many elemental layers probably is not as simple as it would be if the correlation decreased linearly, but should behave somewhat similarly. When $\ell = L$, the correlation sum (Eq. 3.23) becomes

$$C_L = \frac{1}{3} (L - 1)(2L - 1) \quad 3.25$$

or approximately $2L^2/3$. When $\ell > L$, the sum is $(\ell - L) C_L$, and the variance of winds averaged over $\ell = bL$ elemental layers is

$$\begin{aligned} \sigma_{\bar{x}}^2 | \ell = bL &= \left(\frac{\sigma}{bL}\right)^2 \left[bL + L(b-1) \left(\frac{L-1}{3}\right) (2L-1) \right] \\ &= \frac{\sigma^2}{bL} \left[1 + \frac{b-1}{3b} (L-1)(2L-1) \right] \end{aligned} \quad 3.26$$

or somewhat less than $\sigma^2 (L/b)$. The ratio of this variance to that of winds averaged over L layers is

$$\begin{aligned} \frac{\sigma_{\bar{x}}^2 | \ell = bL}{\sigma_{\bar{x}}^2 | \ell = L} &= \frac{\sigma^2/3b^2L}{\sigma^2/3L^2} \frac{3b + (b-1)(2L^2 - 3L + 1)}{2L^2 + 1} \\ &= \frac{b-1}{b^2} \left(1 - \frac{3L}{2L^2 + 1} \right) + \frac{3}{b(2L^2 + 1)} \end{aligned} \quad 3.27$$

or essentially $1/b$, as in the case of independence. Regardless of the number of elemental layers L in the correlation distance, the variance of wind averaged over ℓ elemental layers decreases as ℓ increases. Over thin layers, where correlation is strong, the decrease is rapid, perhaps exponential, and over thick layers it is almost linear.

3.9 WIND DIFFERENCES

Wind shear is theoretically a point function, as discussed in Section 3.2, and was so considered in preceding Sections. In practice, wind shear is estimated from the differences between "observed" components of the wind at two "levels". These "observed" components, in turn, are obtained from the differences in the position of a balloon at successive time intervals, during which the balloon rises through ℓ elemental layers. Hence the variance of such "observed" component winds, which are averages of ℓ elemental layers, decreases as ℓ is increased, as discussed in the preceding Section.

The difference between such "observed" wind components for the i th and j th "levels" is the component wind shear:

$$\text{zonal:} \quad w_{x|ij} = v_{x|i} - v_{x|j}$$

$$\text{meridional:} \quad w_{y|ij} = v_{y|i} - v_{y|j}$$

3.28

Thus $w_{ij} = (w_{x|ij}^2 + w_{y|ij}^2)^{1/2}$ is the magnitude of the vector wind shear, which has a χ_2 distribution (Eq. 3.7) in which the parameter is the common standard deviation of $w_{x|ij}$ and $w_{y|ij}$, or some function of these standard deviations if they are unequal (Table 3.1).

When the two ℓ - element levels are separated by more than the correlation distance for elemental layers, the average wind component over one level is independent of that over the other level. Then the variance of the difference between the two average winds is the sum of the variances of the two components, which depend on ℓ . When wind components in all the elemental layers have zero means and the same variance, σ^2 , the parameter in the χ_2 distribution of vector shear is $\sigma_{\bar{x}|\ell} \sqrt{2}$. Then the mean vector wind shear is, from Eq. (3.7)

$$E(w) = \sigma_{\bar{x}|\ell} \sqrt{2} \sqrt{\pi/2} = \sigma_{\bar{x}|\ell} \sqrt{\pi} \quad , \quad 3.29$$

or 1.77 times the standard deviation of an "observed" wind component. If the decrease in the correlations of wind components of elemental layers is linear with increasing layer separation, this would be approximately, from Eq. (3.23)

$$E(w) = \sigma \sqrt{\pi} (1 - \ell/3L) \quad . \quad 3.30$$

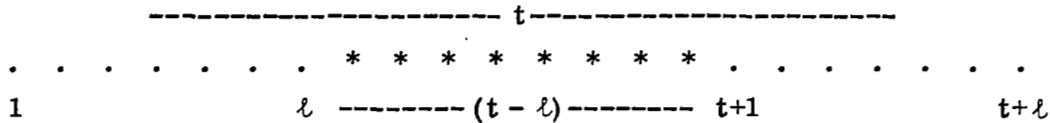
In this case, mean vector shear depends on ℓ/L , the ratio of averaging distance to correlation distance, but not on the distance over which the shear is computed. The characteristic extreme of a χ_2 variate also is proportional to the mean, as well as to the square root of the logarithm of sample size (Eq. 3.12). Thus, the characteristic extreme of vector wind shear also depends on ℓ/L , and not on the shear interval, when that interval is greater than the correlation distance.

More realistically, when the correlation of wind components in elemental layers decreases so slowly that the separation between "levels" is less than the correlation distance, the elemental winds which are averaged for the "observed" winds are not independent, and neither are the "observed" winds. Then the vector wind shear still has a χ_2 distribution, but with a parameter which depends on the interlevel correlation as well as on the thickness of the "levels". In general, the parameter

is $(1 - \rho_{ij})^{1/2}$ times that for the case of independence, so that

$$E(w) = \sigma_{\bar{x}|\ell} \sqrt{\pi} \sqrt{1 - \rho_{ij}}, \quad 3.31$$

where ρ_{ij} is the correlation between the ℓ -element average winds over layers which are $|i - j| = t$ units apart, with $\ell < t$. Since i and j refer to the midpoints of the ℓ -element "levels," the actual separation between these levels is $t - \ell/2 - \ell/2 = t - \ell$:



Assuming zero means and constant variance σ^2 for the winds in each elemental layer yields

$$\begin{aligned} \rho_{ij} &= E(\bar{x}_{\ell|i} \bar{x}_{\ell|j}) \\ &= \ell^{-2} E \left[(x_1 + \dots + x_{\ell})(x_{t+1} + \dots + x_{t+\ell}) \right] \\ &= \ell^{-2} \left[\ell \rho_t + \sum_{k=1}^{\ell-1} k (\rho_{t+\ell-k} + \rho_{t-\ell+k}) \right] \end{aligned} \quad 3.32$$

If the correlation decrease is linear, (Eq. 3.23), and $t < L$,

$$\begin{aligned} \rho_{ij} &= \ell^{-2} \left[\ell \frac{L-t}{L} + \sum_{k=1}^{\ell-1} k \left(\frac{L-t-\ell+k}{L} + \frac{L-t+\ell-k}{L} \right) \right] \\ &= 1 - t/L \end{aligned} \quad 3.33$$

Introducing this result for ρ_{ij} and that previously found (Eq. 3.23) for $\sigma_{\bar{x}} | \ell$ into Eq. (3.31) yields

$$E(w | \ell < t < L) = \sigma \sqrt{\pi t} \sqrt{L - \ell/3 - 1/3\ell} / L \quad 3.34$$

If $\ell \ll L$, which is likely if $\ell < t < L$, this is approximately $\sigma \sqrt{\pi t/L}$: for a fixed, large correlation distance L , the mean vector wind shear between two "levels" is approximately proportional to the square root of the distance between levels, under all the simplifying assumptions. The actual wind speed difference (not divided by the separation to give shear) would be proportional to the 3/2 power of the separation. The characteristic extreme of wind shear also would be proportional to \sqrt{t} .

3.10 CONCLUSION

Vector wind shear has been shown, in the preceding discussion, to be a complicated variate, with statistical characteristics depending primarily on the statistical behavior of winds in elemental layers and, especially, the correlations between such winds. To derive any useful results, many simplifying assumptions were made: that the mean wind in each elemental layer is zero, that winds in all elemental layers have the same variance, and that the two components in each layer are independent. Under these conditions, vector wind shear has a central circular χ_2 distribution, readily studied. None of these assumptions is actually valid, so that vector wind shear generally has a non-central elliptical χ_2 distribution, which is so complicated that it has been studied very little. However, this distribution can be approximated with a computer, and should be examined to determine how far the results for the artificially simple case apply in practice.

Another simplifying assumption is that the correlation of elemental winds decreases linearly over a fixed correlation distance, beyond which it is zero. While quite unrealistic, this model falls generally between two others which may apply to

winds: the exponential decay and the damped wave. Hence it provides some insight into the effect of correlation on wind shear.

If vector wind shear has a central circular χ_2 distribution, its mean is proportional to the standard deviation of the difference in "observed" wind speed components at the two "levels" between which the shear is computed. This standard deviation, in turn, is the product of the standard deviations of the two wind components at the two levels and $(1 - \rho_t)^{1/2}$, where ρ_t is the correlation between the components.

In general, ρ_t is proportional to $f(t)$, some function of t ; a linear function was assumed in much of the preceding discussion. Hence the mean vector wind shear, \bar{w} , also depends on some other function, $g(t) = (1 - f(t))^{1/2}$. Until the form of $f(t)$ is established, $g(t)$ cannot be defined. It has been approximated, in several studies, by a fractional power: $g(t) = t^\alpha$. If $f(t) = 1 - t/L$, a linear decrease, $g(t) = t^{1/2}$, so $\alpha = 1/2$. If $f(t) = 0$, for complete independence, then $g(t) = 1$ and $\alpha = 0$. The few studies relating vector wind shear to t^α suggest that $0 < \alpha < 1$, with no theoretical basis.

The preceding discussion shows that $g(t) = t^\alpha$ is a crude approximation for the actual behavior of wind shear. However, if such an assumption is made, the magnitude of the exponent α will depend on the rate of which ρ_t decreases: for zero correlation, $\alpha = 0$, for rapid decrease of ρ with t , α must be small; for slow decrease, it must be larger. Obviously, understanding the variation of wind correlation with layer thickness is essential for any discussion of the variation of vector wind shear with layer thickness.

Section 4

OBSERVED RELATIONS BETWEEN WIND SHEAR OVER VARIOUS ALTITUDE INTERVALS

4.1 INTRODUCTION

The 1194 Jimsphere soundings were used to compute the scalar, vector, zonal and meridional layer shears for shear layer thicknesses, Δz , from 50 to 5000 meters. The layer shear in meters/second is equal to the finite difference approximation of the point shear, defined in Section 3, multiplied by Δz . The scalar, zonal, and meridional layer shears may also be defined as the difference in scalar, zonal and meridional wind speeds at two altitudes separated by a distance Δz ; the vector layer shear is the magnitude of the vector difference between the horizontal wind vectors at the altitudes separated by a distance Δz ; thus the various layer shears are all scalar quantities. The following convention is used: The layer shear over the altitude difference $\Delta z = A - B$ ($A > B$) is defined as the layer shear at A . All the results on "shears" to be described in this section and the sections to follow refer to layer shears; therefore, for the sake of brevity the word "shear" is used instead of layer shear.

4.2 MEANS AND VARIANCES OF SHEARS

The estimated climatological mean scalar, vector, zonal and meridional shears for shear layer thickness from 100 through 5000 m are plotted as a function of altitude in Figures 4.1 through 4.4. It is suggested that over certain altitude intervals there is a consistent relationship between mean shear and shear layer thickness. This is particularly noticeable for mean vector and zonal shears at altitudes from 5.5 to 12 km (Figures 4.2 and 4.3) and for mean scalar shears at altitudes from 8 to 12 km (Figure 4.1). The absolute magnitude of the mean meridional shear increases with increasing shear layer thickness but it is evident from Figure 4.4 that the relation between mean shear and thickness is not clearly defined at any altitude or range of altitudes.

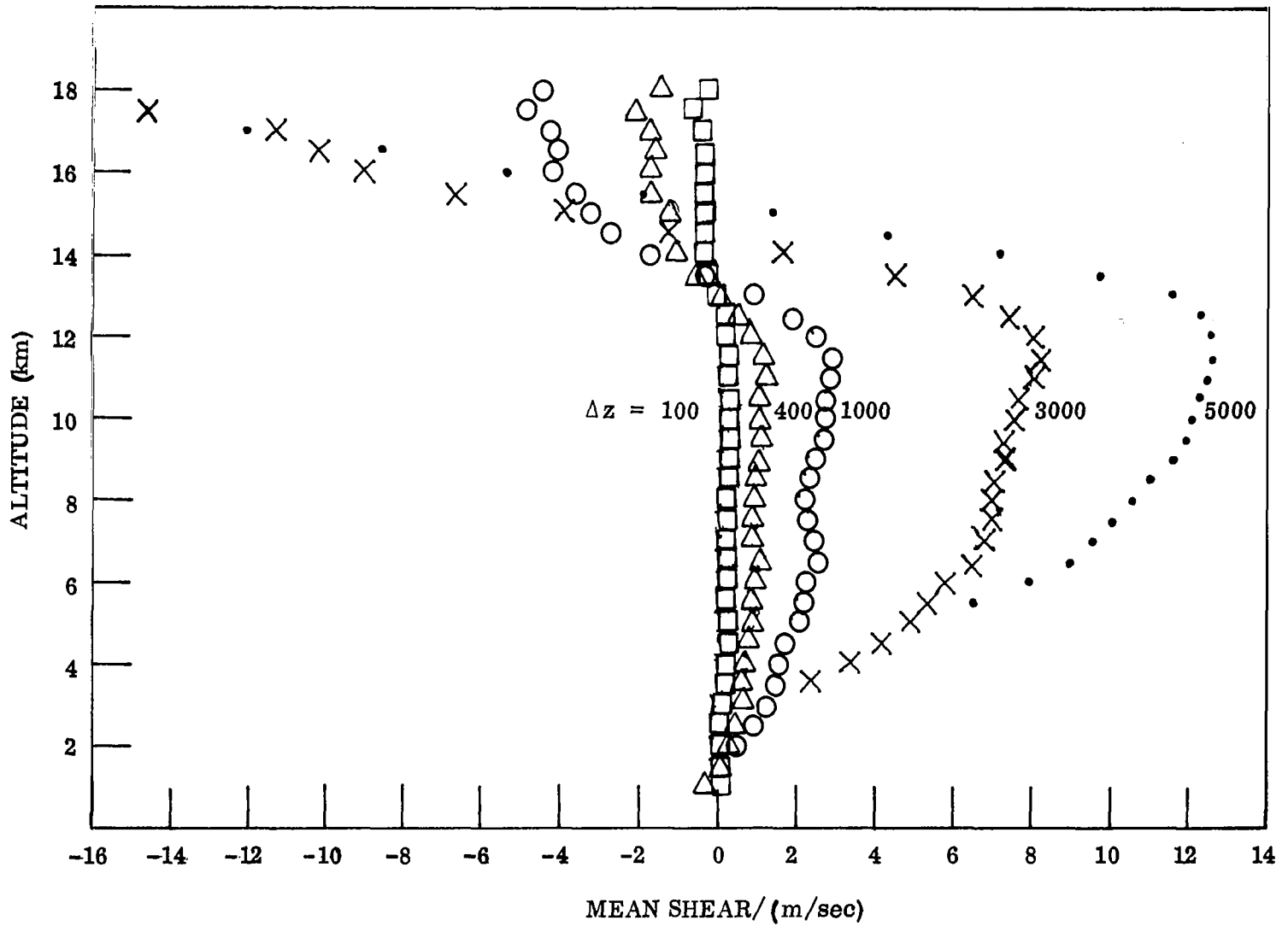


Figure 4.1 Mean Scalar Shear as a Function of Altitude for Various Shear Layer Thicknesses, Δz (m)

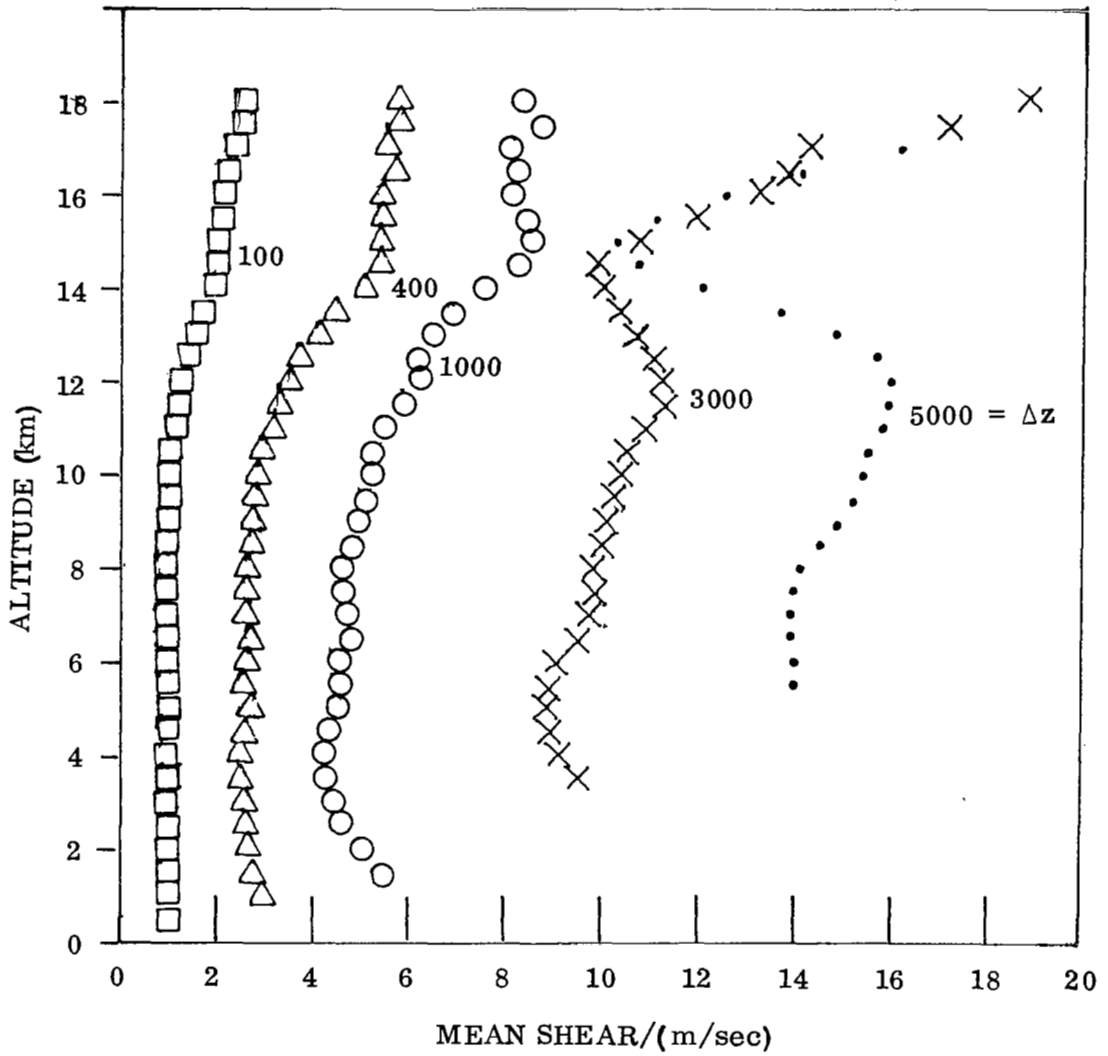


Figure 4.2 Mean Vector Shear as a Function of Altitude for Various Shear Layer Thicknesses, Δz (m)

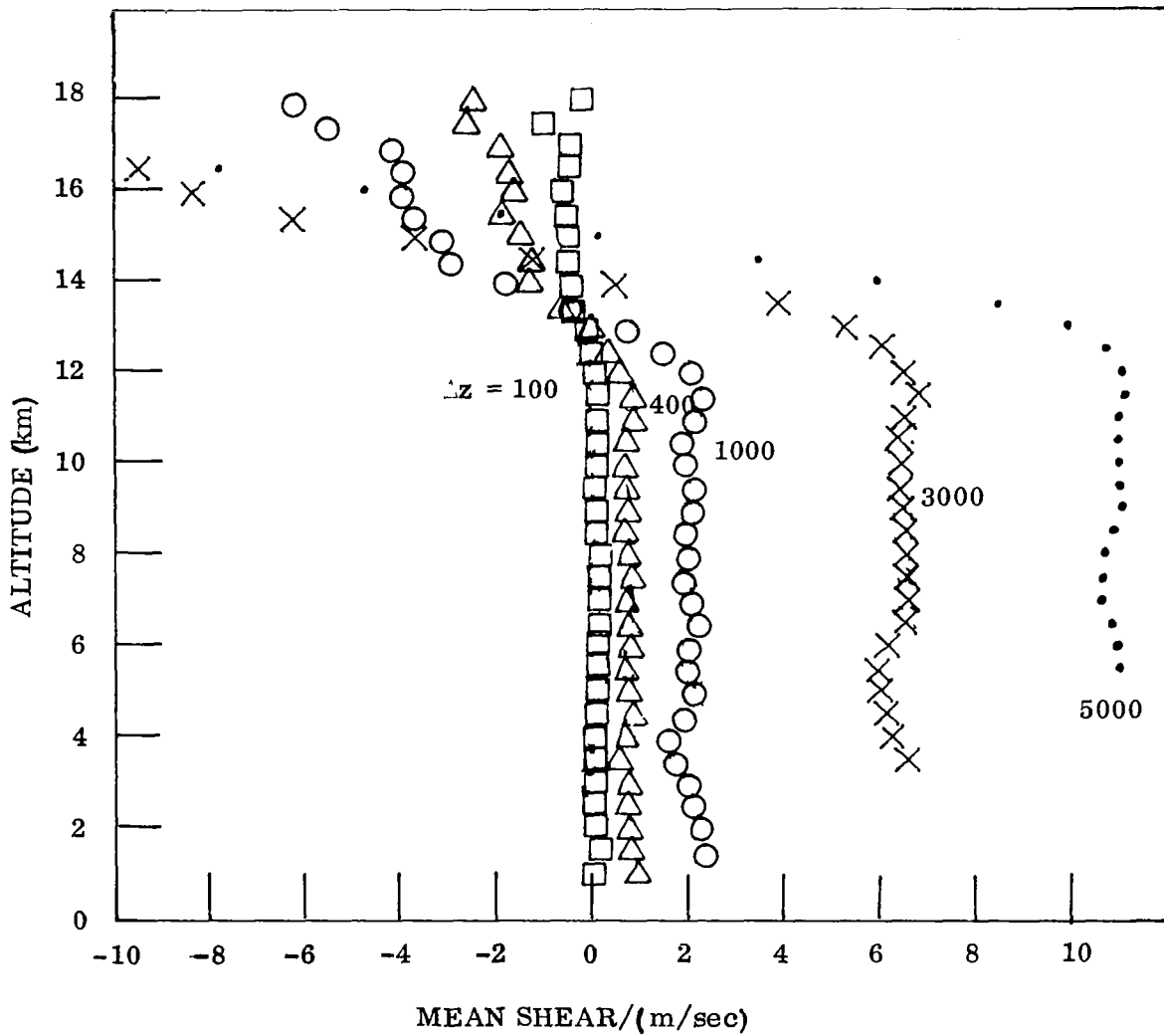


Figure 4.3 Mean Zonal Shear as a Function of Altitude for Various Shear Layer Thicknesses, Δz (m)

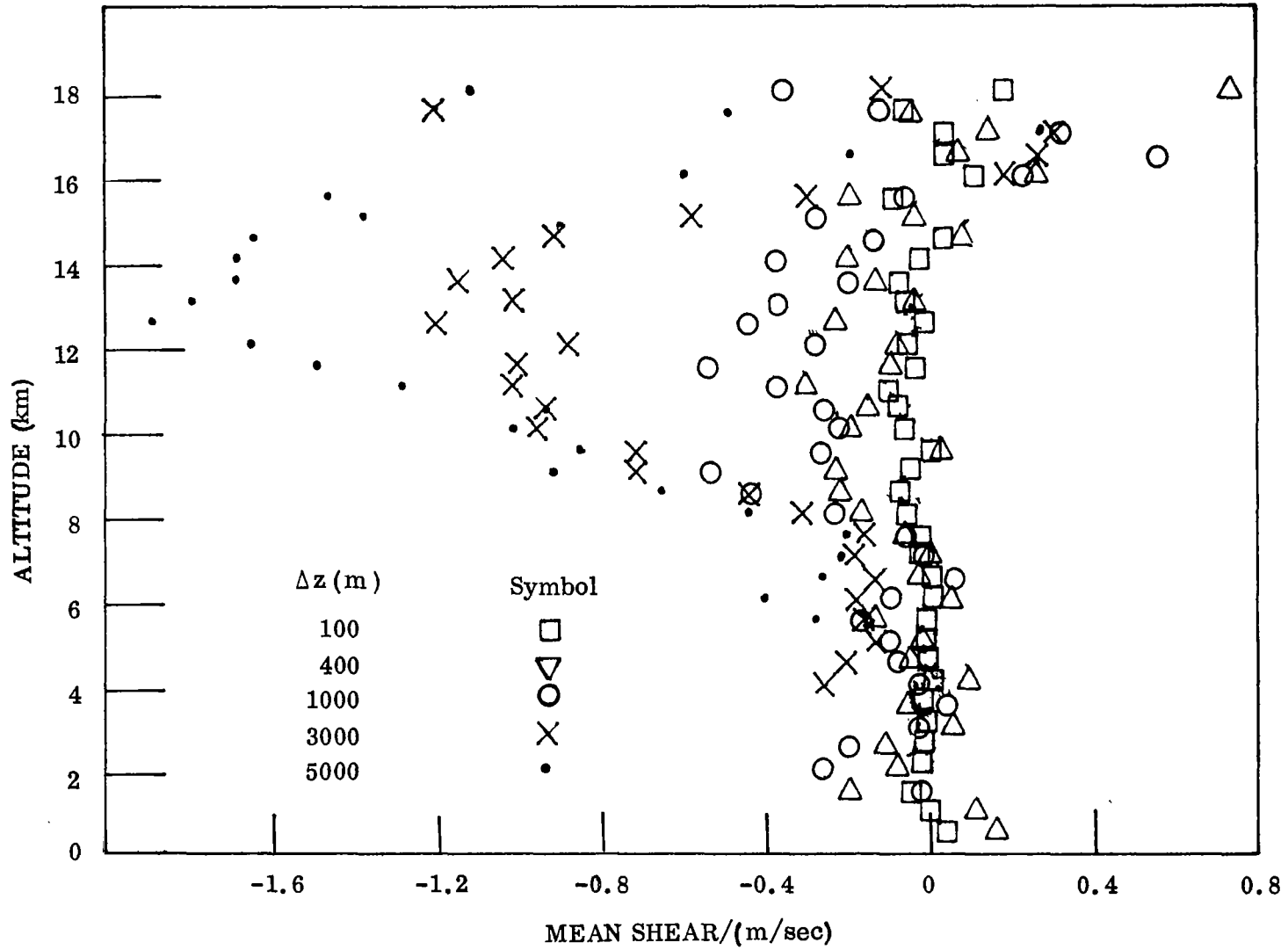


Figure 4.4 Mean Meridional Shear as a Function of Altitude for Various Shear Layer Thicknesses, Δz (m)

The estimated climatological variance of the scalar, vector, zonal, and meridional shears for various shear layer thicknesses are plotted as a function of altitude in Figures 4.5 through 4.8.

4.3 OBSERVED DISTRIBUTION OF ZONAL, MERIDIONAL AND VECTOR SHEARS

The percentile bounds of the empirical distribution of zonal and meridional shears at 1, 4, 7, 10, 13, and 16 km for shear layer thicknesses of 50, 100, 400, 1000, 3000 and 5000 m are given in Figures 4.9 through 4.14; the percentile bounds for vector shears at 12 km for the same shear layer thicknesses are given in Figure 4.15.

Since the zonal and meridional winds are approximately normal (as shown in Section 2) and since the difference of two normal distributions is also a normal distribution, it follows that the zonal and meridional shears should also be normal. The straight lines of Figures 4.9 through 4.14 represent normal distributions for the zonal and meridional shears; the plotted points are the observed distributions. These results strongly support the conclusion that this particular distribution of Jimsphere zonal and meridional winds is normal from 1 to 16 km for the 2.5 through 97.5 percentile bounds. Although there are specific cases when there is good agreement between the shears of the theoretical normal distribution and the observed distribution for percentiles greater than 97.5 and less than 2.5 (for example, the zonal 3000 m shears at 16 km deviate little from the normal distribution at all percentiles, Figure 4.13), the observed shears for these percentiles generally show a deviation from normality which increases as the percentile becomes more extreme. The observed distribution of vector shears shown in Figure 4.15 differs considerably from the distributions discussed above. Theoretically there is no justification for comparison of this distribution with a normal distribution; this is verified by these results.

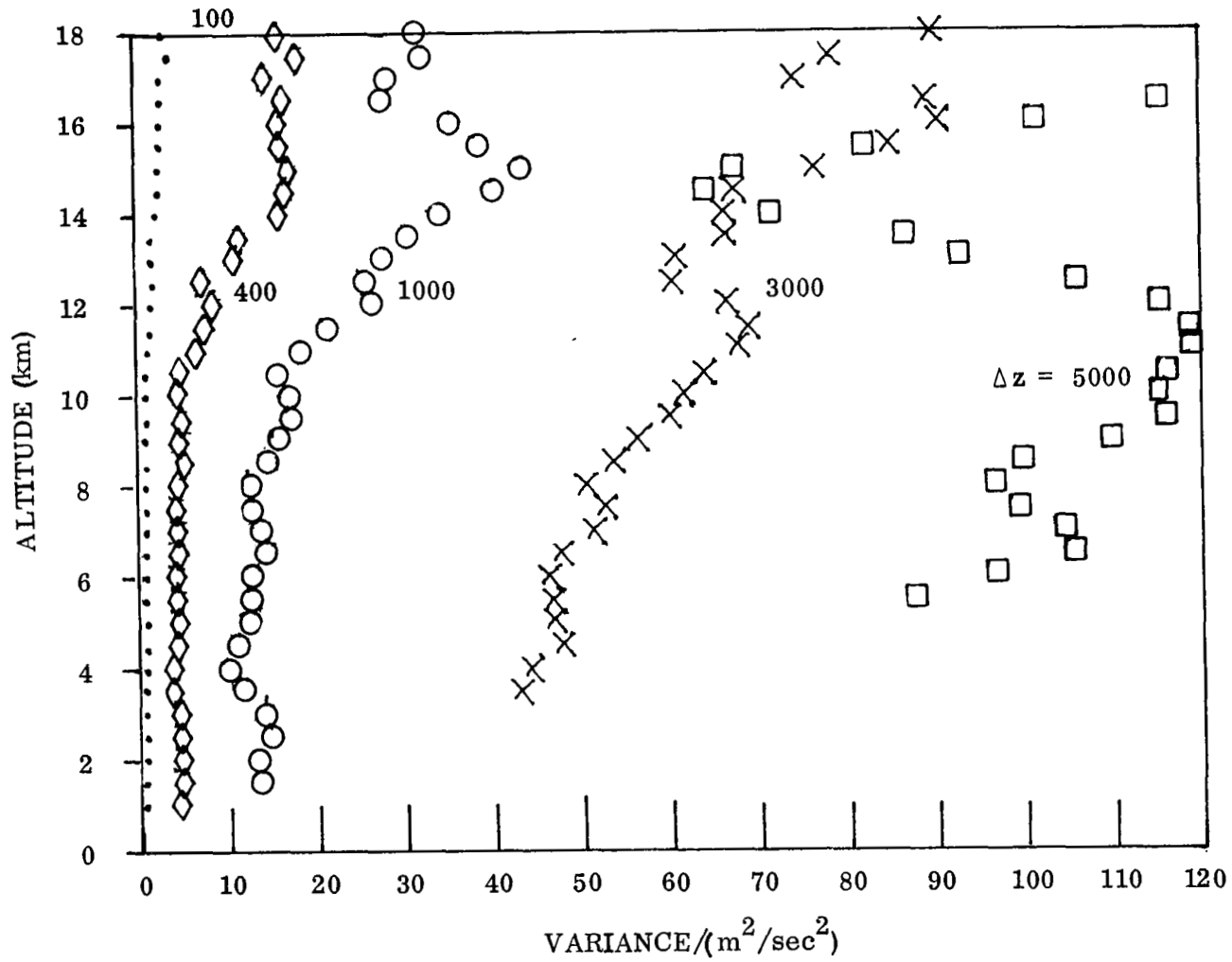


Figure 4.5 Variance of Scalar Shear as a Function of Altitude for Various Shear Layer Thicknesses, Δz (m)

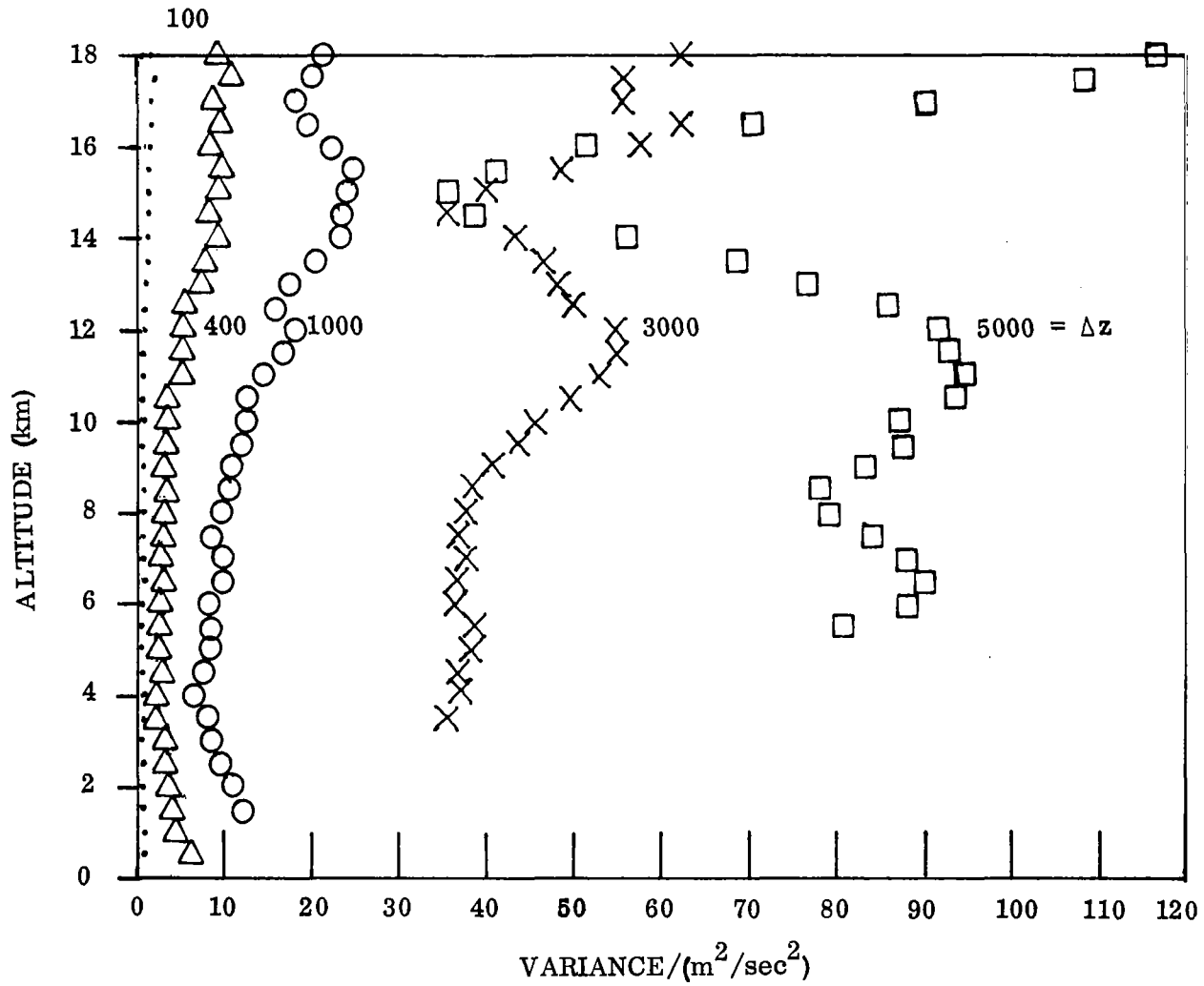


Figure 4.6 Variance of Vector Shear as a Function of Altitude for Various Shear Layer Thicknesses, Δz (m)

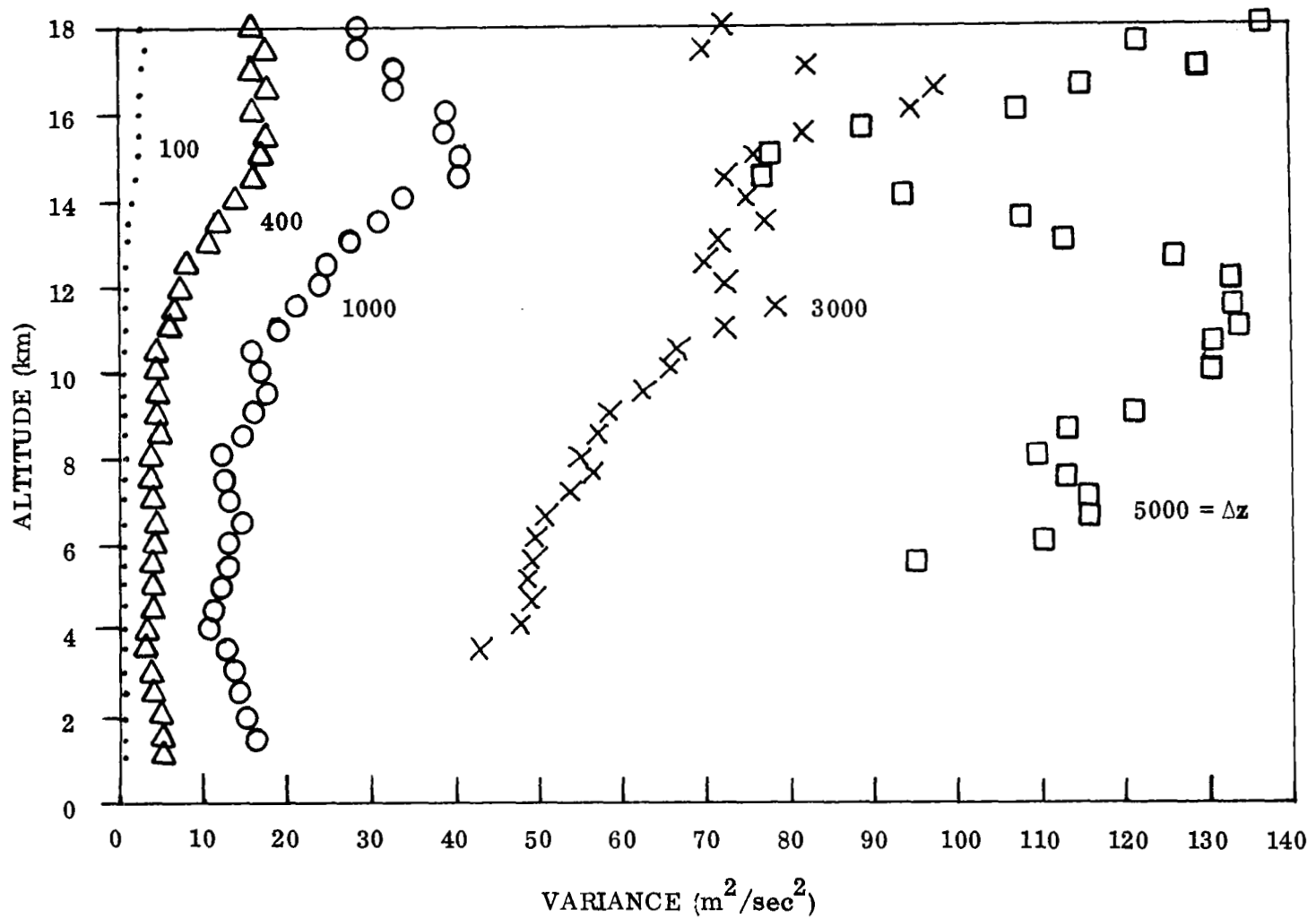


Figure 4.7 Variance of Zonal Shear as a Function of Altitude for Various Shear Layer Thicknesses, Δz (m)

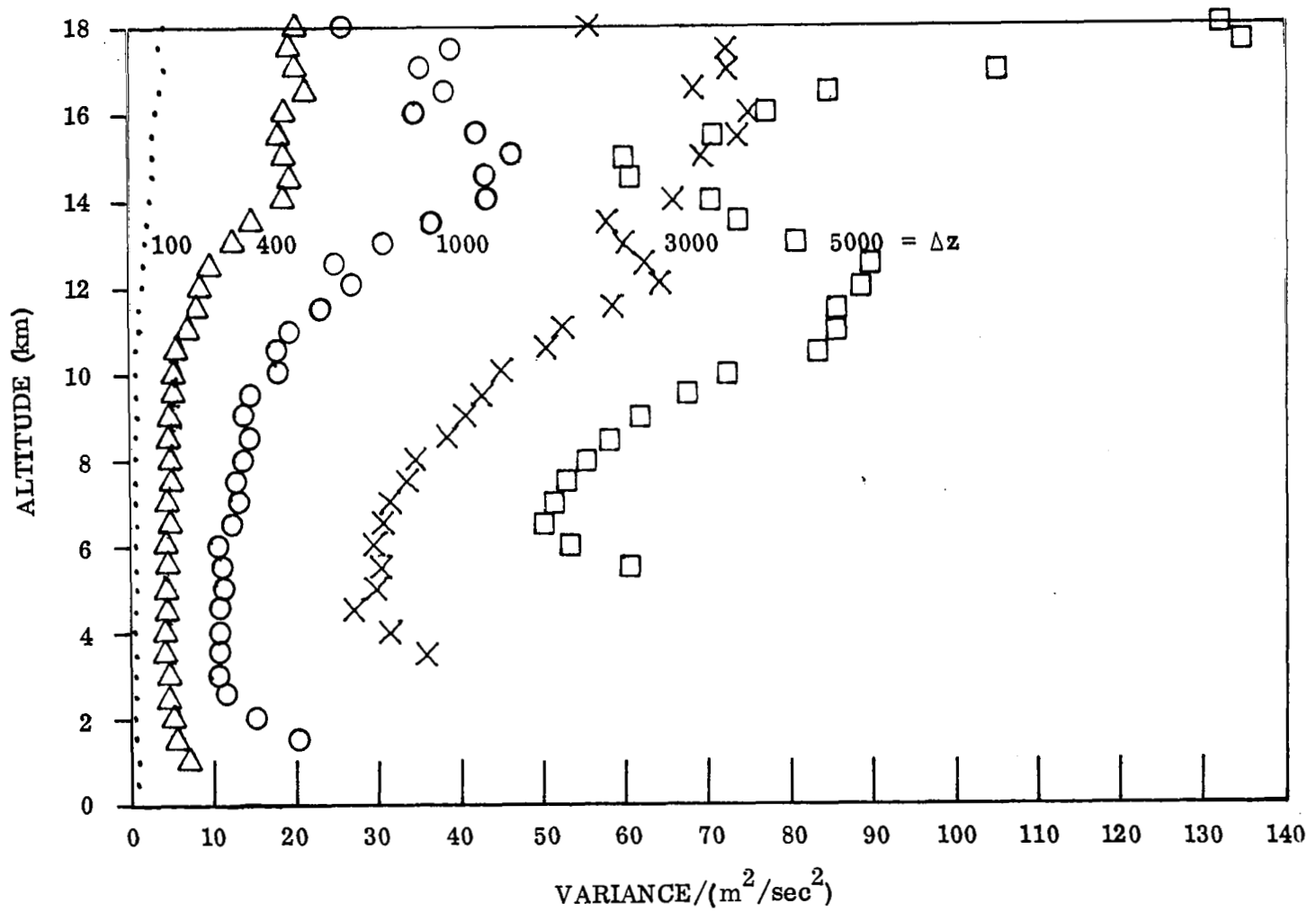


Figure 4.8 Variance of Meridional Shear as a Function of Altitude for Various Shear Layer Thicknesses, Δz (m)

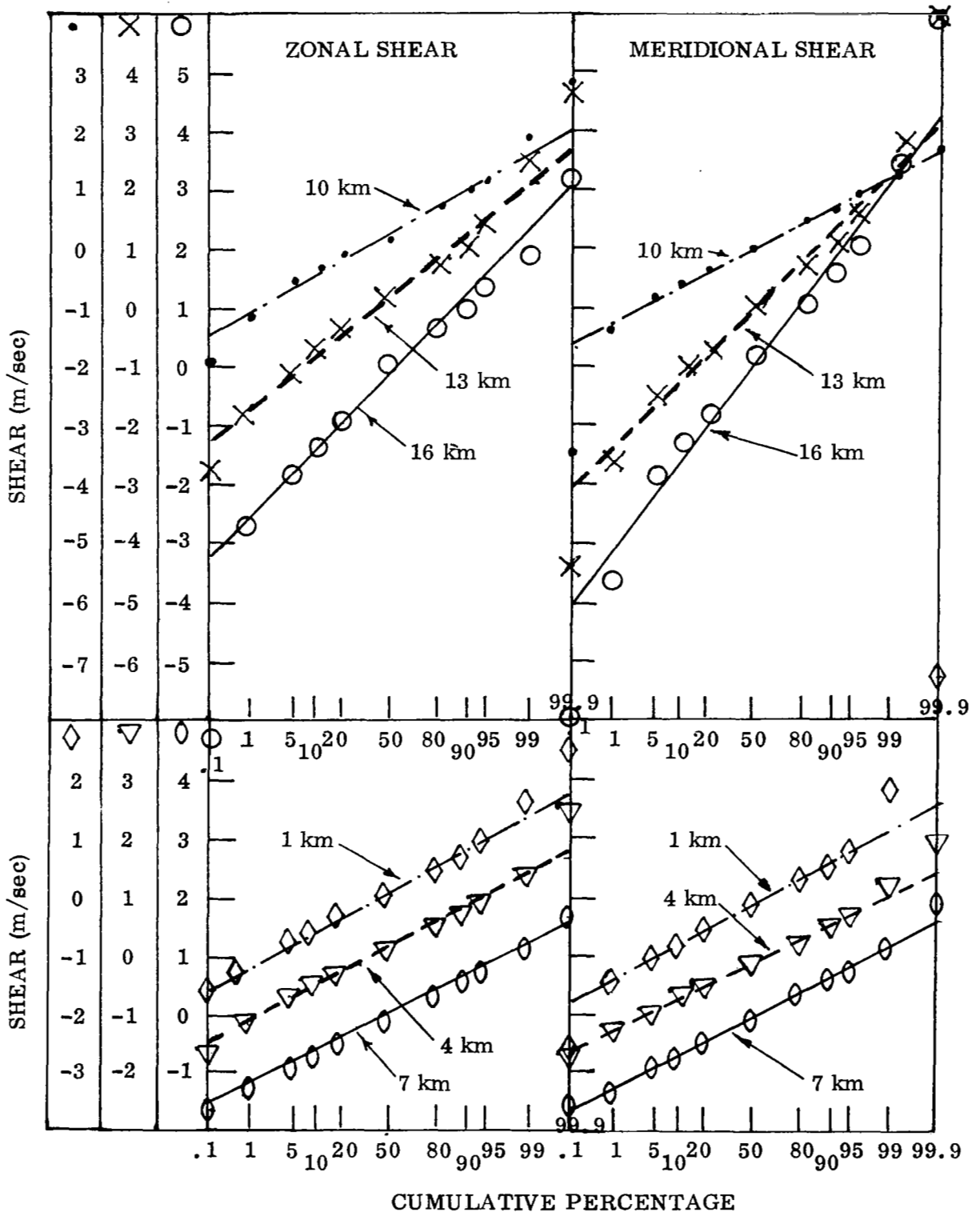


Figure 4.9 Observed and Normal Distribution of 50 m Zonal and Meridional Shears

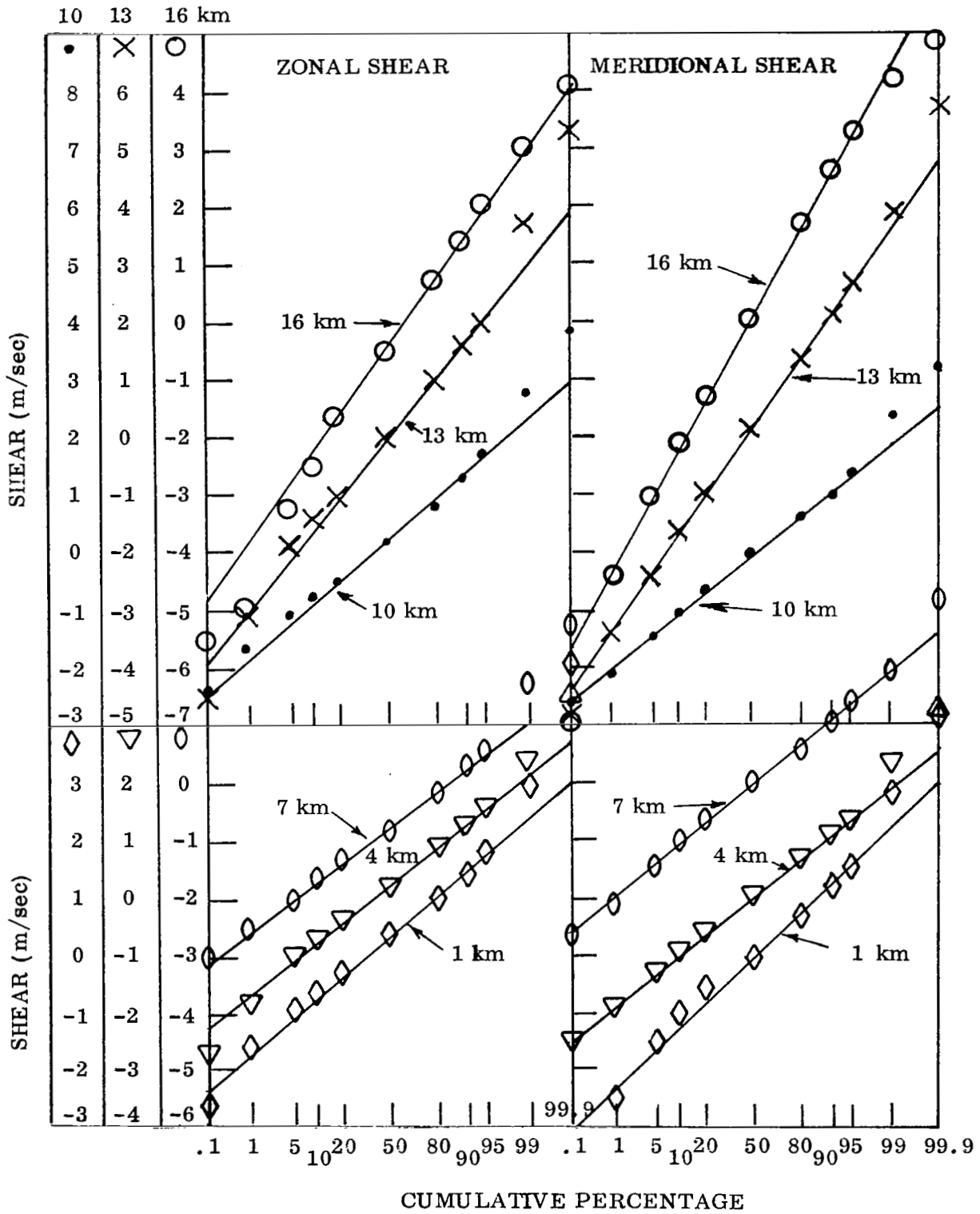


Figure 4.10 Observed and Normal Distribution of 100 m Zonal and Meridional Shears

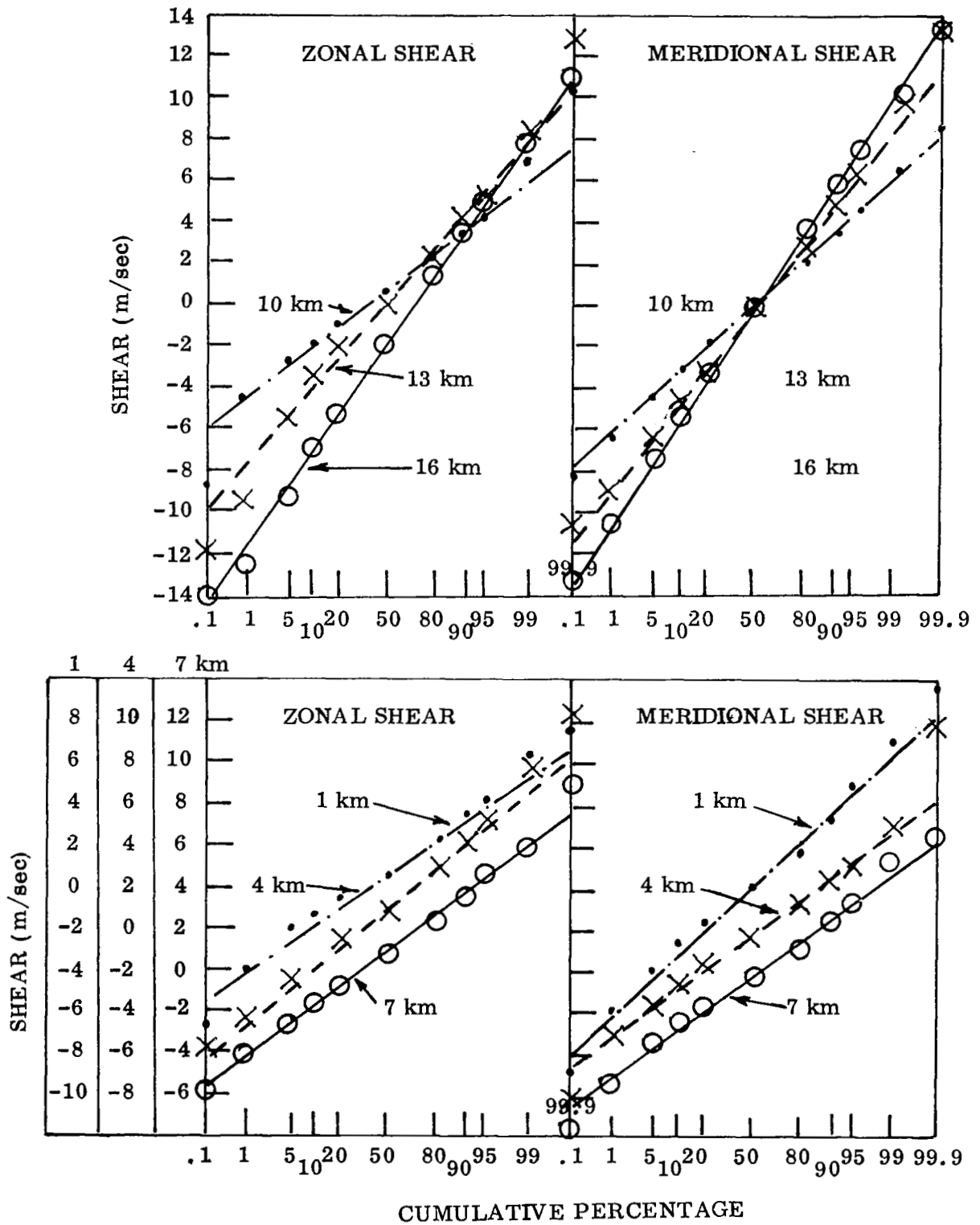


Figure 4.11 Observed and Normal Distribution of 400 m Zonal and Meridional Shears

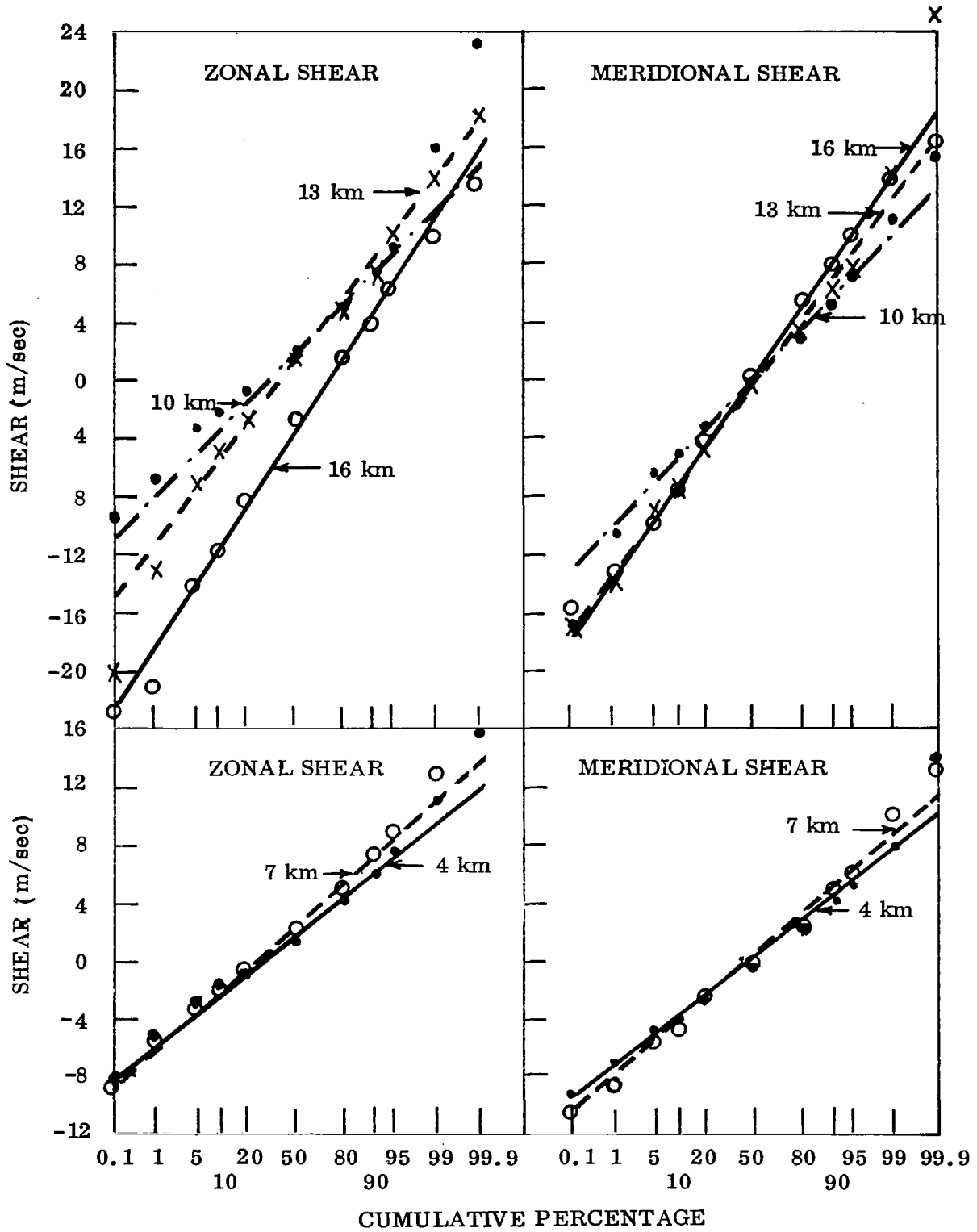


Figure 4.12 Observed and Normal Distribution of 1000 m Zonal and Meridional Shears

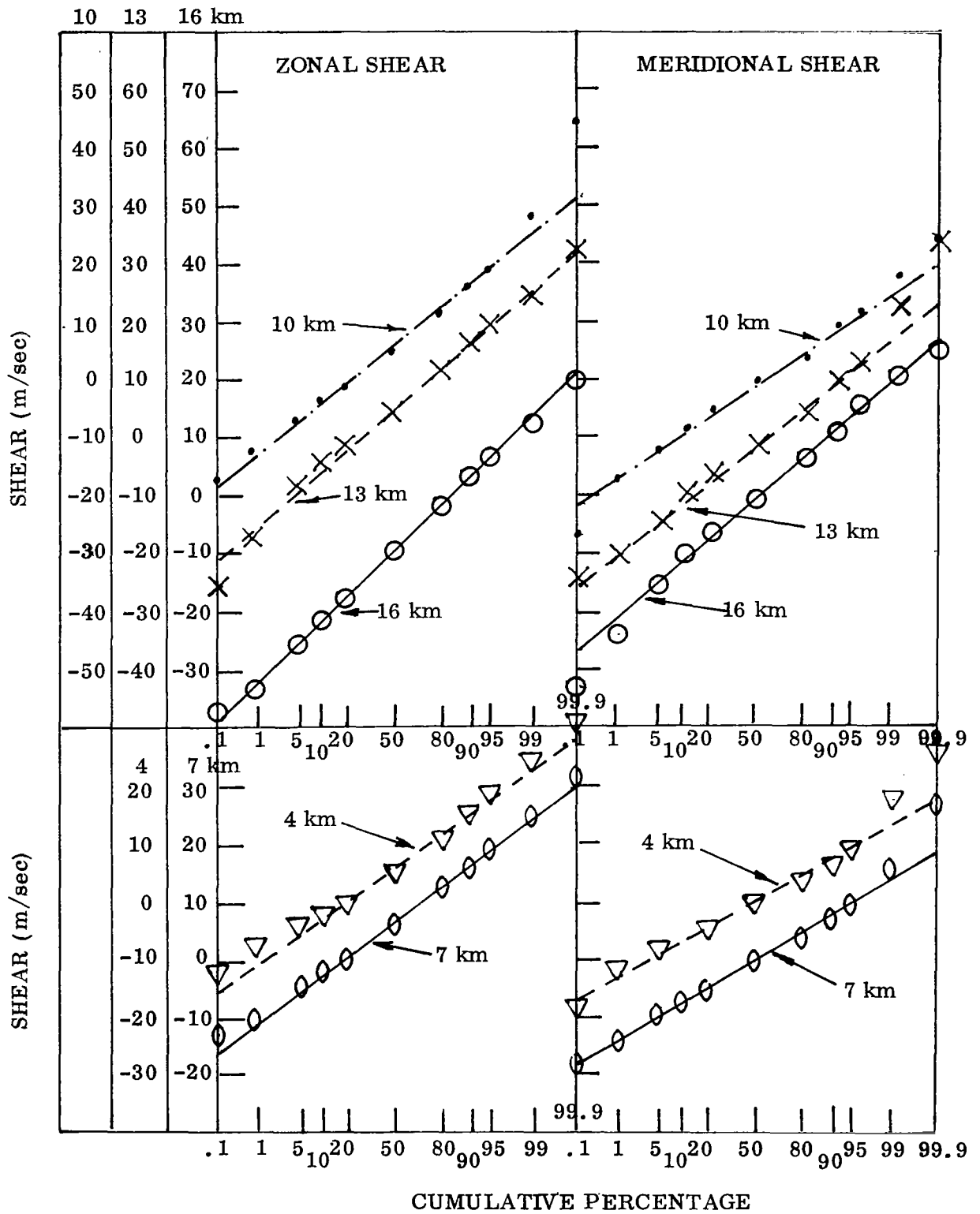


Figure 4.13 Observed and Normal Distribution of 3000 m Zonal and Meridional Shears

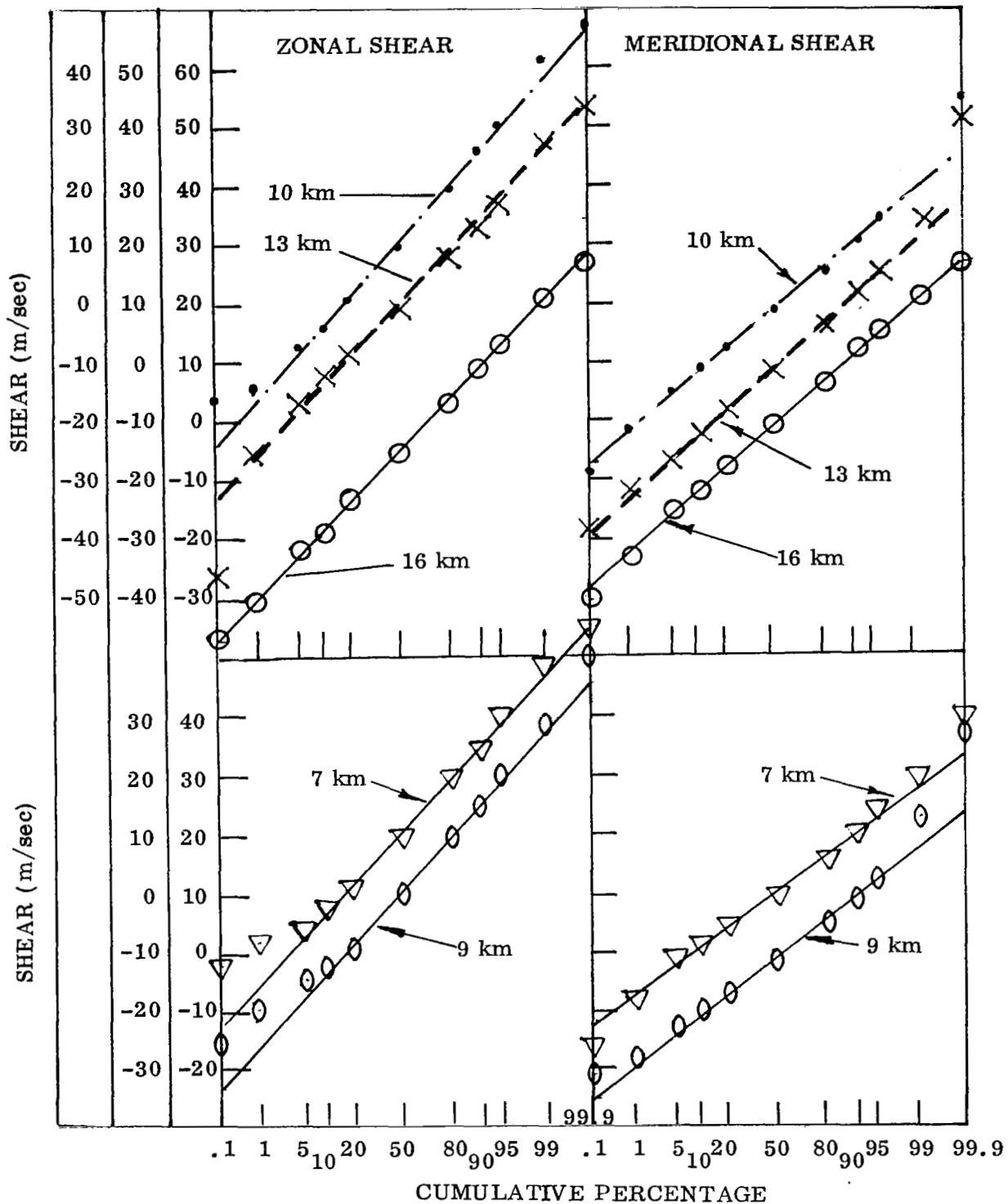


Figure 4.14 Observed and Normal Distribution of 5000 m Zonal and Meridional Shears

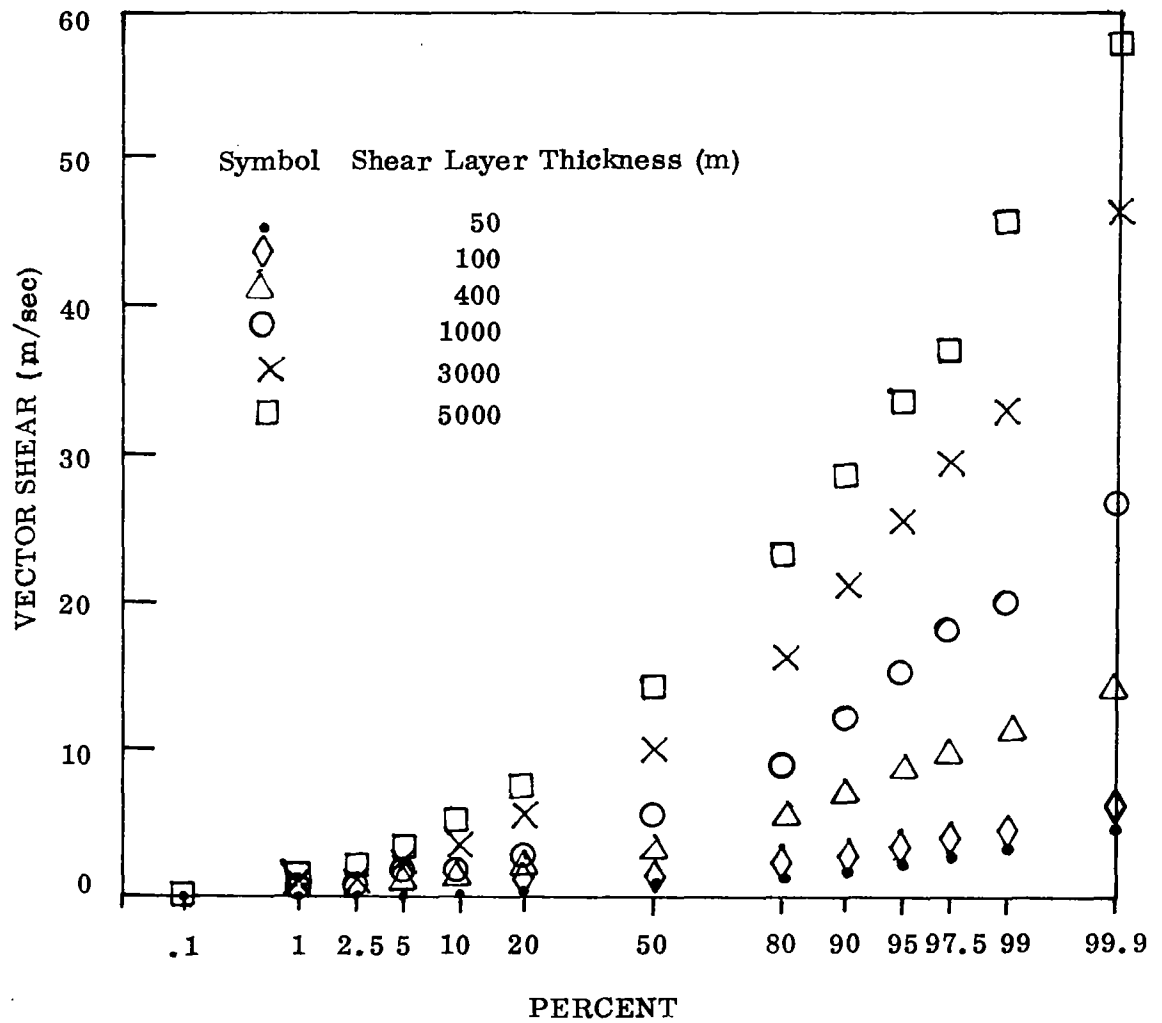


Figure 4.15 The Cumulative Distribution of Vector Shears at 12 km For Shear Layer Thicknesses of 50, 100, 400, 1000, 3000, and 5000 Meters

4.4 MEAN, STANDARD DEVIATION, AND EXTREME SHEAR AS A FUNCTION OF SHEAR LAYER THICKNESS

The means of the scalar, vector, zonal, and meridional shears at 8, 12, and 16 km are plotted in Figure 4.16 as a function of shear layer thickness, Δz in meters. It is shown that the mean magnitude of the vector shear, \bar{w} in m/sec, is a function of Δz , of the form

$$\bar{w} = C (\Delta z)^{2/3}, \quad 4.1$$

where C is a constant equal to 0.047 at 8 km, 0.062 at 12 km, and 0.10 at 16 km. Essenwanger (Ref. 6) found that the mean vector shear at Cape Kennedy during August could also be expressed by a similar relation but with a power of 0.44; similarly, Armendariz and Rider (Ref. 3) obtained a power of 0.38 for data obtained at White Sands Missile Range with a smooth 100 gm balloon during September 1964. In a comparative study of simultaneous wind profiles Rider and Armendariz (1968) used the data from a smooth 100 gm spherical balloon and a Jimsphere balloon. They found that the average vector shears for the Jimsphere data follow Eq. (4.1) with $C = 0.04$, whereas the data for the smooth balloon fit the relation,

$$\bar{w} = 0.15 (\Delta z)^{0.41}; \quad 4.2$$

Rider and Armendariz conclude that the relation obtained with the smooth balloon is relatively inaccurate because of erratic balloon motion due to aerodynamic instability. The average vector shears for the investigations cited above were obtained by averaging the shears determined at various elevations of a particular sounding. In contrast, for this study of Jimsphere winds, the averages are time averages computed at a particular altitude for all the available Jimsphere wind profiles. These results support the conclusion that a general power law relation of the form of Eq. (4.1) exists at Cape Kennedy and White Sands. This does not seem to be affected by the different averaging techniques used.

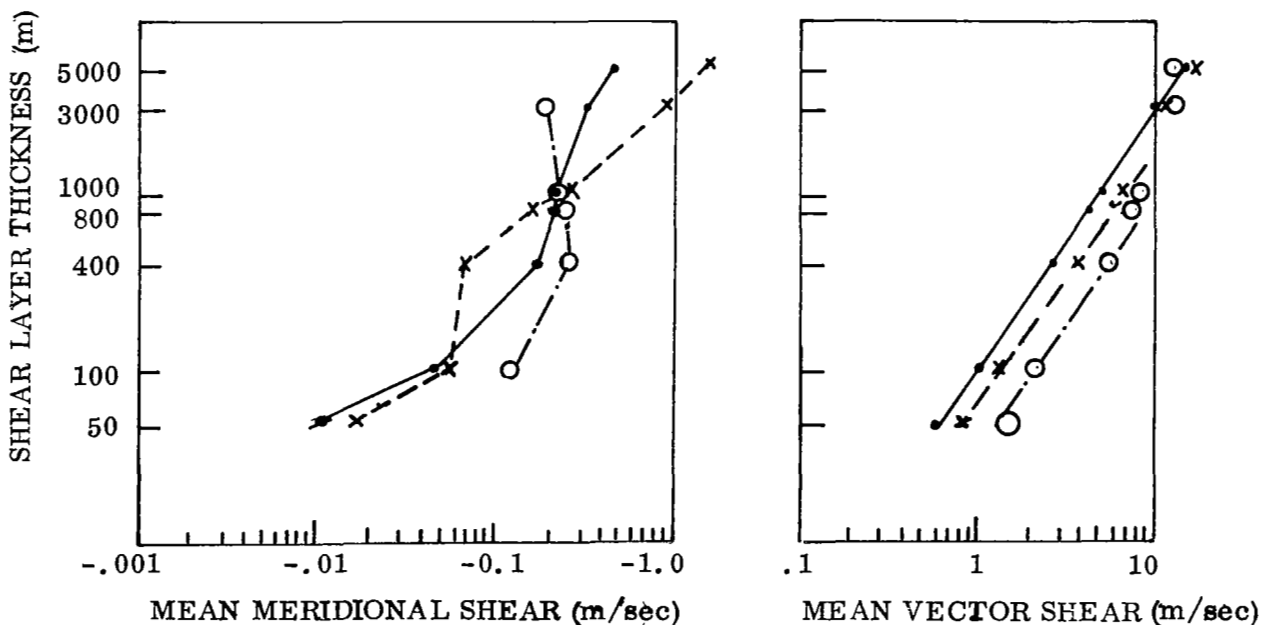
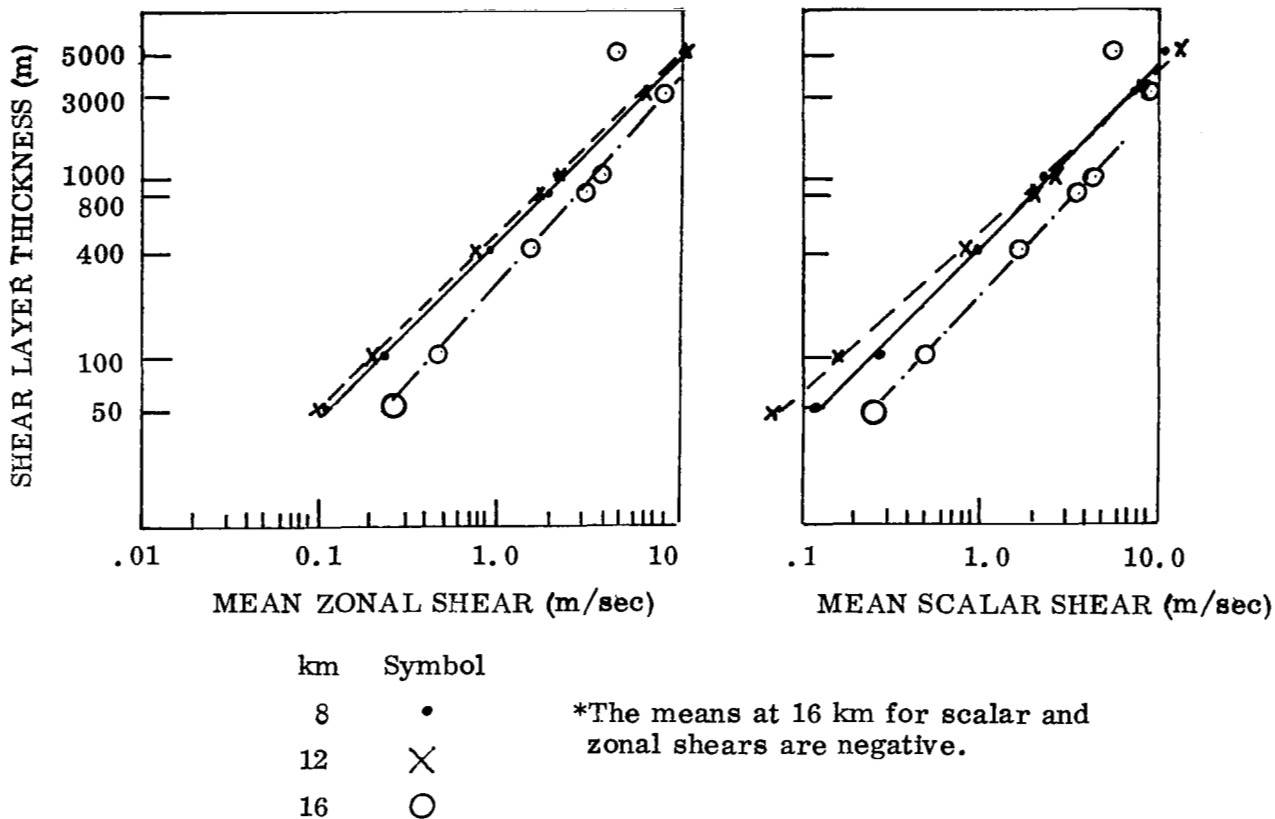


Figure 4.16 The Mean Zonal, Meridional, Scalar and Vector Shear at 8, 12, and 16 km, as a Function of Shear Layer Thickness

The mean zonal shear, \bar{w}_x , at 8 and 12 km and the mean scalar shear, \bar{w}_s , at 8 km are linearly related to Δz , such that

$$\bar{w}_x = \bar{w}_s = 0.0025 (\Delta z) \quad 4.3$$

The mean scalar shears at 12 km fit Eq. (4.3) for Δz greater than 400 meters; for Δz less than 400 meters, the observed mean scalar shear is significantly less than that given by Eq. (4.3). The mean zonal and scalar shears at 16 km are negative; they may be represented roughly for shear layer thicknesses from 50 to 1000 m by the function

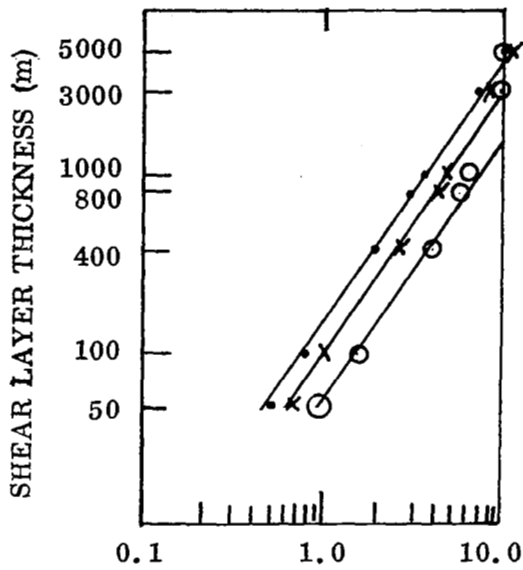
$$\bar{w}_x = \bar{w}_s = - 0.0055 \Delta z ; \quad 4.4$$

for shear layer thicknesses greater than 1000 m, these shears are significantly smaller than those given by Eq. (4.4). The rather irregular behavior of the mean meridional shear leads to the conclusion that it cannot be expressed by a power of Δz , or alternatively the behavior of the mean meridional shear when it is near zero may be beyond the observational capability of the Jimsphere.

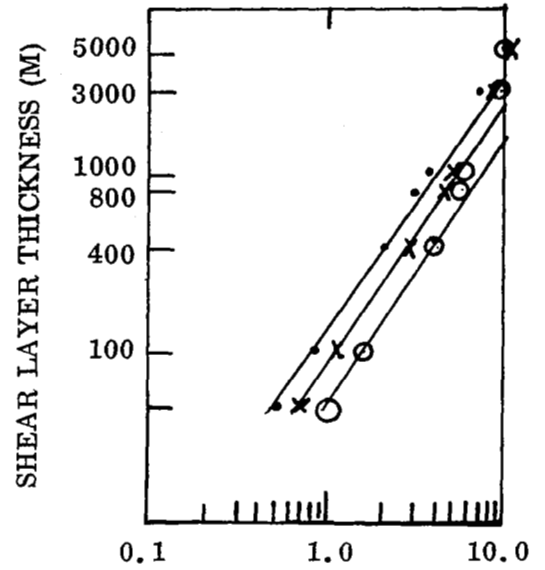
The standard deviations of scalar, vector, zonal, and meridional shears at 8, 12, and 16 km are plotted in Figure 4.17, as a function of shear layer thickness Δz . With minor exceptions, these results support the conclusion that the standard deviation of scalar, vector, zonal and meridional shears for shear layer thicknesses from 50 to 1000 m are given by the following general relation

$$\sigma = D (\Delta z)^{2/3} \quad 4.5$$

where σ is the standard deviation of shear in m/sec and D is a constant for a particular shear type at a particular altitude. The values of D are given in Table 4.1. A value for D for the standard deviation of meridional shear at 16 km is not given because the data seem to follow the relation

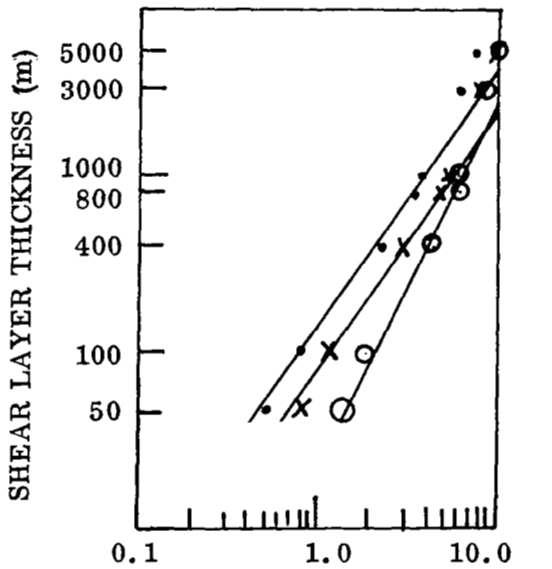


STANDARD DEVIATION OF ZONAL SHEAR (m/sec)

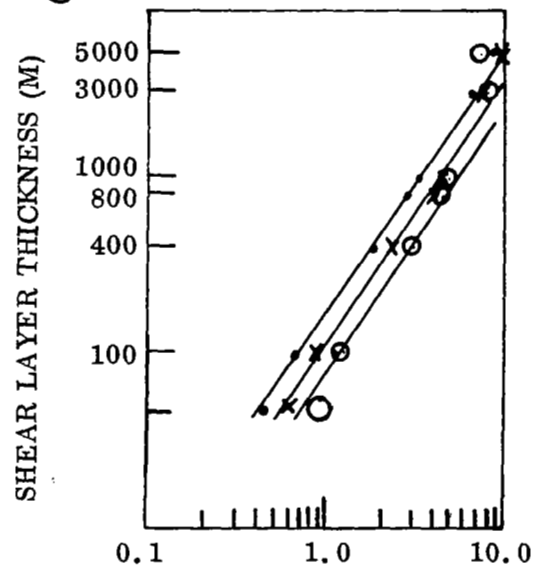


STANDARD DEVIATION OF SCALAR SHEAR (m/sec)

km	Symbol
8	•
12	×
16	○



STANDARD DEVIATION OF MERIDIONAL SHEAR (m/sec)



STANDARD DEVIATION OF VECTOR SHEAR (m/sec)

Figure 4.17 Standard Deviation of Zonal, Meridional, Scalar, and Vector Shears as a Function of Shear Layer Thickness at 8, 12, and 16 km

$$\sigma = 0.23 (\Delta z)^{0.48} . \quad 4.6$$

TABLE 4.1

THE VALUE OF THE CONSTANT D OF EQUATION 4.5

ALTITUDE (km)	8	12	16
Shear Type			
Scalar	0.036	0.052	0.077
Vector	0.036	0.045	0.055
Zonal	0.036	0.050	0.075
Meridional	0.036	0.062	-

The 95% and 99% zonal, meridional, and vector shears at 12 km are plotted in Figure 4.18 as a function of shear layer thickness, Δz . The relation that best fits the data for the 95% meridional and vector shears for Δz from 50 to 1000 m is

$$w/95 = w_y/95 = G(\Delta z)^{2/3} \quad 4.7$$

where G is .085 for meridional shears and .15 for vector shears. For Δz greater than 1000 m this relation overestimates the 95% shears. The 99% vector shears for Δz from 50 to 1000 m may be described by

$$w/99 = 0.21 (\Delta z)^{2/3} , \quad 4.8$$

whereas the 99% zonal and meridional shears deviate rather widely from a power law relation.

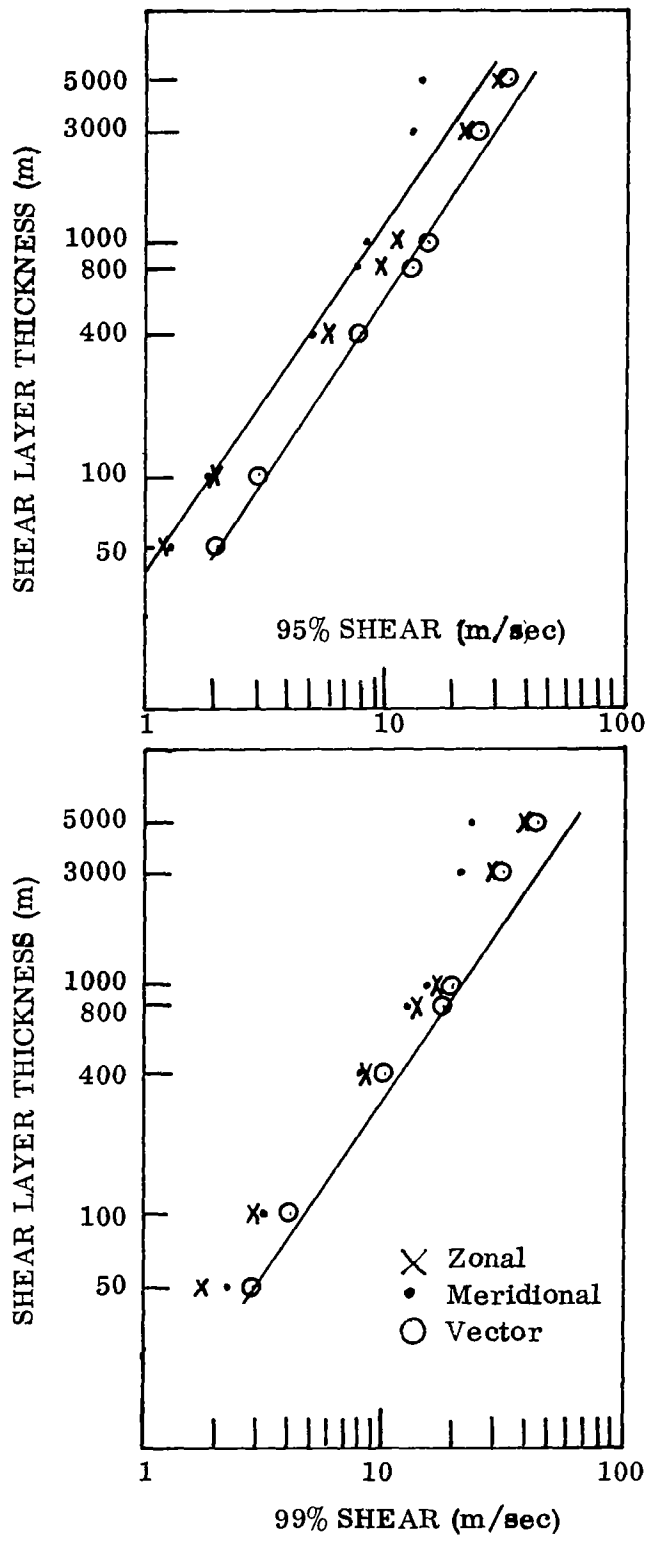


Figure 4.18 95% and 99% Zonal, Meridional, and Vector Shears at 12 km as a Function of Shear Layer Thickness

The rather large deviation of the 95% zonal shear from the power law relation described above may be explained in the following way. If it is assumed that the zonal shears are normally distributed (this is supported by the results of Part D), then it follows that the Pth percentile zonal shears are given by

$$w_x/P = \bar{w}_x + n\sigma \quad 4.9$$

where n is the number of standard deviations from the mean of the Pth percentile zonal shear. For zonal shears at 12 km from Eq. 4.5 and Table 4.1 \bar{w}_x and σ are

$$\begin{aligned} \bar{w}_x &= 0.0025 \Delta z \\ \sigma &= 0.0500 (\Delta z)^{2/3} \end{aligned} \quad 4.10$$

Therefore, the 95% ($n = 1.645$) zonal shear at 12 km is given by

$$\bar{w}_x/95 = 0.0025 \Delta z + 0.082 (\Delta z)^{2/3} \quad 4.11$$

This function is plotted in Figure 4.19; it is shown that the observed 95% zonal shears (indicated by the crosses) for shear layer thicknesses of 50 to 5000 m are in agreement with those predicted by Eq. (4.11).

4.5 CORRELATION OF SHEARS

The linear correlation coefficient (defined in Section 3.6) was computed for adjacent pairs of scalar, vector, zonal, and meridional shears over non-overlapping intervals of 50, 100, 400, and 1000 m at and immediately below 10, 12, and 14 km. As shown in Figure 4.20, the 100 m shears have the highest correlation (with a single exception the correlation for 50 m vector shear near 14 km exceeds the

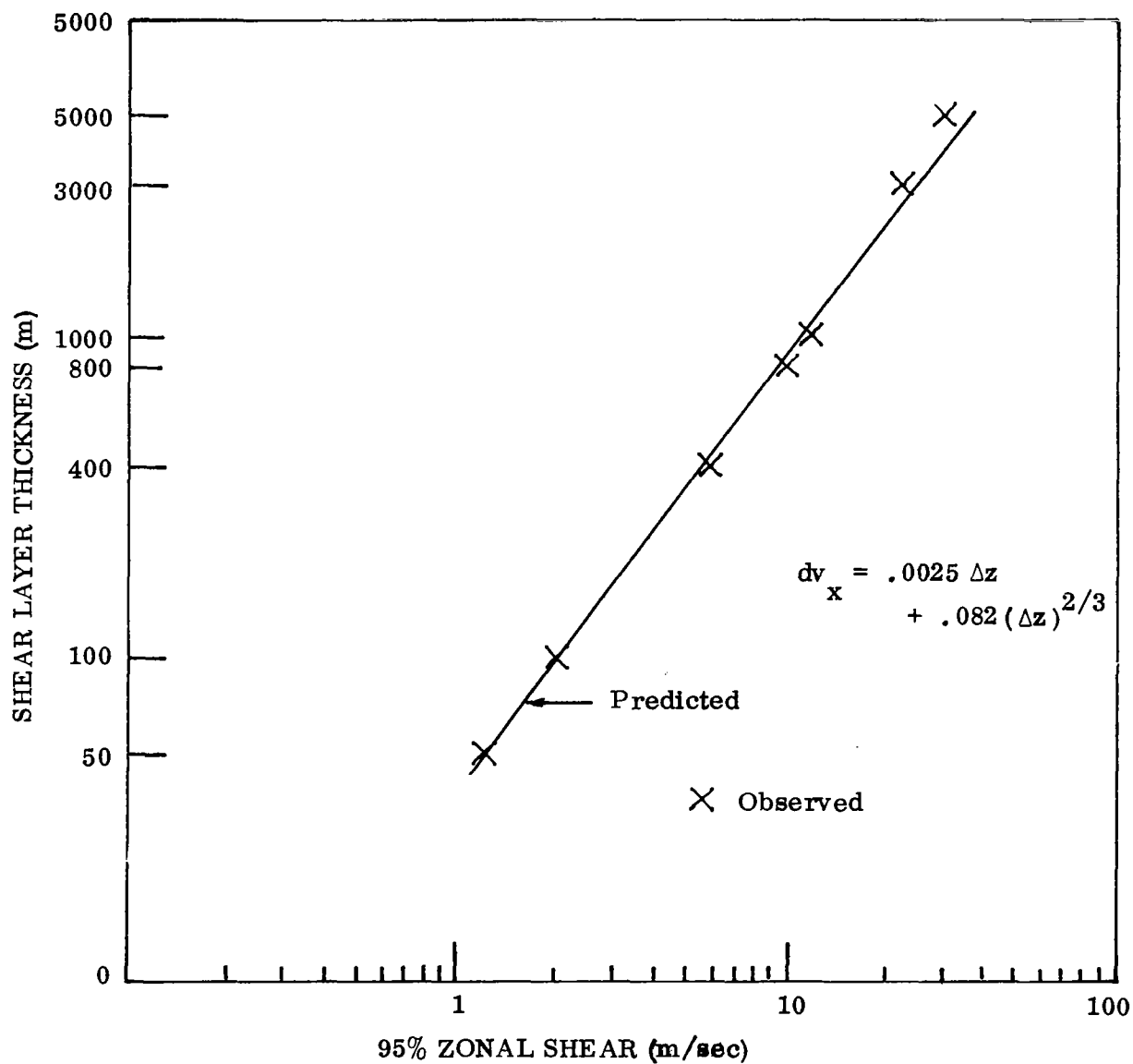


Figure 4.19 Comparison of Observed and Predicted 95% Zonal Shear at 12 km as a Function of Shear Layer Thickness

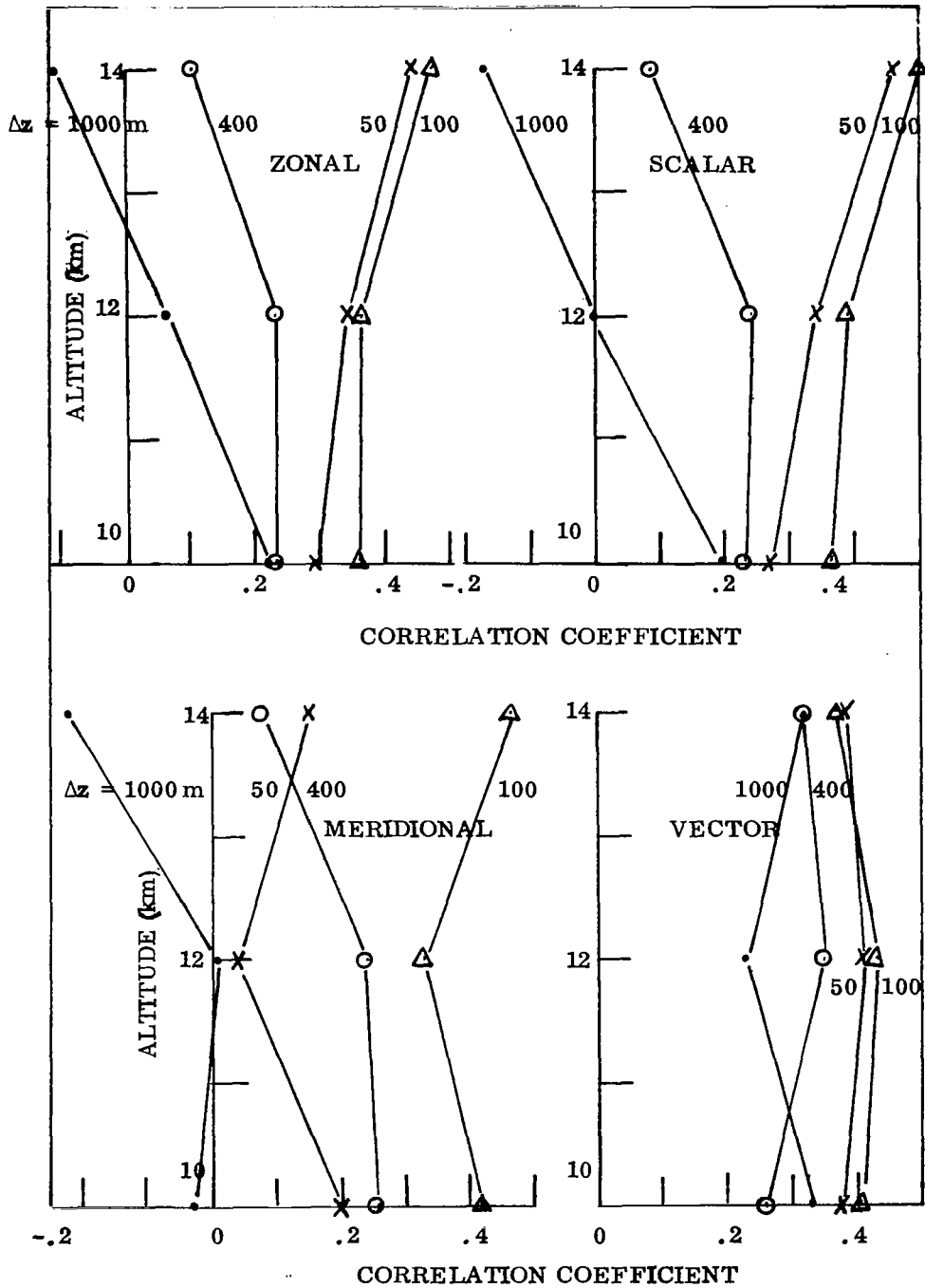


Figure 4.20 Correlation of Adjacent Pairs of Scalar, Vector, Zonal, and Meridional Shears Over Non-Overlapping Intervals (Δz) of 50, 100, 400, and 1000 Meters at and Immediately Below 10, 12, and 14 km

correlation for 100 m shears) ; on the average the correlation between 100 m shears is 0.4. The variation of the correlation of vector shear for the various altitudes and shear layer thicknesses is significantly less than the variation of the correlation for the other shear types. The 1000 m zonal, scalar, and meridional shears have a correlation near zero at 12 km; the correlation of 1000 m vector shears is significantly larger at all altitudes.

The linear correlation between 50 m vector shears and overlapping 100, 400, 800, 1000, 3000, and 5000 m vector shears at 12 km are plotted in Figure 4.21. The correlation decreases steadily from a value of .66 for overlapping 50 and 100 m vector shears to a minimum of .14 for overlapping 50 and 3000 m shears; the correlation increases somewhat to .18 for overlapping 50 and 5000 m shears.

These results support the conclusion that the relations between overlapping or non-overlapping shears for the various altitudes and shear layer thicknesses considered cannot be accurately described with linear equations.

The linear correlation between zonal and meridional shears for shear layer thicknesses of 50, 400, 1000, 3000 and 5000 meters are plotted in Figure 4.22. A rather low correlation between zonal and meridional shear is indicated. There is a tendency for the correlation to increase with increasing shear layer thickness but this may be of minor significance since the maximum correlation is only .31 for the 5000 m shears at 11 km; for shear layer thicknesses of 1000 m or less the maximum correlation is less than $\pm .07$. These results support the conclusion that zonal and meridional shears are not linearly dependent.

The coefficient of multiple correlation, $R_{x/yz}$ between the dependent variable, X, and the independent variables, Y and Z, is given by

$$R_{x/yz} = \sqrt{\frac{\rho_{xy}^2 + \rho_{xz}^2 - 2\rho_{xy}\rho_{xz}\rho_{yz}}{1 - \rho_{yz}^2}} \quad 4.12$$

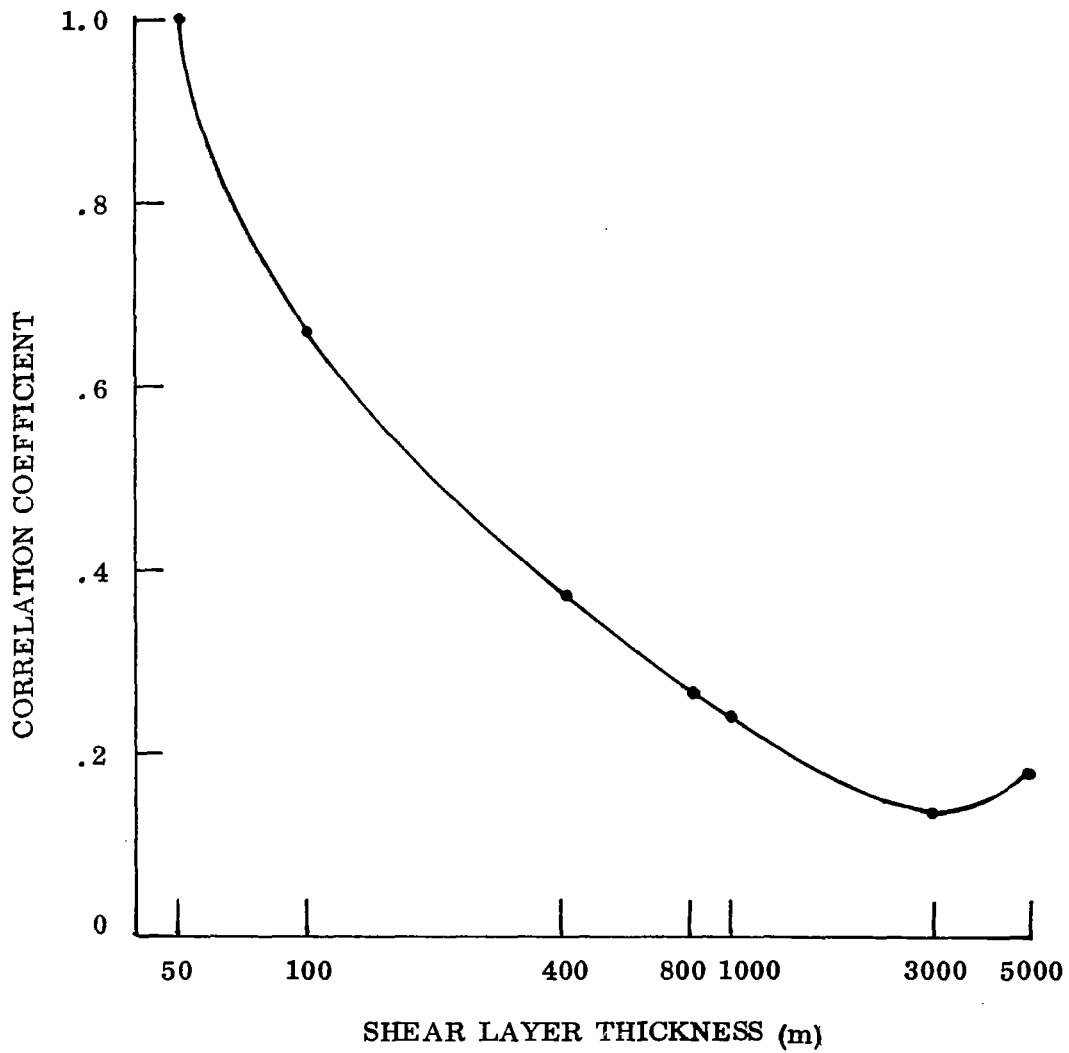


Figure 4.21 The Correlation of 50 m Vector Shears with Vector Shears of Various Thicknesses at 12 km

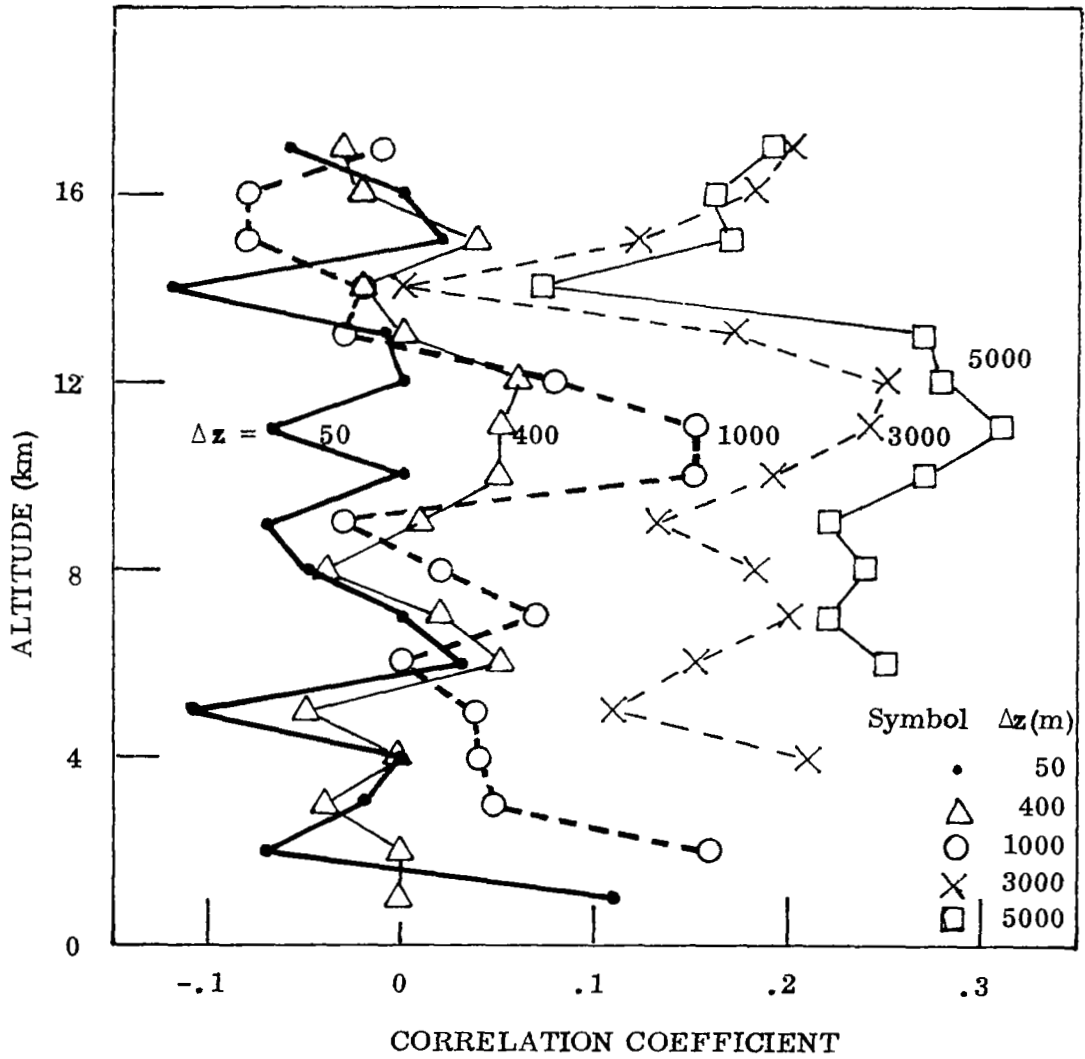


Figure 4.22 The Correlation Between Zonal and Meridional Shears, as a Function of Altitude, for Shear Layer Thicknesses, Δz , of 50, 400, 1000, 3000, and 5000 m

where ρ_{xy} , ρ_{xz} , and ρ_{yz} are linear correlation coefficients.

$R_{x/yz}$ is a pure number in the closed interval bounded by 0 and 1. When $R_{x/yz} = 1$, a perfect linear relation exists between x , y , and z of the form,

$$x = ay + bz + c \quad 4.13$$

where a , b , and c are constants. When $R_{x/yz}$ is 0, there is no linear relation between x , y , and z .

$R_{x/yz}$ was computed for overlapping vector shears at 12 km. For a fixed dependent variable x (50 m vector shear) and four pairs of independent variables yz (100 and 400, 400 and 800, 800 and 1000, and 1000 and 3000 m vector shears), the results are given in Table 4.2.

TABLE 4.2

$R_{x/yz}$ THE COEFFICIENT OF MULTIPLE CORRELATION FOR
VECTOR SHEARS AT 12 km

<u>x/yz</u>	<u>$R_{x/yz}$</u>
50/100 400	.67
50/400 800	.38
50/800 1000	.44
50/1000 3000	.29

It is shown that the multiple correlation between overlapping vector shears at 12 km is dependent on the amount of overlap; the multiple correlation decreases as the overlap decreases. Therefore, this supports the conclusion that shears with small layer thicknesses are not linearly dependent on pairs of shears with large layer thicknesses.

4.6 EMPIRICAL CONDITIONAL PROBABILITIES FOR 95% ZONAL AND VECTOR SHEARS

The conditional probability of extreme ($\geq 95\%$) non-overlapping zonal and vector shear at altitudes above and below 12 km, given that the shear at 12 km is extreme ($\geq 95\%$) was estimated by first identifying the N_0 soundings at a pivotal level Z (12 km) in which the shears over the layer $Z - \Delta z$ to Z equal or exceed a pre-determined percentile limit ($\geq 95\%$); of the N_0 soundings there may be N_1 soundings for which the shears over the layer $Z - \Delta z$ to $Z - 2\Delta z$ equal or exceed the percentile limit in combination with exceedence of the shear over the layer Z to $Z - \Delta z$. Thus the estimated probability, given the extreme values at Z , that extreme values occur at $Z - \Delta z$ is N_1/N_0 . The conditional probabilities computed in this manner for shear layer thicknesses (Δz) of 50, 100, 800, and 1000 m are plotted in Figure 4.23 for zonal shears, and Figure 4.24 for vector shears. If these adjacent non-overlapping extreme shears are independent of the extreme shear at 12 km, the conditional probability should be 0.05. The consistently low conditional probabilities below 11 km and above 13 km support the conclusion that the extreme 50, 100, 800, and 1000 m zonal and vector shears below 11 km and above 13 km are independent of the extreme shears at 12 km.

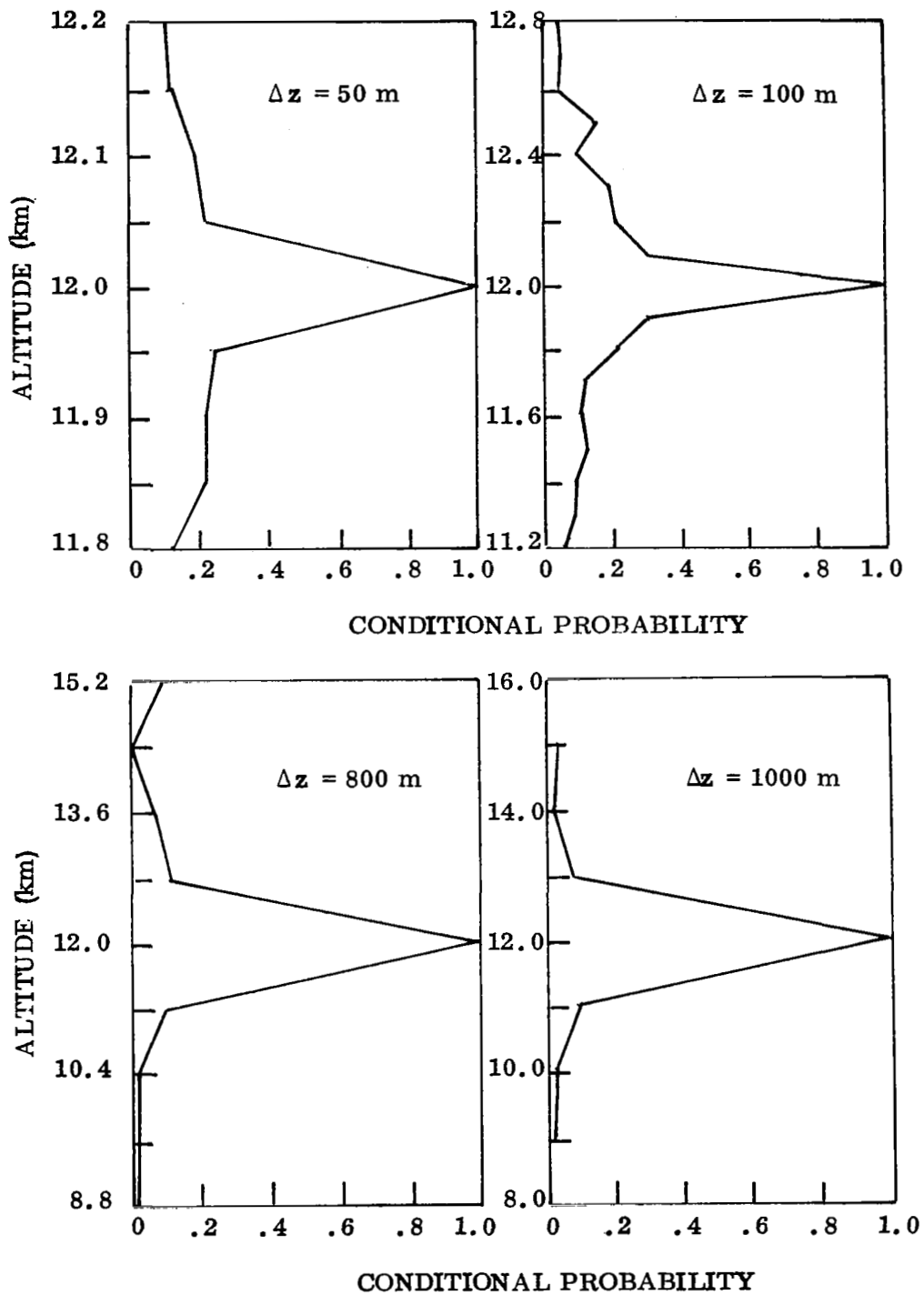


Figure 4.23 Conditional Probability of Exceedance in Combination of 95% Zonal Shear at Indicated Altitude, Given the 95% Zonal Shear at 12 km, For Shear Layer Thicknesses (Δz) of 50, 100, 800, and 1000 Meters

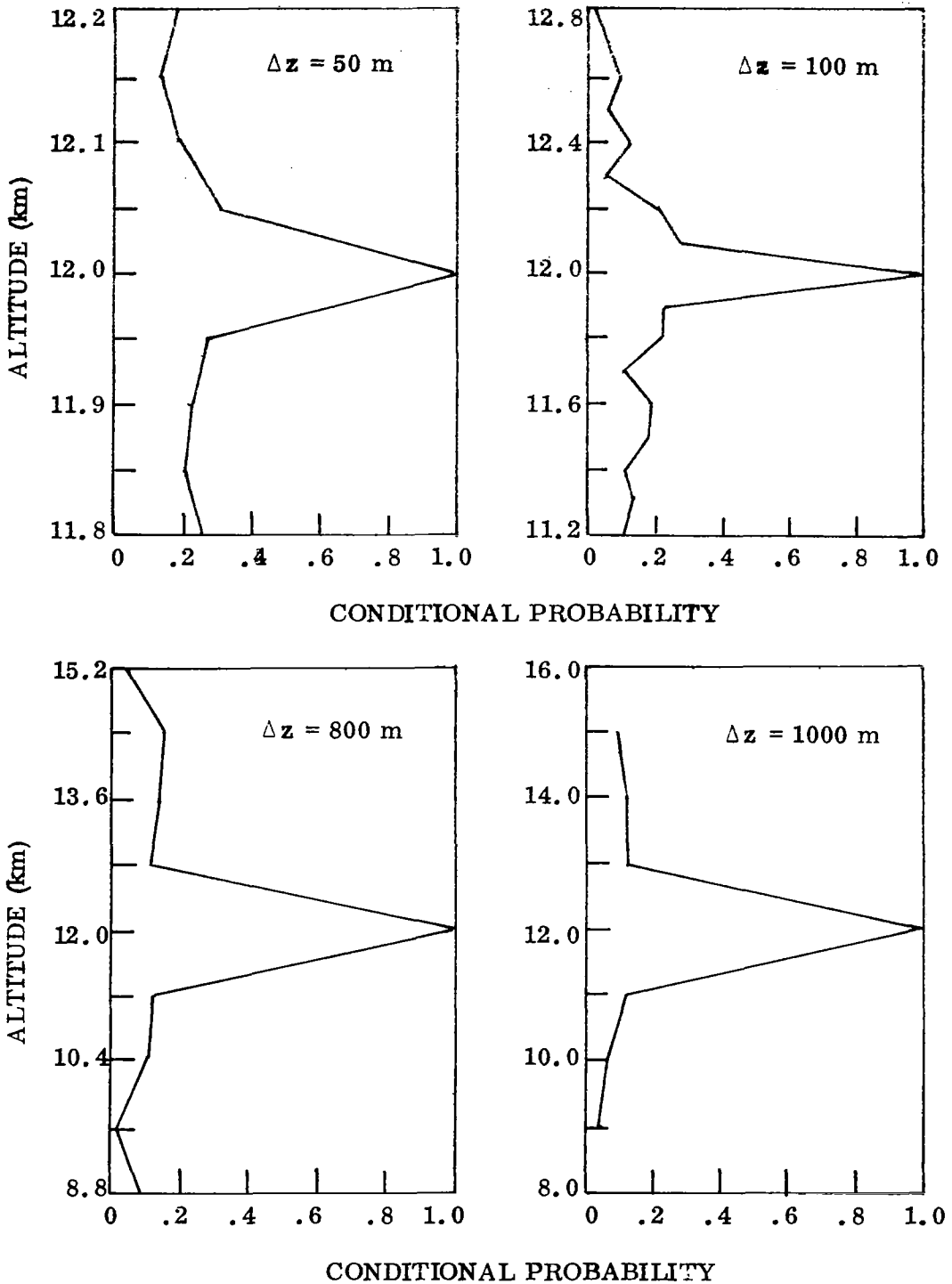


Figure 4.24 Conditional Probability of Exceedance in Combination of 95% Vector Shear at the Indicated Altitude Given the 95% Vector Shear at 12 km for Shear Layer Thicknesses (Δz) of 50, 100, 800, and 1000 Meters

Section 5

SHEAR ENVELOPES FOR 95 AND 99 PERCENT ZONAL AND VECTOR SHEARS

The shear envelopes are derived by determination of the 95 and 99 percent values of the observed distribution of shear, at 500 m altitude intervals. These shear envelopes are given in Figures 5.1 and 5.2 for zonal shears with layer thicknesses from 50 to 5000 m, and 5.3 and 5.4 for vector shears with layer thicknesses from 50 to 5000 meters.

The probability is extremely low that any of these extreme shear profiles occur. This is supported by the computation of conditional probabilities given in Section 4. These computations indicated that the extreme ($\geq 95\%$) zonal or vector shears below 11 km or above 13 km are independent of the extreme ($\geq 95\%$) zonal or vector shears at 12 km. Therefore, it follows, for example, that given the extreme ($\geq 95\%$) 1000 m zonal shears at 12 km, the probability that the 1000 m zonal shear will also be extreme at 9, 10, and 11 km is $(.05)^3$.

Independence of extreme shears is also indicated from computations of the conditional probability of exceedence in combination which, from the example in the previous paragraph, is predicted to be near zero. This conditional probability may be stated in the following way: Given the extreme shear ($\geq 95\%$) at 12 km we wish to compute the probability that the shears for a succession of non-overlapping intervals of equal thickness will also be extreme.

This conditional probability is estimated by first identifying the N_0 soundings at a pivotal level Z (12 km) in which the shears over the layer $Z - \Delta z$ to Z exceed a pre-chosen percentile limit. Of the N_0 soundings there may be N_1 soundings which contain shears that exceed the percentile limit at $Z - \Delta z$ in combination with exceedance at Z . Thus, the estimated probability, given the extreme values at Z , that extreme values occur at $Z - \Delta z$, is N_1/N_0 .

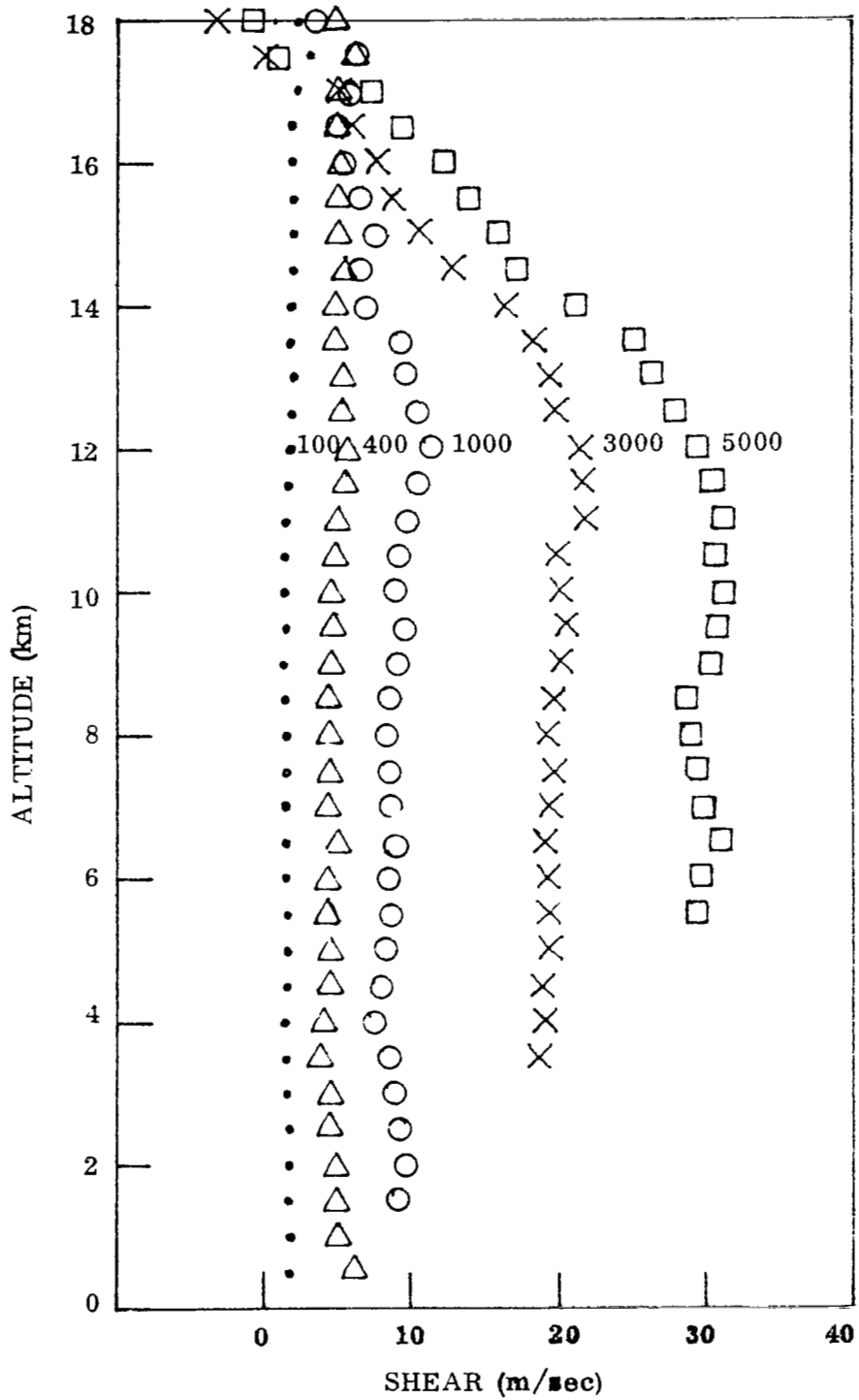


Figure 3.1 95% Zonal Shear as a Function of Altitude for Various Shear Layer Thicknesses

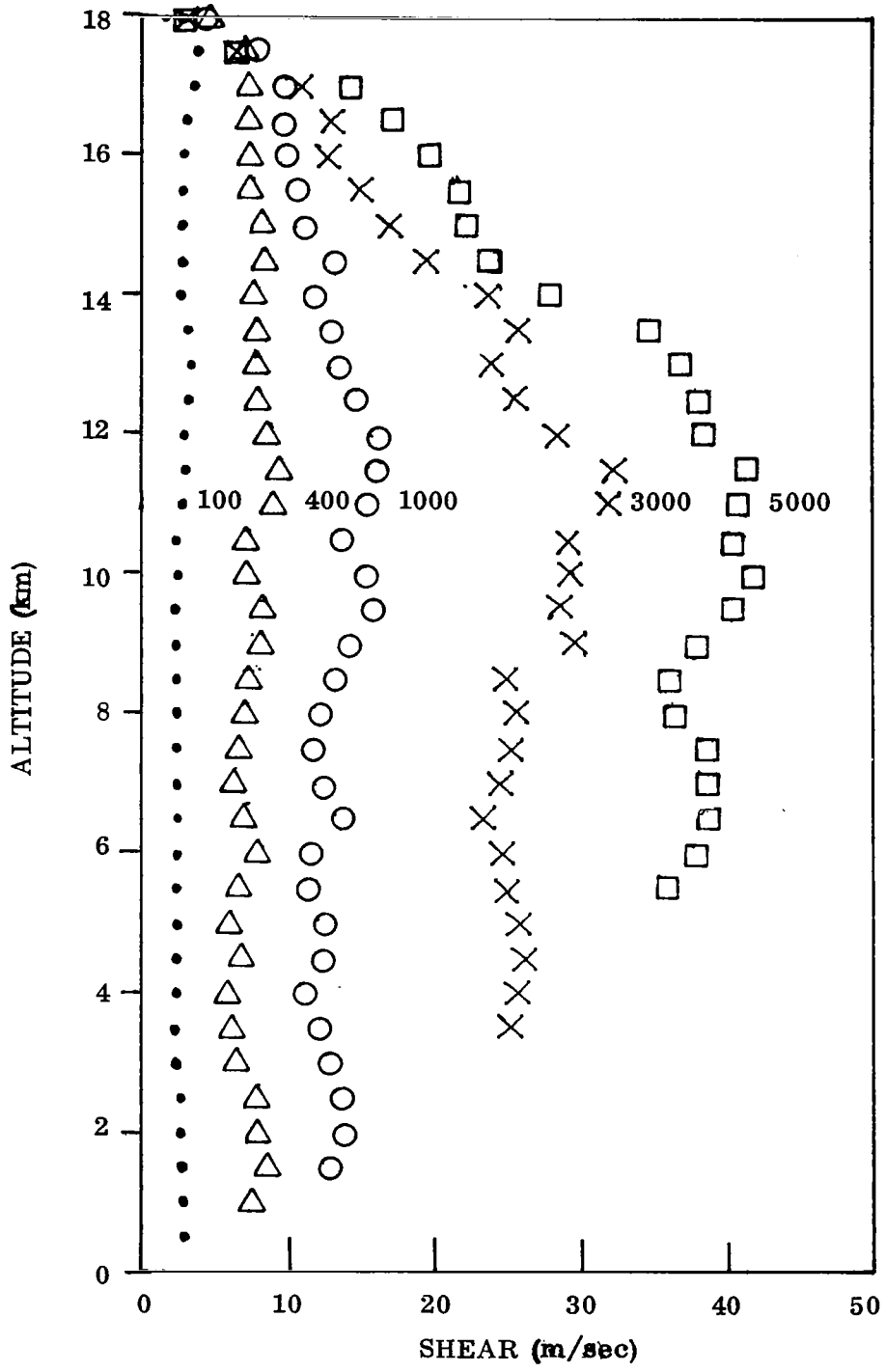


Figure 5.2 99% Zonal Shear as a Function of Altitude for Various Shear Layer Thicknesses, Δz (m)

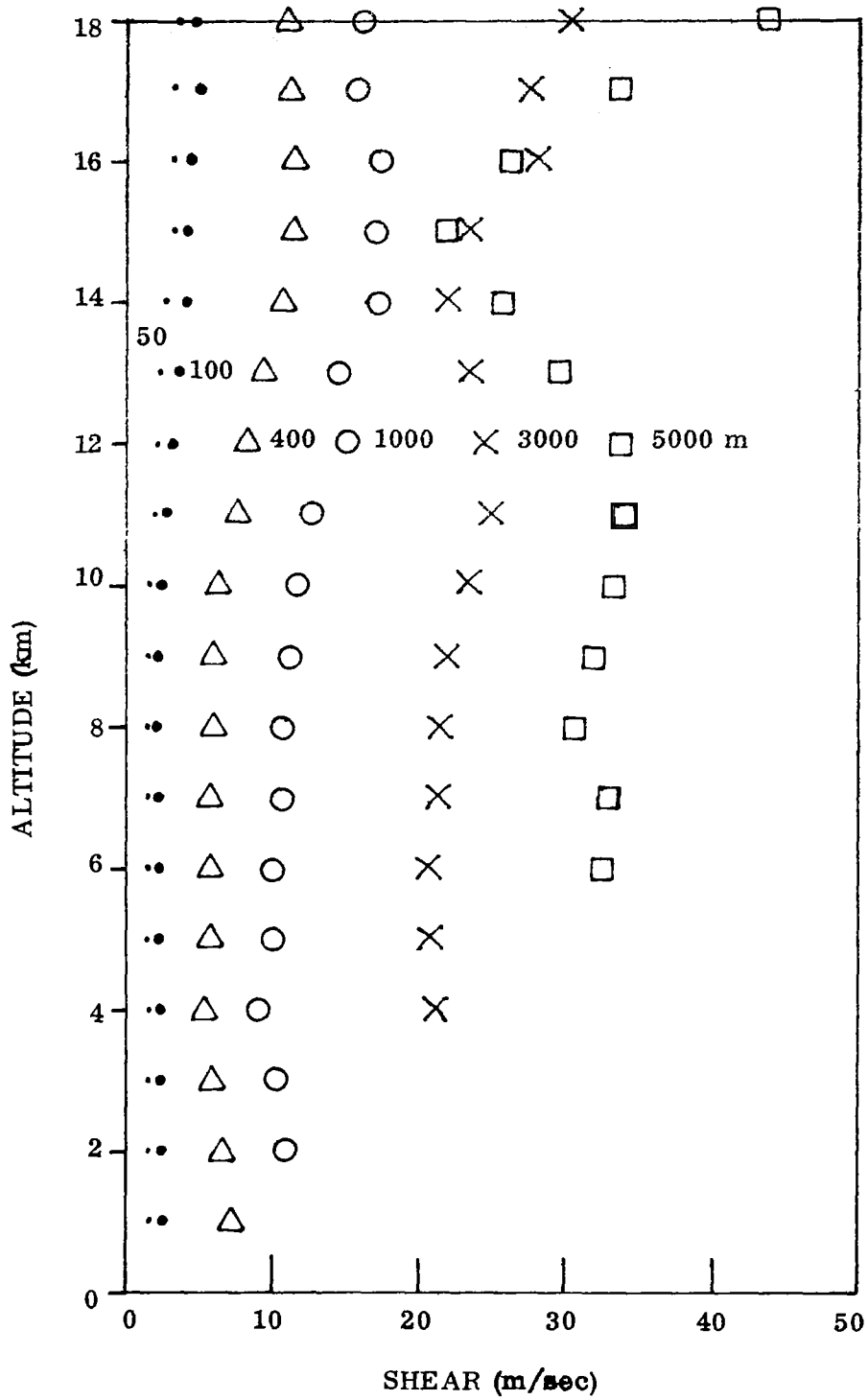


Figure 5.3 95% Vector Shear as a Function of Altitude for Various Shear Layer Thicknesses, Δz (m)

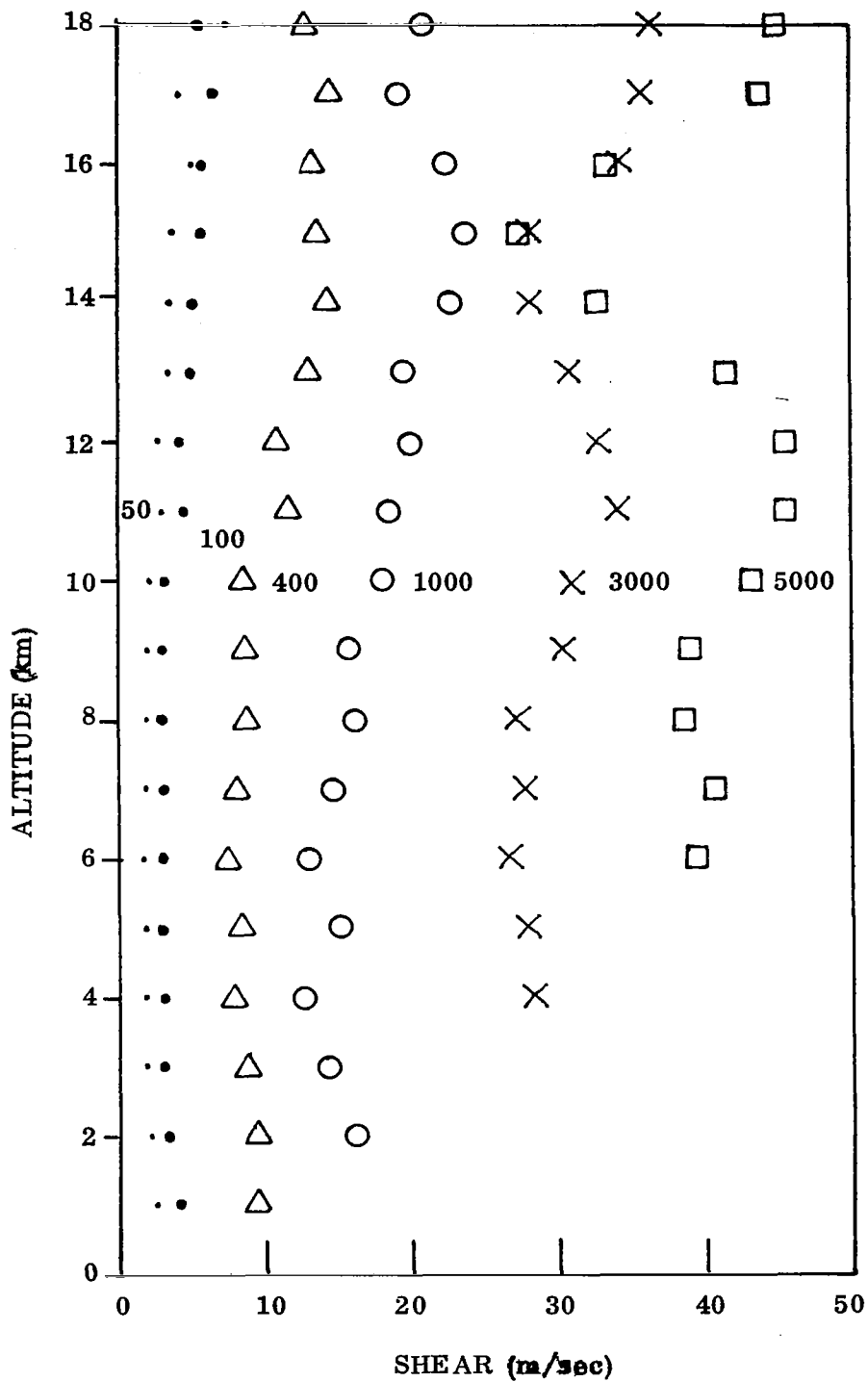


Figure 5.4 99% Vector Shear as a Function of Altitude for Various Shear Layer Thicknesses, Δz (m)

We wish now to compute the conditional probability of exceedance at $Z - 2 \Delta z$ in combination with exceedance at $Z - \Delta z$ and also at Z . In the N_1 soundings for which the extreme values have occurred simultaneously at levels Z and $Z - \Delta z$, some N_2 will show exceedance of the percentile limit at $Z - 2 \Delta z$, as well. The estimated probability, given exceedance at Z , is N_2/N_0 that the exceedance will also occur at $Z - \Delta z$ and $Z - 2 \Delta z$. Similarly conditional probabilities may be computed for as many increments of Δz as desired, depending on how rapidly the probability decreases.

As shown in Figure 5.5, for a pivotal level of 12 km, the conditional probability for exceedance in combination of the 95% 1000 m zonal (or vector) shear at 9, 10, and 11 km given the 95% shears at 12 km, is estimated to be zero. Figure 5.5 also gives the conditional probabilities of exceedance in combination for 50, 100, 400, and 800 m shear layer thicknesses.

Conditional probabilities have also been computed for exceedance of the 95% zonal or vector 50, 100, and 400 m shears given that the 1000 m 95% shear at 12 km is exceeded. The results plotted in Figure 5.6 for zonal and vector shears show that the exceedance of the 95% 50, 100, and 400 m shears below 10.8 km and above 12.4 km is nearly independent of exceedance of the 95% 1000 m zonal shear at 12 km.

In summary, it may be concluded from these results that: 1) The simultaneous occurrence of non-overlapping extreme vector and zonal shears measured over altitude layers of 50 through 1000 meters, given that the shear is extreme at 12 km, is a low probability event. This is also supported by the finding (Section 3) that extreme non-overlapping shears below 11 km and above 13 km are independent of the extreme shears at 12 km. 2) The extreme 50, 100, or 400 m vector and zonal shears below 10.8 and above 12.4 km are nearly independent of the extreme 1000 m shear at 12 km.

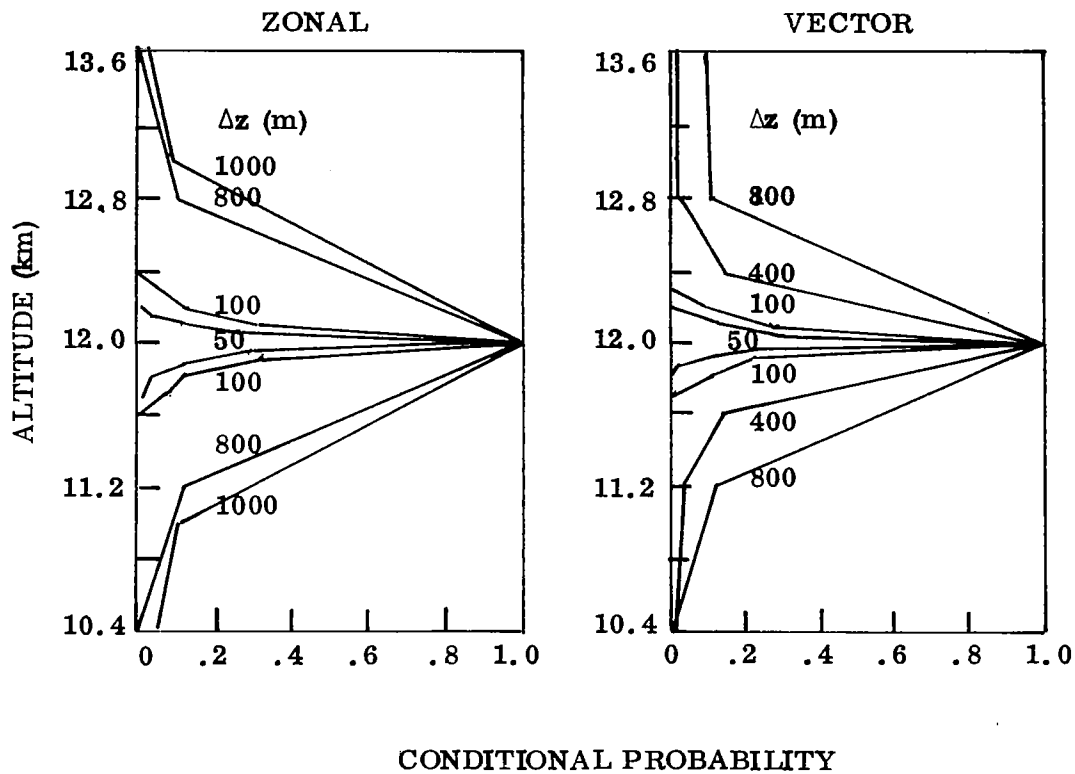


Figure 5.5 Conditional Probability of Exceedance in Combination of Non-Overlapping 95% Zonal (Vector) Shears at Altitudes Between 12 km and the Indicated Altitude Given the 95% Zonal (Vector) Shear at 12 km. For Shear Layer Thicknesses (Δz) of 50, 100, 800, and 1000 Meters

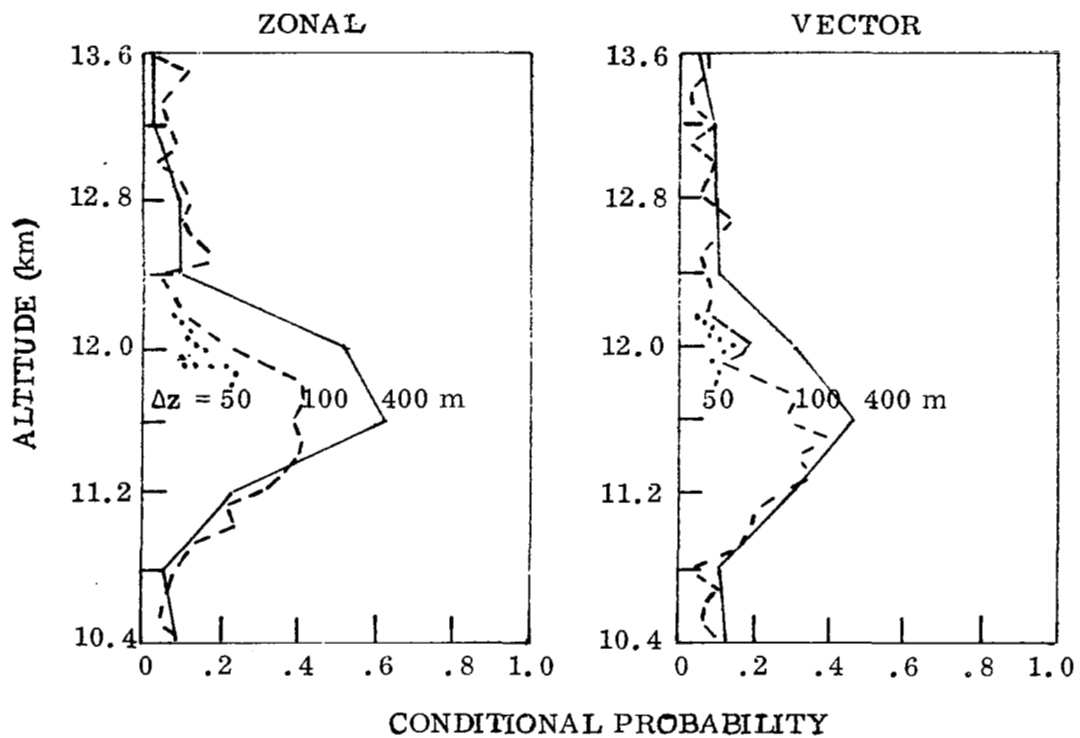


Figure 5.6 Conditional Probability of Exceedance in Combination of 95% 50, 100, and 400 Meter Zonal (Vector) at the Indicated Altitude Given the 95%, 1000 Meter Shear at 12 km

Section 6

THE DEFINITION OF THE STEADY STATE WIND AND GUSTS

Defining a steady state wind for any application clearly involves some kind of low pass filtering. The purpose of filtering is to sort out the low frequency information from a wide banded spectrum of fluctuations. The information removed is sometimes called "turbulence".

Defining a steady state wind meteorologically raises the question: What steady state wind? There are as many steady state wind definitions as there are interesting scales of atmospheric motion.

A steady state wind as defined for one problem may not be steady state for another problem. Therefore, a desirable part of the definition of the steady state wind could be a statement of the scale of the perturbations of interest. The advent of Jimsphere and other high resolution-high accuracy systems for upper air wind measurements has extended the spectrum of observable wavelengths, and thus the possible scales of interest, by almost an order of magnitude. For the meteorological definitions of steady state wind, we can propose a few filter types that may be useful in possible applications of Jimsphere data to current problems in meteorology.

The definition of a steady state wind for a space vehicle is further complicated by the varying velocity with which the vehicle moves through the wind field. Hence, the same wind fluctuations with altitude that are sensed by the vehicle as a low frequency input at one altitude may be sensed as a high frequency input at another altitude.

A logical approach would be to re-define the wind fluctuations in terms of vehicle flight time*. The re-definition or transformation of the original wind data into

*Vehicle Flight Time, Vehicle Time Domain, or Time Domain, all refer to Time after launch of the Vehicle.

the time axis would necessarily be a function of the particular vehicle and mission. The Jimsphere wind profiles may then be filtered to separate the "steady state" from the interesting scales of motion. For example, the important bending mode frequencies of the Saturn V Launch Vehicle range from about 1 to 3 cycles per second. For the particular problem of determining the severity of wind perturbation inputs at these frequencies, perturbations at lower frequencies are of no importance. Hence, these low frequency perturbations can be defined as the steady state wind for this particular problem.

Before proposing a procedure for the derivation of steady state wind profiles, it would be helpful to first determine the maximum possible frequency range of Jimsphere data. According to Pasquill (Ref. 11) the following basic properties of equally spaced data can be used for the determination of the maximum frequency range of a typical Jimsphere profile:

1. T , the length of the data record, assumed to be 18×10^3 meters.
2. S , the averaging interval for each observation, assumed to be 50 meters.
3. H(n) , a transfer function, depending on T and S :

$$H(n) = \left[1 - \frac{\sin^2 \pi n T}{\pi n T} \right] \frac{\sin^2 \pi n S}{(\pi n S)^2} \quad 6.1$$

where n is the frequency in cycles per meter. The range of frequencies for which H(n) is greater than 0.50 will be arbitrarily defined as the frequency range or "spectral window" of the Jimsphere data. In Figure 6.1, H(n) is plotted as a function of n for $T = 18 \times 10^3$ m and $S = 50$ m . According to our definition, the maximum possible frequency range of the Jimsphere data is 9×10^{-5} to 1×10^{-2} cycles per meter. The spectral energy of wind profile perturbations with frequencies outside this range are attenuated by a factor of greater than 0.5 .

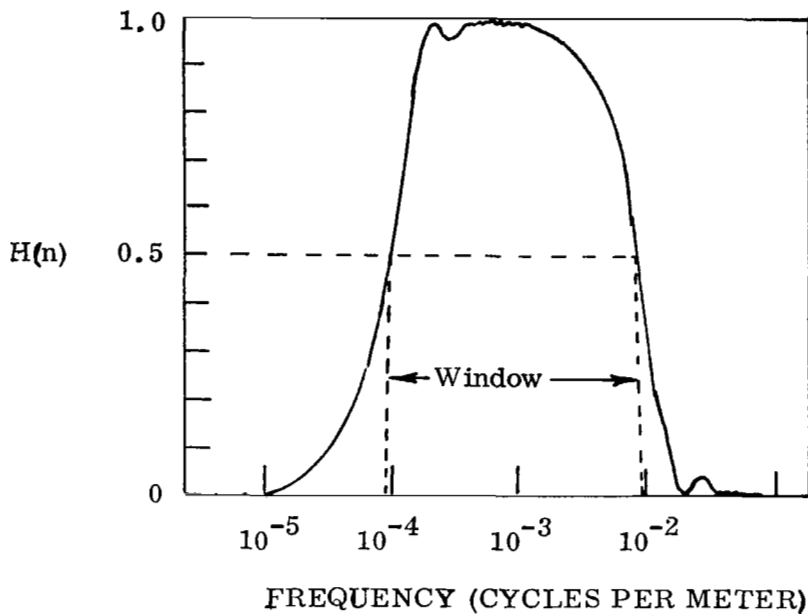


Figure 6.1 Spectral Window for Jimsphere Profiles

To study how winds, as observed with the Jimsphere system, affect space vehicles, requires the frequency range of the wind inputs as observed in the time domain of the vehicle. The limits of the frequency range in the vehicle time domain are obtained by multiplying the limits of the frequency range in the space domain by the velocity. The limits computed for the Saturn AS-504 Vehicle (using a typical reference trajectory), are given in Table 6.1. This subject is developed further along slightly different lines in a later paragraph.

TABLE 6.1

FREQUENCY RANGE OF JIMSPHERE DATA IN THE TIME
DOMAIN FOR THE SATURN AS-504 VEHICLE *

<u>Flight Time</u> <u>Sec</u>	<u>Altitude</u> <u>km</u>	<u>Vertical Velocity</u> <u>m/sec</u>	<u>Minimum Freq.</u> <u>cps</u>	<u>Maximum Freq.</u> <u>cps</u>
51	4	195	0.0175	1.95
67.5	8	290	0.0261	2.90
79.5	12	365	0.0328	3.65
89.5	16	435	0.0392	4.35

The steps required in a procedure for the derivation of a steady state wind profile with respect to a space vehicle are given below.

- A. Transformation of the Jimsphere data, assumed to be a function of altitude only, to the vehicle time coordinate system.
- B. Definition of the wind perturbations of interest. Saturn vehicles have significant response to wind perturbations at the control frequency (.15 cps), and the first and second bending mode frequencies (1, 2 cps).
- C. Application of a low pass digital filter to the transformed Jimsphere profiles obtained in A. For Saturn V applications, the basic characteristics of the filter is its insignificant energy transmission at frequencies above .15 cps. The result is a steady state wind profile in the vehicle time domain with respect to Saturn V control and bending problems.

*Flight time and altitude data obtained from Jacobs (Ref. 10).

D. Application of the inverse of the transformation in A to the result of C . This yields a steady state wind profile with respect to the vehicle as a function of altitude.

This procedure yields steady state wind profiles which have a constant cut-off frequency when viewed in the vehicle time domain. In the procedure used by Bieber (Ref. 4), the Jimsphere profiles are filtered in the space domain before transformation to the time domain. Bieber used a filter derived by Alfriend (Ref. 1) which has essentially zero energy transmission above a cut-off frequency, f_c , equal to .002 cycles/meter. But in the vehicle time domain, this filter has a variable cut-off frequency, f_c^* (cycles per second), which is a function of the vehicle vertical velocity:

$$f_c^* = .002 V(t) \quad 6.2$$

Values of f_c^* for various velocities and corresponding altitudes of the Saturn AS-504 vehicle trajectory are given in Table 6.2.

TABLE 6.2

CUT-OFF FREQUENCY OF THE ALFRIEND FILTER AS A FUNCTION
OF FLIGHT TIME OF THE SATURN AS-504 VEHICLE

<u>Flight Time (sec)</u>	<u>Altitude (km)</u>	<u>Vertical Velocity (m/s)</u>	<u>Alfriend Filter Cut-Off Frequency f_c^* (cycles per second)</u>
51	4	195	.39
67.5	8	290	.58
79.5	12	365	.73
89.5	16	435	.87

Further discussion is needed of the important assumption, made in Step A, that the Jimsphere data are a unique function of altitude. During the hour required for the Jimsphere balloon to reach an altitude of 18 km, the horizontal displacement from its launch position may be several tens of kilometers. Therefore, the observed winds depend on time and horizontal displacement as well as altitude. In contrast, a Saturn V reaches 18 km after approximately 94 seconds of flight and a horizontal displacement of approximately 10 km. The successful use of Jimsphere winds for pre-launch decision making hinges upon an affirmative answer to the question: Are the features of the wind profile observed over the one hour period of balloon ascent to 18 km, which are important in the frequency range of vehicle response, applicable to a vehicle ascent to 18 km in 94 seconds? Progress towards answering this question has been reported by Scoggins and Vaughan (Ref. 15), who have found high persistence in a significant number of small-scale features of selected representative Jimsphere profiles approximately 1 1/2 hours apart in time. Further contributions to an affirmative answer could result from future research into the persistency of spectral energy of wind inputs at the frequency of significant spacecraft response to wind inputs in the space vehicle time domain.

Jimsphere winds can be transformed to the vehicle time domain by evaluating the Jimsphere data at altitudes corresponding to the altitude of the vehicle at equally spaced time intervals. The resulting time series is suitable for application of digital time domain filters and spectral analysis. The maximum possible information with the least distortion will be obtained from the Jimsphere profiles by specifying a time interval small enough to include all the Jimsphere data. In the following paragraphs an expression for the time interval is derived in terms of vehicle altitude versus time relations and the resolution of the wind profile. An expression for the maximum observable frequency of wind fluctuations from wind profiles as a function of the vehicle vertical velocity is also given.

Assume that a wind profile contains independent estimates of wind at equal intervals of altitude, R , in meters, representing the resolution of the profile. The number of wind values per second, N , "seen" by a vehicle with a time dependent vertical velocity, $V(t)$, in meters per second, is given by

$$N = V(t)/R \quad 6.3$$

The time interval, ΔT , in seconds, between wind values as seen by the vehicle, is N^{-1} , where

$$\Delta T = N^{-1} = R/V(t) \quad 6.4$$

In the altitude range of a Jimsphere sounding, the vertical velocity of the vehicle increases with altitude as shown in Figure 6.2 for various vehicles.* Therefore, ΔT , decreases with altitude, and choice of ΔT for the maximum vehicle velocity will insure that all information in the original data is transformed to the vehicle time domain. Assume that 16 km is the maximum altitude used for a study of vehicle response to Jimsphere winds. Figure 6.3, which gives the altitude of various vehicles as a function of flight time, shows that the Saturn AS-504 vehicle reaches 16 km 89.5 seconds after launch. At that time the vertical velocity of the vehicle is approximately 435 m/sec. From Eq. (6.4), for $R = 50$ meters, $\Delta T = 0.11$ seconds.

The maximum observable frequency, f_m , in cycles per second for equally spaced observations ΔT seconds apart is given by

$$f_m = 1/2 \Delta T = V(t)/2R, \quad 6.5$$

obtained by substituting for ΔT from Eq. (6.4).

Figure 6.4 gives the maximum observable frequency, obtained from Eq. (6.5), for a wind profile resolution of 50 meters. From step B above we have defined the range of frequencies (0.15 to 3.0 c.p.s.) over which the vehicle would be expected to have significant response to wind inputs. From Figure 6.4, for a resolution of 50 meters, which is the resolution of present compilations of Jimsphere winds, a maximum observable frequency of 3.0 c.p.s. is attained at flight

*It should be noted that these time altitude and velocity values vary somewhat for a particular vehicle depending on its mission.

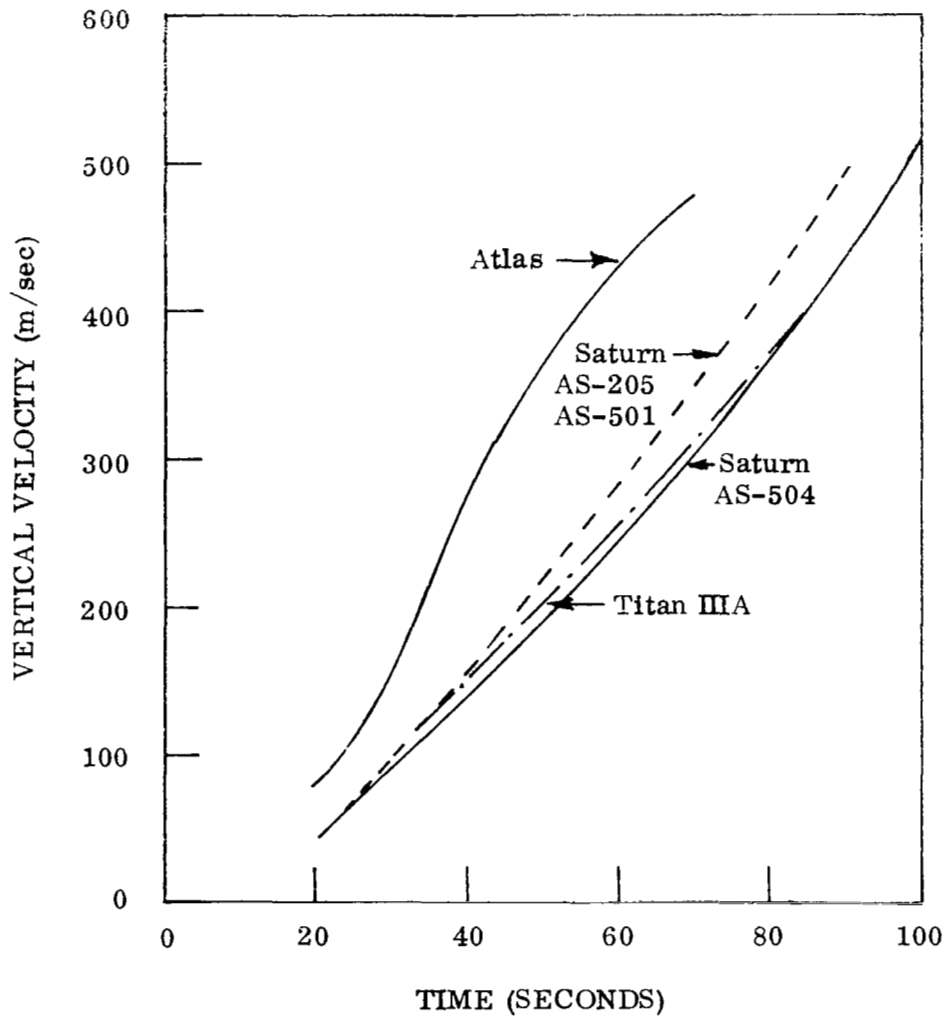


Figure 6.2 Vertical Velocity of Various Vehicles as a Function of Flight Time

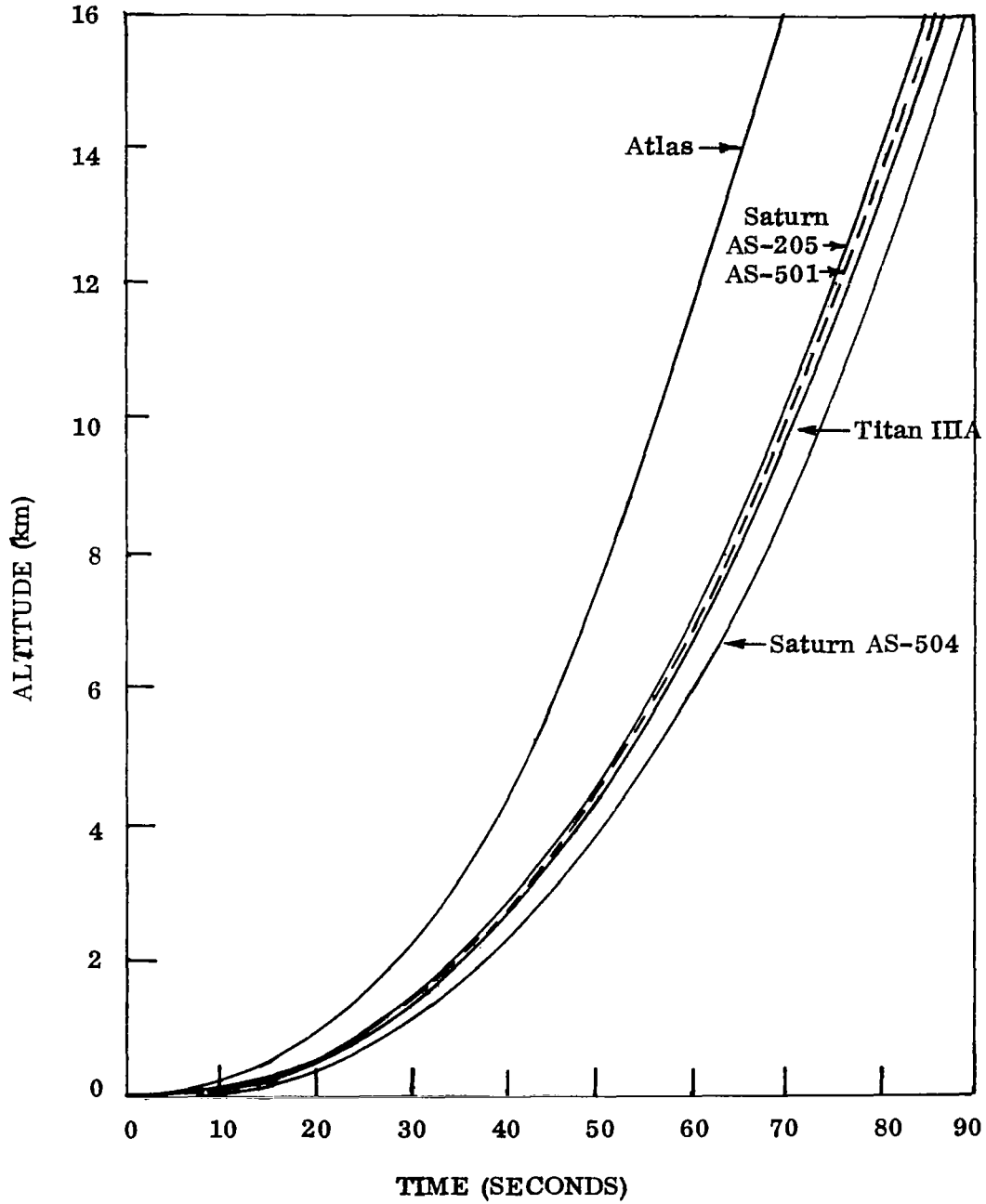


Figure 6.3 Altitude of Various Vehicles as a Function of Flight Time

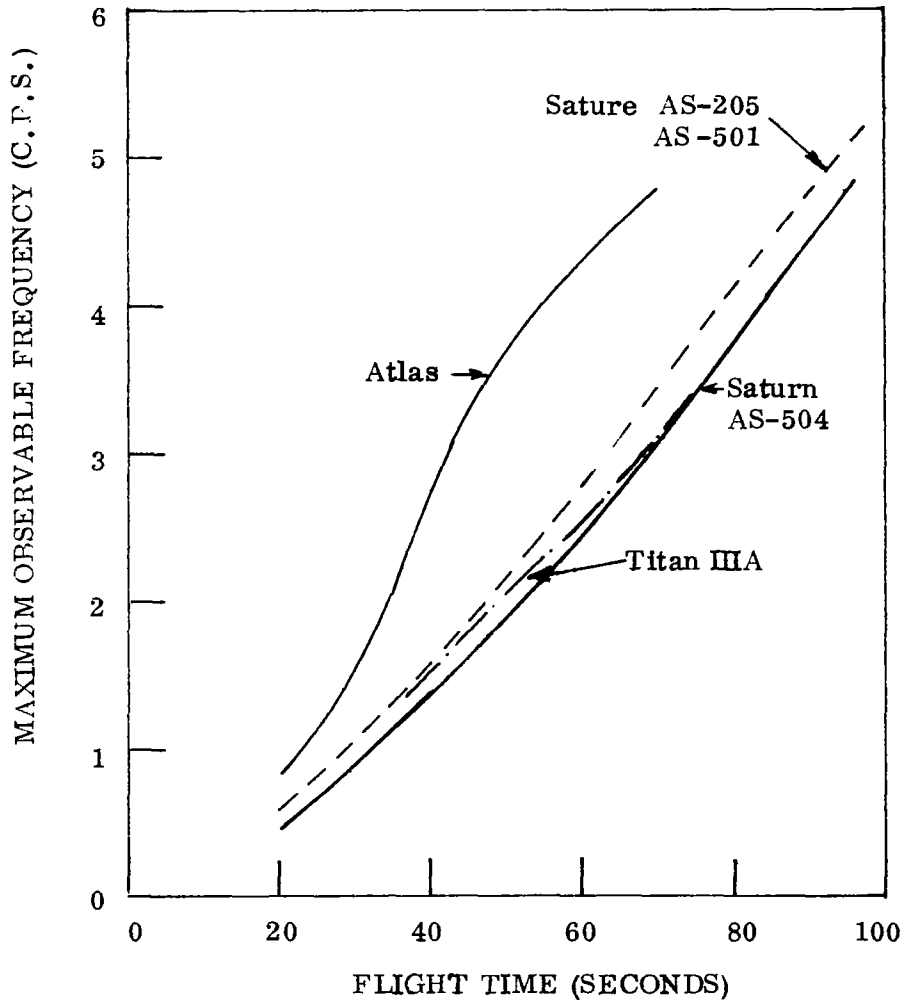


Figure 6.4 Maximum Observable Frequency of Wind Fluctuations from Wind Profiles with an Altitude Resolution of 50 Meters as a Function of Flight Time for Various Vehicles

times that range from 42 seconds for the Atlas to 70 seconds for the Saturn AS-504.

Figure 6.5 gives f_m as a function of altitude for various vehicles. For $R = 50$, and $f_m = 2$ cps the wind profile as viewed by the vehicle cannot contain frequencies as high as 2 cps at altitudes below, 2.6 km for Atlas, 3.8 km for Saturn AS-205 and AS-501, and 4.2 km for Saturn AS-504, and Titan IIIA. Therefore, the limitation imposed by the 50 m resolution of Jimsphere winds in combination with the velocity of the vehicles effectively imposes altitude limits below which studies of wind inputs with frequencies as high as 2 cps would progressively lose their meaning, and above which wind perturbations in the range 0 to 2 cps are completely observable. The range of observable frequencies is extended to higher frequencies at higher altitudes: at 16 km it is 4.35 cps for the Saturn AS-504, and 4.80 cps for Atlas.

The definition of gusts with respect to a space vehicle, as obtained from Jimsphere wind profiles, depends on the same basic considerations that were outlined above for the definition of the steady state wind. The basic idea is that the wind profile as seen by an ascending vehicle is composed of a continuous spectrum of perturbations with a frequency range which is a function of the velocity of the vehicle, the resolution of the profile, and the length of the profile.

The frequency range of significant space vehicle dynamic response to wind inputs is generally known and in the procedure outlined above the frequency below which significant space vehicle dynamic response to the wind profile characteristics does not exist is stated for the Saturn V class of vehicles. Wind profiles which contain perturbations which are never less than this frequency may be defined as gust profiles. These gust profiles are not necessarily composed solely of small spatial scale turbulent motions. It follows from the definition of the gust profile that, when the vehicle velocity is large, non-turbulent motions of relatively large spatial scale may result in significant space vehicle responses.

Gust profiles may be obtained by adding the following steps to the procedure outlined for the derivation of the steady state wind with respect to a space vehicle:

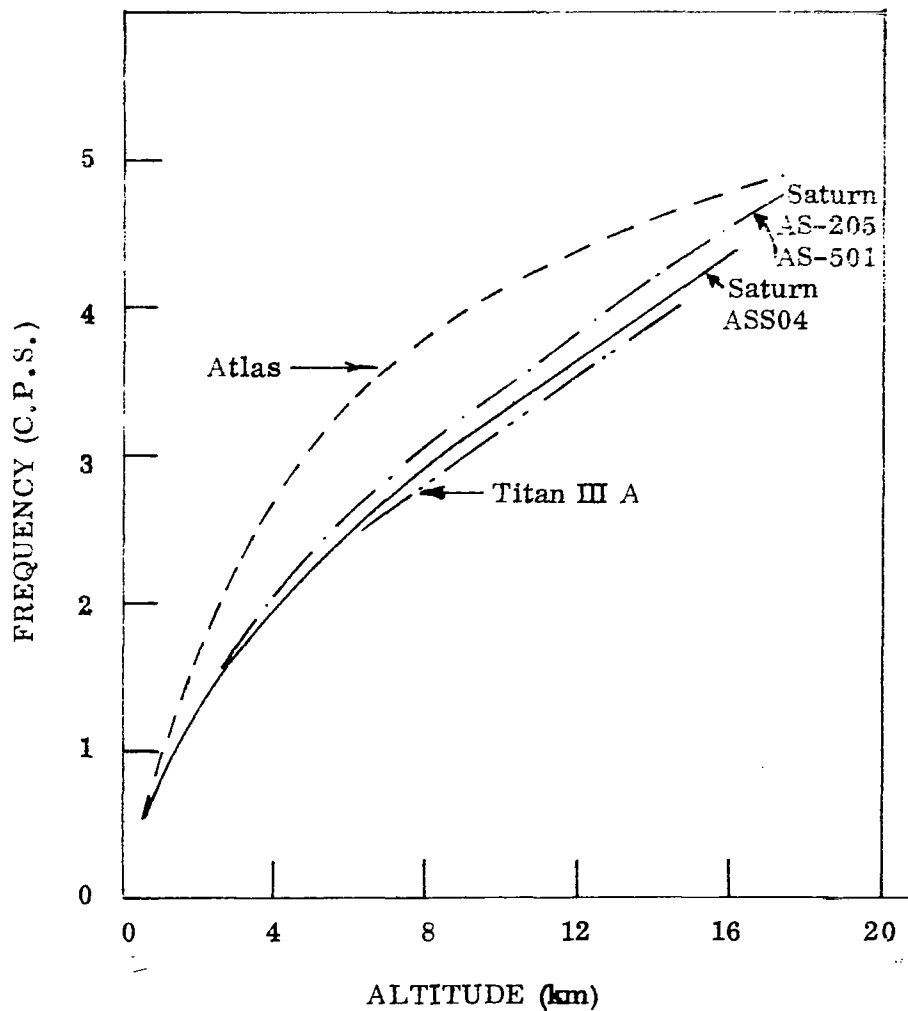


Figure 6.5 Maximum Observable Frequency from Wind Profiles with an Altitude Resolution of 50 Meters as a Function of Altitude for Various Vehicles

Subtract the steady state wind profile in the time domain from the total wind profile in the time domain. The result is a gust profile in the time domain.

Subtract the steady state wind profile in the space domain from the total wind profile in the space domain. The result is a gust profile in the space domain.

In principle, the gust profiles derived according to this procedure are not comparable with gust profiles derived according to the procedure outlined by Bieber (Ref. 4). The difference between the gust profiles may be attributed to the fact that Biebers filter, applied in the space domain, has a variable cut-off frequency when viewed in the vehicle time domain (Table 6.2), whereas the filter used in this procedure has a constant cut-off frequency in the vehicle time domain.

Section 7

RELATION BETWEEN WIND SPEEDS, SHEARS, AND GUSTS

Conditional probabilities were used to examine the relation between wind shear and wind speed at 12 km.

According to the proposed definition of gusts given in Section 6 and according to Eq. 6.5, shears at 12 km measured over an altitude interval up to 200 m may result in significant bending mode response of the Saturn V class of vehicles, and shears at 12 km measured over an interval of 1000 m may result in significant response at the control frequency. Therefore, the results discussed below for the shear layer thicknesses of 100, 400, and 1000 m are related to the gusts as seen by the Saturn V vehicle when it is near an altitude of 12 km.

Conditional probabilities were computed for exceedance of the 50, 80, 95, and 99 percent vector shears at 12 km for shear layer thicknesses of 100, 400, 1000, 3000, and 5000 m, given that the 95% scalar wind at 12 km is exceeded. These probabilities are given in Figure 7.1; and similarly the conditional probabilities for zonal shears, given the extreme ($> 95\%$) zonal wind speed at 12 km were computed and are given in Figure 7.2. The highest probability of extreme shear, given the extreme wind speed, occurs for the large shear layer thicknesses (1000, 3000, 5000 m). For shear layer thicknesses of 100 through 3000 m, the conditional probability of extreme vector shears, given the extreme scalar wind, is consistently higher than for zonal shear with zonal winds. The conditional probability for vector shears decreases with increasing shear layer thickness 100 to 400 m whereas the conditional probability for zonal shears is nearly constant for the same thickness range. These results may be applied for the estimation of the probability of wind build-up rates based on simultaneous exceedance of specific wind and shear percentiles at 12 km. For example, given the 95% scalar wind at 12 km, the conditional probability that the 5000 m vector shear exceeds the 99% value is .15 and the conditional probability is .83 that the same shear exceeds the 80% value.

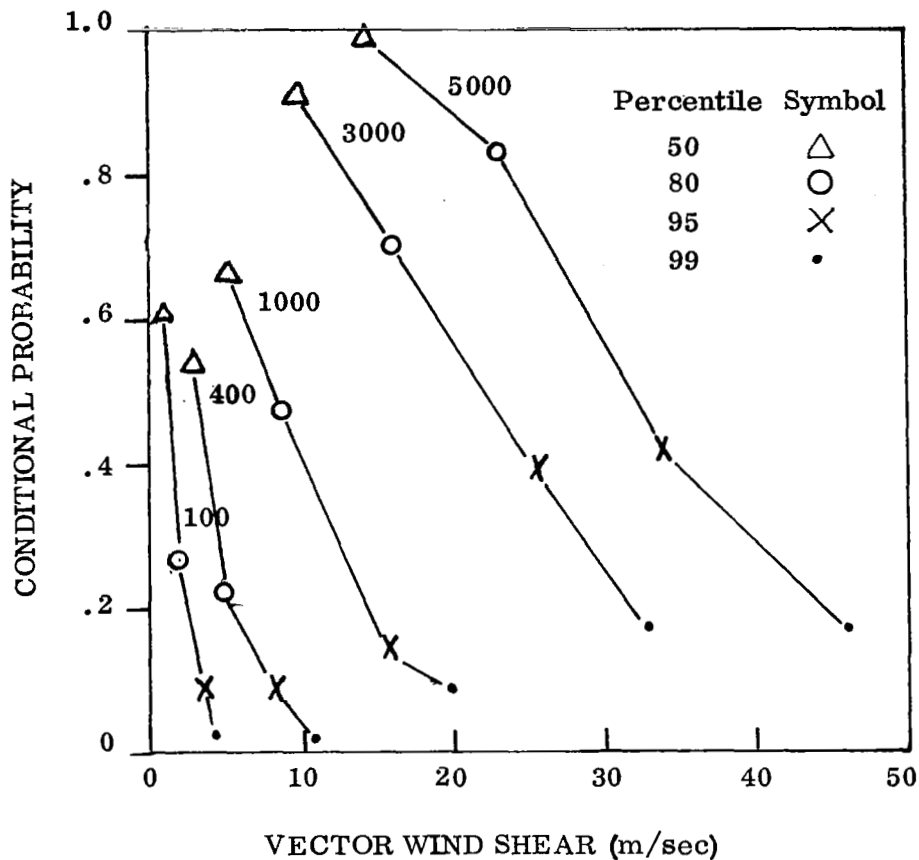


Figure 7.1 Conditional Probability for Exceedance of the Indicated Vector Shear Percentiles at 12 km, for Shear Layer Thicknesses of 100, 400, 1000, 3000 and 5000 m, Given that the Scalar Wind Speed at 12 km Exceeds the 95 Percent Value

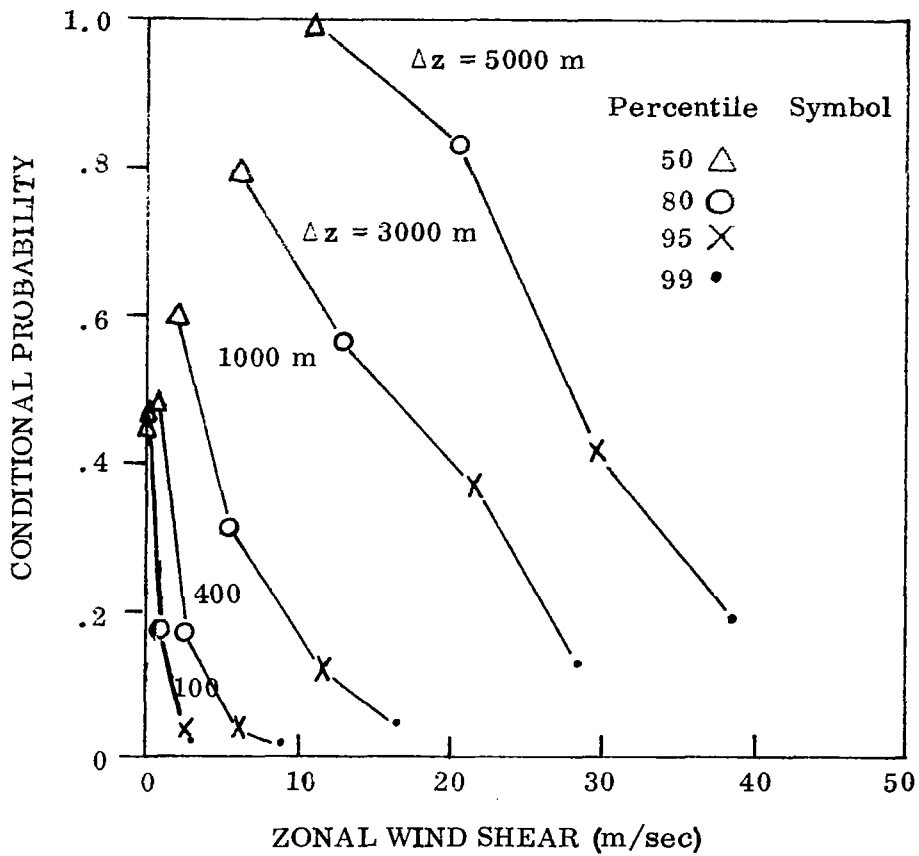


Figure 7.2 Conditional Probability for Exceedance of the Indicated Zonal Shear Percentiles at 12 km, for Shear Layer Thicknesses of 100, 400, 1000, 3000, and 5000 m, Given that the Zonal Wind Speed at 12 km Exceeds the 95 Percent Value

A comparison of the conditional probabilities discussed above with the conditional probabilities of dependent and independent wind and shear distributions is given in Table 7.1 for scalar wind with vector shear and in Table 7.2 for zonal wind with zonal shear. The Tables show that the estimated conditional probabilities for the 5000 m shears obtained from the Jimsphere data are in most cases only slightly less than that predicted for perfect dependence; the conditional probabilities decrease rapidly as the shear layer thickness decreases indicating that the 1000, 400, and 100 m shears have conditional probabilities only slightly higher than that predicted for perfect independence.

These results support the conclusion that extreme large scale ($\Delta z > 3000$ m) shears at 12 km are dependent on the wind speed at 12 km whereas small scale shears ($\Delta z < 1000$ m) are independent of the wind speed at 12 km.

TABLE 7.1

COMPARISON OF CONDITIONAL PROBABILITIES OF DEPENDENT AND INDEPENDENT SCALAR WIND SPEED AND VECTOR SHEAR WITH CONDITIONAL PROBABILITIES ESTIMATED FROM JIMSPHERE OBSERVATIONS FOR VARIOUS SHEAR LAYER THICKNESSES, Δz

Conditional Probability of exceedance of the indicated percentile vector shear at 12 km given exceedance of the 95% scalar wind at 12 km.

Percentile Vector Shear	99	95	80	50
Independent	.01	.05	.20	.50
Dependent	.20	1.00	1.00	1.00
Estimated from Observations				
Δz (m)				
5000	.17	.42	.83	.99
3000	.17	.39	.70	.91
1000	.09	.14	.47	.66
400	.02	.09	.22	.54
100	.02	.09	.27	.61

TABLE 7.2

COMPARISON OF CONDITIONAL PROBABILITIES OF DEPENDENT AND INDEPENDENT ZONAL WIND SPEED AND ZONAL SHEAR WITH CONDITIONAL PROBABILITIES ESTIMATED FROM JIMSPHERE OBSERVATIONS FOR VARIOUS SHEAR LAYER THICKNESSES, Δz

Conditional Probability of exceedance of the indicated percentile zonal shear at 12 km given exceedance of the 95% zonal wind at 12 km.

Percentile Zonal Shear	99	95	80	50
Independent	.01	.05	.20	.50
Dependent	.20	1.00	1.00	1.00
Estimated from Observations				
Δz (m)				
5000	.19	.42	.83	.99
3000	.13	.37	.56	.79
1000	.05	.12	.31	.59
400	.02	.04	.17	.48
100	.02	.04	.17	.47

Section 8

RECOMMENDATIONS FOR FUTURE ANALYSIS OF DETAILED WIND PROFILES

A number of recommendations for future analysis of Jimsphere wind profiles have evolved based on the experience and knowledge gained during the present study. These are summarized as follows:

A. Gust Studies

It has been suggested (Section 6) that gusts be defined in the time domain of vehicle flight and in terms of space vehicle characteristics such as vertical velocity and the frequencies of significant response to wind inputs. Future work should have emphasis on a statistical analysis of gust profiles which are derived according to these procedures as recommended in Section 6. The aim of the statistical analysis, which should include studies of the distributions of gust amplitudes and peaks and gust spectra, is to provide more realistic representations of gusts which may be used with synthetic wind profiles (or wind profiles with poor high frequency characteristics such as rawinsonde profiles) and which are applicable to a variety of vehicle characteristics.

Persistence is another aspect of gust profiles which should be further studied. Of particular importance is the persistence of severe gust profiles. A measure of the severity of a gust profile is the amount of spectral energy in the wind profile at the frequencies of maximum vehicle response. Future studies should be directed towards the determination of the persistence of spectral energy in the critical 10 to 14 km altitude range from series Jimsphere gust profiles.

B. Theoretical Distribution Functions for Wind and Shear

Theoretical distribution functions for wind and shear have been discussed in Section 3. The observed distributions of zonal and meridional wind and shear (Section 2 for wind, Section 4 for shear) are in general agreement with the theory which predicts normality for these distributions. From the results of Section 4, which led to the conclusion that zonal and meridional shears are independent for shear layer thicknesses less than 1000 meters, it follows that the distribution function for vector shear would be similar to the non-central elliptical chi distribution shown in Table 3.1. Although this function is too complicated for complete tabulation, it can be tabulated and fitted to particular sets of observations, and the fit criteria can be used to estimate the degree of correspondence of theory and observation. The same applies to the distribution of scalar wind with the following additional comment: The zonal and meridional wind speeds have not yet been shown to be independent; if they are not independent the distribution function becomes more cumbersome but still approachable as discussed in Section 3. The distribution of scalar shear known as the chi-dif is apparently in the same stage of development.

In summary, the partial tabulation of these proposed distribution functions must be accomplished to test their validity by comparison with observed distribution.

C. Analysis of Jimsphere Data Obtained at Other Locations

The Jimsphere profiles taken at White Sands, Wallops Island, and at the Western Test Range (Pt. Mugu) can be analyzed to establish relations between shears over various altitude intervals. One aim of this analysis is to compare the results with the Cape Kennedy results to seek generalizations which represent certain aspects of wind shear behavior at all four locations. For example, in Section 4.4, a comparison suggested that the mean vector shears at both Cape Kennedy and White Sands are proportional to the two-thirds power of the shear layer thickness. A more detailed analysis should be made

to support this result, and to determine how far it is applicable also at the Western Test Range; similarly, the behavior of the extreme shears ($\geq 95\%$, $\geq 99\%$), which have also been shown to be proportional to the two-thirds power of shear layer thickness, (Section 4.4) at Cape Kennedy, should be studied at the other locations.

In general, the aim of the analysis would be to provide more information for design and operation of space vehicles at these locations.

D. Classification of Wind Profiles with Respect to Space Vehicle Performance and Synoptic Meteorology

Based on present knowledge of wind profile influences on space vehicle performance the various wind profile types which cause severe space vehicle responses can be extracted from the larger body of Jimsphere wind profiles. These profiles can then be classified according to their general behavior. For example, Ryan, Scoggins, and King (Ref. 13) mention four types of behavior that are important for the Saturn V; they are: High wind speed with moderate shear, low wind speed with high shear, fluctuations at bending mode frequencies, and shears that have the characteristic of a step function. The final and most important aspect of the classification is the study of the association of each type of severe wind profile with particular synoptic meteorology patterns. The degree of association may be expressed by a statement of the probability that the particular severe profile type will occur for a particular meteorological situation.

This classification scheme can be used as an aid in forecasting severe wind profiles.

Section 9

REFERENCES

1. Alfriend, K. T., "Design of a Digital Filter for Application to Wind/Turbulence Data", Lockheed Missiles and Space Company, LMSC/HREC A 710908 (1965).
2. Anonymous, "Synoptic Meteorology as Practiced by the National Meteorological Center," the NAWAC Manual, U.S. Department of Commerce, Washington, D.C., (October 1960).
3. Armendariz, M., and Rider, L. J., "Wind Shear for Small Thickness Layers," J. Appl. Meteor., 5, 810-815 (1966).
4. Bieber, R. E., "Relative Influence of Atmosphere Properties on Launch Vehicle Design", J. Spacecraft, Vol. 4, No. 2, 224-229 (1967).
5. Court, A., "The Difference of Two CHI Variates," Lockheed-California Company Report LR 21269 (Jan. 1968).
6. Essenwanger, O., "On the Derivation of Frequency Distributions of Vector Wind Shear Values for Small Shear Intervals," Geofis. Pura. Appl., 56, 216-224 (1963).
7. Gordon, A. H., "Elements of Dynamic Meteorology", (D. Van Nostrand Company, New York, 1962), First Edition, Chap. 7, p. 113.
8. Gumbel, E. J., "Statistics of Extremes," (Columbia University Press, New York, 1958).
9. Huschke, R. E., "Glossary of Meteorology," (American Meteorology Society, Boston, Mass. 1959).
10. Jacobs, D. B., "Saturn V AS-504 Launch Vehicle Reference Trajectory" Document D5-15481-1 Vol. 2, Contract NAS 8-5608, The Boeing Company (May, 1967).
11. Pasquill, F., "Atmospheric Diffusion," Van Nostrand, New York (1962).
12. Rider, L. J., and Armendariz, M., "A Comparison of Simultaneous Wind Profiles Derived from Smooth and Roughened Spheres," J. Appl. Meteor., 7, 293-296 (1968).
13. Ryan, R. S., Scoggins, J. R. and King, A., "Use of Wind Shears in the Design of Aerospace Vehicles," AIAA J. 4, 1526-1532 (1967).
14. Scoggins, J. R., "An Evaluation of Detailed Wind Data as Measured by the FPS-16 Radar/Spherical Balloon Techniques," NASA Technical Note D-1572, Washington, D.C., (May 1963).

15. Scoggins, J. R., and Vaughan, W. W., "Some Properties of Atmospheric Turbulence for Space Vehicles," AIAA Paper No. 65-509 presented at AIAA Second Annual Meeting, San Francisco, California, July 26-29, 1965.
16. Anonymous, "Atlantic Missile Range Reference Atmosphere for Cape Kennedy, Florida (Part I)", IRIG Document 104-63 Range Commanders Council, White Sands New Mexico, April 16, 1963.
17. Vaughan, W. W., "Interlevel and Intralevel Correlations of Wind Components for Six Geographical Locations," NASA TN-D-561 (Dec. 1960).